ALEX(01)-TR-78-08

EVENT IDENTIFICATION – APPLICATIONS TO AREA OF INTEREST EVENTS

TECHNICAL REPORT NO. 28
VELA NETWORK EVALUATION AND AUTOMATIC PROCESSING RESEARCH

Prepared by
R. L. Sax and Technical Staff

TEXAS INSTRUMENTS INCORPORATED
Equipment Group
Post Office Box 6015
Dallas, Texas 75222

Prepared for

AIR FORCE TECHNICAL APPLICATIONS CENTER
Alexandria, Virginia 22314

Sponsored by

ADVANCED RESEARCH PROJECTS AGENCY
Nuclear Monitoring Research Office
ARPA Program Code No. 7F10
ARPA Order No. 2551

13 November 1978

Acknowledgment: This research was supported by the Advanced Research Projects Agency, Nuclear Monitoring Research Office, under Project VELA-UNIFORM, and accomplished under the technical direction of the Air Force Technical Applications Center under Contract Number F08606-77-C-0004.

Equipment Group
8705-79-015

UNCLASSIFIED

SECURITY CLASSIFICATION OF THIS PAGE (When Data Entered)

REPORT DOCUMENTATION PAGE		READ INSTRUCTIONS BEFORE COMPLETING FORM
1. REPORT NUMBER	2. GOVT ACCESSION NO.	3. RECIPIENT'S CATALOG NUMBER
4. TITLE (and Subtitle) (6) EVENT IDENTIFICATION - APPLICATIONS TO AREA OF INTEREST EVENTS. (14) TI		5. TYPE OF REPORT & PERIOD COVERED (9) Technical rept.,
		6. PERFORMING ORG. REPORT NUMBER ALEX(01)-TR-78-08
7. AUTHOR(s) R. L. Sax and Technical Staff		8. CONTRACT OR GRANT NUMBER(s) (15) F08606-77-C-0004 ARPA Order-2551
9. PERFORMING ORGANIZATION NAME AND ADDRESS Texas Instruments Incorporated Equipment Group Dallas, Texas 75222 (12) 194 p.		10. PROGRAM ELEMENT, PROJECT, TASK AREA & WORK UNIT NUMBERS VELA T/8705/B/PMP
11. CONTROLLING OFFICE NAME AND ADDRESS Advanced Research Projects Agency Nuclear Monitoring Research Office Arlington, Virginia 22209		(11) 12. REPORT DATE 13 November 1978
		13. NUMBER OF PAGES 193
14. MONITORING AGENCY NAME & ADDRESS (if different from Controlling Office) Air Force Technical Applications Center VELA Seismological Center Alexandria, Virginia 22314		15. SECURITY CLASS. (of this report) UNCLASSIFIED
		15a. DECLASSIFICATION/DOWNGRADING SCHEDULE

16. DISTRIBUTION STATEMENT (of this Report)

This document has been approved for public release and sale; its distribution is unlimited.

17. DISTRIBUTION STATEMENT (of the abstract entered in Block 20, if different from Report)

(10) R. L. Sax A. G. R. Bell, D. L. Dietz, A. C. Strauss J. S. Shaub

18. SUPPLEMENTARY NOTES

ARPA Order No. 2551

19. KEY WORDS (Continue on reverse side if necessary and identify by block number)

Seismology
Seismic event identification
Seismic discrimination
Multivariate seismic discrimination

20. ABSTRACT (Continue on reverse side if necessary and identify by block number)

An integrated event identification system has been developed to operate on an 'Area of Interest' data base. This system includes an automated measurement and analysis section using the IBM 360/44 computer and an interactive editing and identification section using the PDP-15/50 computer. Amplitude measurements are made on both short-period and long-period data and serve as the basis for computing most of the discriminants. Other discriminants include mean instantaneous frequency and

DD FORM 1 JAN 73 1473 EDITION OF 1 NOV 65 IS OBSOLETE

UNCLASSIFIED 405 076 mtt

SECURITY CLASSIFICATION OF THIS PAGE (When Data Entered)

19. (continued)

Automatic seismic detection
Automated seismic processing
Interactive seismic processing systems
Maximum likelihood seismic magnitude estimation

20. (continued)

mean instantaneous phase standard deviation, and complexities. Ringdal's maximum likelihood technique is used to generate 'unbiased' event measurements from the individual station measurements obtained for each event. At present, a set of 35 events has been processed with this system. A multivariate analysis technique was used to classify the events either as earthquakes or as particular types of anomalous events. The results indicate that the system makes it possible to achieve good separation between anomalous events and a selected set of normal shallow-depth earthquakes.

LIST OF AUTHORS

Principal authors of this report are listed below.

Section	Authors
I.	A. C. Strauss
II.	A. G. R. Bell, and R. L. Sax
III.	A. G. R. Bell, D. L. Dietz, A. C. Strauss, and R. L. Sax
IV.	D. L. Dietz, J. S. Shaub, and R. L. Sax
V.	R. L. Sax
VI.	R. L. Sax
Appendix A	D. L. Dietz

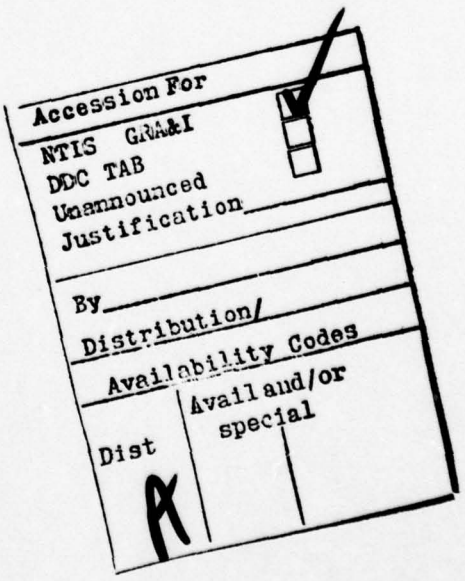

ABSTRACT

An integrated event identification system has been developed to operate on an 'Area of Interest' data base. This system includes an automated measurement and analysis section using the IBM 360/44 computer and an interactive editing and identification section using the PDP-15/50 computer. Amplitude measurements are made on both short-period and long-period data and serve as the basis for computing most of the discriminants. Other discriminants include mean instantaneous frequency and mean instantaneous phase standard deviation, and complexities. Ringdal's maximum likelihood technique is used to generate 'unbiased' event measurements from the individual station measurements obtained for each event. At present, a set of 35 events has been processed with this system. A multivariate analysis technique was used to classify the events either as earthquakes or as particular types of anomalous events. The results indicate that the system makes it possible to achieve good separation between anomalous events and a selected set of normal shallow-depth earthquakes.

ACKNOWLEDGMENTS

The authors would like to thank Frode Ringdal for his help in applying his maximum likelihood magnitude estimation method to the event identification system; Dave Black for his assistance in programming routines for the PDP-15/50 computer; Bill Schmidt for his help in programming and processing on the IBM 360/44 computer; Ruud Unger for consulting on this project and for his help in editing this report; and Helmut Y.A. Hsiao for contributing to the theoretical section (Section II) of this report.

TABLE OF CONTENTS

SECTION	TITLE	PAGE
	LIST OF AUTHORS	iii
	ABSTRACT	iv
	ACKNOWLEDGMENTS	v
I.	INTRODUCTION	I-1
	A. THE TASK	I-1
	B. THE AREA OF INTEREST DATA BASE	I-5
	C. REPORT ORGANIZATION	I-11
II.	THEORETICAL MOTIVATION	II-1
	A. THEORETICAL EARTHQUAKE AND UNDERGROUND EXPLOSION SOURCE MODELS	II-1
	B. MOTIVATIONS FOR THE DISCRIMINANTS USED IN THIS STUDY	II-4
	C. REGIONAL PHASE RATIO DISCRIMINANTS	II-8
	D. THE TELESEISMIC M_s - m_b DISCRIMINANT	II-10
	E. COMPLEXITY	II-14
	F. VARIABLE FREQUENCY MAGNITUDE METHODS	II-15
	G. INSTANTANEOUS PHASE AND FREQUENCY MEASUREMENTS	II-18
III.	MEASUREMENT OF EVENT IDENTIFICATION PARAMETERS	III-1
	A. OVERVIEW OF THE MEASUREMENT PROGRAM	III-1

TABLE OF CONTENTS
(continued)

SECTION	TITLE	PAGE
	B. SHORT-PERIOD EVENT MEASUREMENT	III-5
	C. LONG-PERIOD EVENT MEASUREMENT	III-24
	D. EXAMPLES OF SHORT-PERIOD AND LONG-PERIOD EVENT MEASUREMENT	III-30
IV.	MULTIVARIATE DISCRIMINATION	IV-1
	A. OVERVIEW	IV-1
	B. THE EVENT DISCRIMINANT DATA BASE	IV-3
	C. APPLICATION OF DISCRIMINATION OPERATORS TO THE EVENT DISCRIMINANT DATA BASE (EDDB)	IV-21
	D. EXAMPLES OF DISCRIMINATION OPERATOR APPLICATION	IV-36
V.	RESULTS	V-1
VI.	CONCLUSIONS	VI-1
VII.	REFERENCES	VII-1
Appendix A	VFM NARROWBAND FILTER DESCRIPTION	A-1

LIST OF FIGURES

FIGURE	TITLE	PAGE
I-1	WORLD-WIDE TECTONIC REGIONS	I-4
I-2	LOCATIONS OF STATIONS	I-7
I-3	LOCATIONS OF EVENTS	I-10
II-1	P CODA FOR EASTERN KAZAKH EXPLOSION AND EARTHQUAKE AS RECORDED AT MAIO	II-16
III-1	GENERALIZED FLOW DIAGRAM OF THE EVENT IDENTIFICATION PARAMETER MEASUREMENT PROGRAM	III-3
III-2	SHORT-PERIOD DISCRIMINANT MEASUREMENT LOGIC FLOW	III-6
III-3	SP SIGNAL DETECTION AND TIMING (Unger, 1978a)	III-7
III-4	STEPBACK PROCEDURE IN SP SIGNAL TIMING (Unger, 1978a)	III-9
III-5	SCHEMATIC ILLUSTRATION OF SHORT-PERIOD EDIT COMPRESSION	III-14
III-6	BROADBAND SHORT-PERIOD (A/T) MEASUREMENT LOGIC FLOW	III-18
III-7	SHORT-PERIOD VARIABLE FREQUENCY MAGNITUDE (VFM) MEASUREMENT LOGIC FLOW	III-21
III-8	LONG-PERIOD VARIABLE FREQUENCY MAGNITUDE MEASUREMENT LOGIC FLOW	III-25
III-9	NORTH AMERICAN CONTINENT DISPERSION FOR WORLD-WIDE STATIONS (Unger, 1978b)	III-26
III-10	ASIAN CONTINENT DISPERSION FOR WORLD-WIDE STATIONS (Unger, 1978b)	III-27
III-11a	SHORT-PERIOD EVENT MEASUREMENT EXAMPLE SHOWING SHORT-PERIOD DATA EDIT AND BROADBAND SIGNAL DETECTION	III-32

LIST OF FIGURES
(continued)

FIGURE	TITLE	PAGE
III-11b, c	SHORT-PERIOD EVENT MEASUREMENT EXAMPLE SHOWING (b) INSTRUMENT RESPONSE REMOVAL, AND (c) SHORT-PERIOD EDIT COMPRESSION	III-33
III-11d, e	SHORT-PERIOD EVENT MEASUREMENT EXAMPLE SHOWING (d) BROADBAND COMPLEXITY, MEAN INSTANTANEOUS FREQUENCY, MEAN PHASE STANDARD DEVIATION, AND (e) BROADBAND $LOG_{10}(A/T)$ MEASUREMENT	III-34
III-11f	SHORT-PERIOD EVENT MEASUREMENT EXAMPLE SHOWING VARIABLE FREQUENCY MAGNITUDE (VFM) $LOG_{10}A$ MEASUREMENT AND NARROWBAND COMPLEXITIES	III-35
III-11g	SHORT-PERIOD EVENT MEASUREMENT EXAMPLE SHOWING INFORMATION CONTAINED IN SHORT-PERIOD EVENT HEADER	III-36
III-12	RAW INPUT SHORT-PERIOD DATA TRACE SHOWING DETECTED P PHASE ARRIVAL AND 51.2 SEC COMPRESSED EDIT	III-37
III-13	NARROWBAND FILTERED SIGNALS, ENVELOPES, AND INSTANTANEOUS FREQUENCIES USED FOR SHORT-PERIOD VFM $LOG_{10}A$ MEASUREMENTS. ALSO SHOWN ARE FILTER CENTER FREQUENCIES (CF), BANDWIDTHS (BW), 10 SECOND SEARCH GATE, AND TIME WITHIN THAT GATE CHOSEN FOR $LOG_{10}A$ MEASUREMENTS (▼)	III-38
III-14a	LONG-PERIOD EVENT MEASUREMENT EXAMPLE SHOWING LONG-PERIOD THREE COMPONENT DATA EDIT AND AUTOMATED QUALITY CHECKS	III-42
III-14b	LONG-PERIOD EVENT MEASUREMENT EXAMPLE SHOWING LONG-PERIOD SYSTEM RESPONSE REMOVAL	III-43
III-14c	LONG-PERIOD EVENT MEASUREMENT EXAMPLE SHOWING LONG-PERIOD VARIABLE FREQUENCY MAGNITUDE (VFM) $LOG_{10}A$ MEASUREMENTS ON VERTICAL (1) AND TRANSVERSE (2) COMPONENTS	III-44

LIST OF FIGURES
(continued)

FIGURE	TITLE	PAGE
III-14d	LONG-PERIOD EVENT MEASUREMENT EXAMPLE SHOWING LONG-PERIOD EVENT HEADER INFORMATION	III-48
III-15	NARROWBAND FILTERED SIGNALS, ENVELOPES, AND INSTANTANEOUS FREQUENCIES USED FOR LONG-PERIOD VFM $LOG_{10}A$ MEASUREMENTS ON VERTICAL AND TRANSVERSE COMPONENTS. ALSO SHOWN ARE FILTER CENTER FREQUENCIES (CF), BANDWIDTHS (BW), AND TIME CHOSEN FOR $LOG_{10}A$ MEASUREMENTS (▼)	III-49
IV-1	EVENT IDENTIFICATION SYSTEM	IV-4
IV-2	GENERAL ORGANIZATION OF EVENT DISCRIMINANT DATA BASE (EDDB)	IV-6
IV-3	STRUCTURE OF THE EVENT DIRECTORY	IV-8
IV-4	STRUCTURE OF A RAW EVENT DISCRIMINANT DATA FILE: "$EDDX_1X_2$"	IV-10
IV-5	STRUCTURE OF AN AVERAGED EVENT DISCRIMINANT CLASS FILE	IV-12
IV-6	STRUCTURE OF THE CLASS DIRECTORY	IV-14
IV-7	GENERAL FLOW OF DDBASE	IV-15
IV-8	GENERAL FLOW OF DLOGD	IV-17
IV-9	SAMPLE DLOGD EXECUTION	IV-18
IV-10	GENERAL FLOW OF CLAVE	IV-19
IV-11	SAMPLE CLAVE EXECUTION	IV-20
IV-12	USER FUNCTION DBOOT	IV-26
IV-13	USER FUNCTION PARM	IV-27
IV-14	USER FUNCTION SETEQ	IV-29
IV-15	USER FUNCTION SETU	IV-30
IV-16	USER FUNCTION EQNRM	IV-32

LIST OF FIGURES
(continued)

FIGURE	TITLE	PAGE
IV-17	USER FUNCTION PXGEN	IV-33
IV-18	USER FUNCTION EXPCL	IV-35
IV-19	USER FUNCTION SUBEX	IV-37
IV-20	EXECUTION OF DBOOT	IV-38
IV-21	EXECUTION OF SETEQ	IV-40
IV-22	EXECUTION OF PARTY	IV-42
IV-23	EXECUTION OF SETU	IV-43
IV-24	EXECUTION OF PARM	IV-44
IV-25	EXECUTION OF EQNRM	IV-47
IV-26	EXECUTION OF PXGEN	IV-48
IV-27	EXECUTION OF EXPCL	IV-49
IV-28	EXECUTION OF SUBEX	IV-50
V-1	SCHEMATIC OF EVENT DISCRIMINANT POPULATIONS	V-5
A-1	NARROWBAND FILTER USED FOR VFM MEASUREMENT. THE WIDTH AT ONE-HALF MAXIMUM AMPLITUDE IS DESIGNATED Δf (Lambert, Bache, and Savino, 1977)	A-2

LIST OF TABLES

TABLE	TITLE	PAGE
I-1	STATION LOCATIONS	I-6
I-2	EVENT PARAMETERS	I-9
IV-1	EVENT DISCRIMINANTS	IV-23
V-1	EVENT DISCRIMINANTS	V-2
V-2	NORMAL EARTHQUAKE STATISTICS	V-7
V-3	UPDATED NORMAL EARTHQUAKE STATISTICS WITH THRESHOLD SET AT 85% LEVEL OF EARTHQUAKE POPULATION	V-8
V-4	CORRELATED GROUP STATISTICS WITH THRESHOLD SET AT 85% LEVEL OF EXPLOSION POPULATION	V-9
V-5	EVENTS SORTED BY MEASURED DISCRIMINANT VALUE	V-11
V-6	EVENT IDENTIFICATION RESULTS	V-24
V-7	DETECTABILITY OF CORRELATED EVENT GROUP NUMBER ONE AND UNCORRELATED UNKNOWNS	V-26

SECTION I

INTRODUCTION

A. THE TASK

Source identification of seismic events has been studied for two decades. As a rule, these research efforts have evaluated discrimination techniques applied to events from a particular region as recorded at a particular station. The drawback to this type of study is that it fails to consider the effects of source, path, and receiver variations on the discriminant. Thus, identification techniques such as first motion or complexity, which initially appeared to be quite promising, were later dropped or downgraded in importance when considered in light of larger data bases. Even a technique such as $M_s - m_b$, which has historically been shown to be highly effective in discriminating between earthquakes and nuclear explosions, must be applied with care. For example, Peppin and McEvilly (1974) used Pn versus 12 second LR (analogous to $M_s - m_b$) to discriminate between Nevada earthquakes and NTS explosions. Their plots of data with M_L less than 5.0 showed good separation between the two populations. However, inclusion in their plots of explosion Pn versus LR points for M_L greater than 5.0 shows that these explosion points fall in the earthquake population. Thus, the discriminant fails for this region when considering large magnitude events.

Since no one discrimination technique can be expected to correctly identify all events from all regions as recorded at all stations, it is necessary at this time to attempt to identify events using all available discrimination information in a multivariate mode of operation. The utility of this type of approach is demonstrated by Anglin (1971), who shows that a complete separation of a suite of Eurasian earthquakes and nuclear explosions

could be achieved by plotting complexity discriminant values against third moment of frequency discriminant values. Used individually, neither of these discriminants completely separated the two populations.

The specific goals of this report are therefore:

- To define a set of identification criteria which can be applied to network data to optimally use the features of each discrimination method.
- To determine the physical source of each discrimination method in order to allow the application of the method to events of similar physical characteristics.
- To assemble a package of discrimination techniques and test this package in order to define how the techniques perform, both individually and in a multivariate mode.
- To recommend further package refinements based on any deficiencies or operational difficulties discovered during the course of this study.

The most significant progress toward these goals last year was the development of an integrated event identification system. The purpose of this system was to automate as fully as possible the routine stages of the data processing so that the analyst can devote as much time as possible to those areas which resist automation. In brief, the system consists of two stages - measurement and analysis. The measurement stage, which is documented by Schmidt and Wilson (1978), edits the data from the event tape, removes the instrument response to produce displacement data, and measures the parameters to be used in the discrimination analysis. This stage of the system is performed on the IBM 360/44 computer. The edited waveforms and measured parameters are written on tape for transfer to the PDP-15/50 computer. At the PDP-15/50, the analyst is able to visually inspect the data

in a quality check mode, override previously made measurements as desired, compute unbiased network magnitudes using Ringdal's technique (Ringdal, 1975), and perform multivariate discrimination. All of this will be more fully discussed in later sections of this report.

It is important to note that the work carried out during the last year had as its principal goal the creation of this system, since the long-term benefits of such a system when fully operational will far outweigh the short-term benefits of measuring a number of discriminant values on any particular data set. The discrimination methods embodied in the current system are not intended to represent all possible methods. The intent in the work performed during the last year was to build in enough recognized discrimination techniques to permit measurement of a data set adequate for the multivariate discrimination effort. By modularizing the system, it will always be possible to add more discriminant-measuring methods at a later date.

An important point to note is that past research has indicated that discriminant measurements are strongly influenced by the tectonic region of the source. Past efforts to minimize the influence of the source tectonic region have generally taken the form of separating the events by geographic region. For example, the M_s - m_b discriminant using SRO data was presented in this fashion by Strauss and Weltman (1977). However, this approach is not optimal, since when studying a large area such as Eurasia many regions, and hence many test events, must be studied. In an attempt to simplify this problem, the events are classed as being located in tectonically active, inactive, or rift regions. Since the tectonic region in which the station is located can also influence discriminant measurements, the stations are also classified as being located in tectonically active, inactive, or rift regions. This results in a total of only nine station-event region tectonic classifications. Figure I-1 illustrates the world-wide distribution of the three tectonic regions.

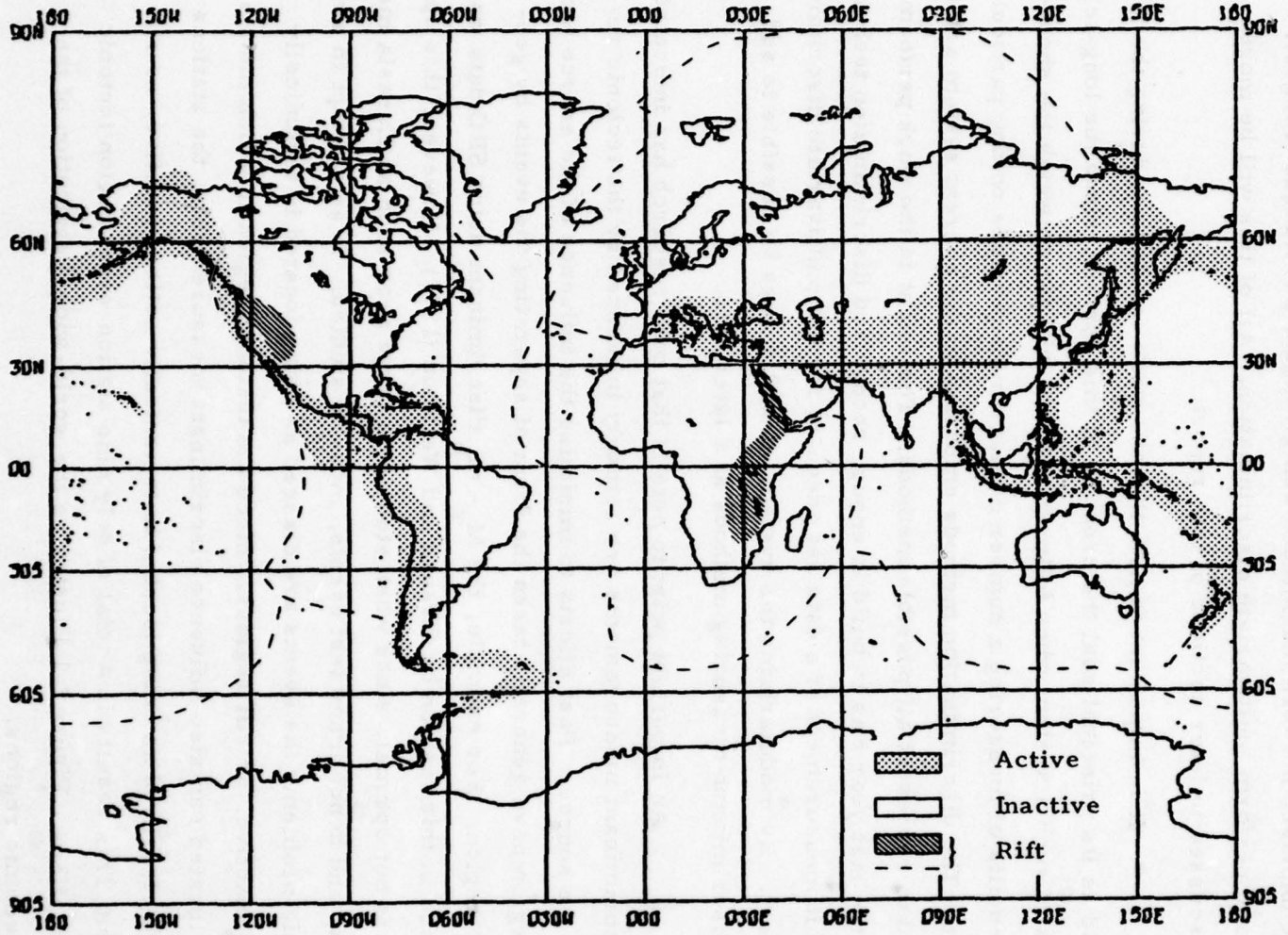

FIGURE I-1

WORLD-WIDE TECTONIC REGIONS

B. THE AREA OF INTEREST DATA BASE

The data base to be used in this event identification study is the suite of 'Area of Interest' (AI) events supplied to all researchers by Teledyne Geotech Incorporated of Alexandria, Virginia. The data supplied for each event consists of edits of the data recorded at the stations listed in Table I-1 and shown in Figure I-2. (An asterisk in Table I-1 denotes that the station was used in this research effort.) These edits nominally consist of 180 seconds of short-period P, 600 seconds of short-period Lg, 240 seconds each of long-period P and S, and 1200 seconds of long-period Rayleigh, where the edit windows are roughly centered about the expected arrival time of the appropriate waveform. The only change made in the data when preparing the AI tapes was to convert the data from digital counts to millimicrons. The data from all stations except RKON and HNME are in the vertical, north, east configuration. The data from RKON and HNME were recorded in a vertical, transverse, radial configuration with respect to the Nevada Test Site.

As of 30 September 1978, the requisite parameters (date, origin time, and epicenter coordinates) for 87 AI events had been supplied to the authors. Since the event identification system as presently constituted is designed for the shallow earthquake/explosion discrimination problem, it was necessary to eliminate from the data base all events with depth unknown or greater than 60 km by searching the National Earthquake Information Service bulletin for depth information. This depth information requirement is only a temporary measure to permit testing of the system as presently designed. Necessary future work on the system will include placing a depth-determination algorithm such as that designed by Page (1976) to provide a screening procedure (Basham and Anglin, 1973) which will eliminate most of those events with focal depths greater than the maximum feasible drilling depth after making allowance for uncertainty in depth determination.

TABLE I-1

STATION LOCATIONS

Site No.	Station	Latitude	Longitude	Tectonic Class†
1	ANMO*	34.94	-106.46	R
2	ANTO	40.00	33.00	A
3	BOCO	5.00	-74.00	A
4	CHTO*	18.80	99.00	A
5	NORS*	60.84	10.89	I
6	GUMO*	13.59	144.87	A
7	MAIO*	36.30	59.49	A
8	LASA*	46.69	-106.22	I
9	NWAO*	-32.93	117.24	I
10	KSRS*	37.45	127.92	I
11	SHIO	25.57	91.88	A
12	TATO*	25.00	121.50	A
13	SNZO*	-41.31	174.70	A
14	ILPA*	35.70	50.61	A
15	ALPA*	65.03	-147.20	A
16	CTAO (ASRO)*	-20.09	146.25	I
17	ZOBO*	-16.27	-68.12	A
18	KAAO*	34.54	69.04	A
19	MAJO*	36.54	138.21	A
20	ATAK*	52.88	173.17	A
21	BFAK*	64.77	-146.89	A
22	CTAO (HGLP)*	-20.09	146.25	I
23	CHGO	18.79	98.98	A
24	TNAK*	62.91	-156.02	A
25	TLOO	39.86	-4.01	I
26	EIAO	29.55	34.95	R
27	KONO	59.65	9.60	I
28	OGDO	41.07	-74.62	I
29	KIPO	21.42	-158.02	A
30	ALQO	34.94	-106.46	R
31	ZLPO	-16.27	-68.12	A
32	MATO	36.54	138.21	A
33	HNME*	46.16	-67.99	I
34	RKON*	50.84	-93.67	I

† A = Active, I = Inactive, R = Rift

* Stations used in this study.

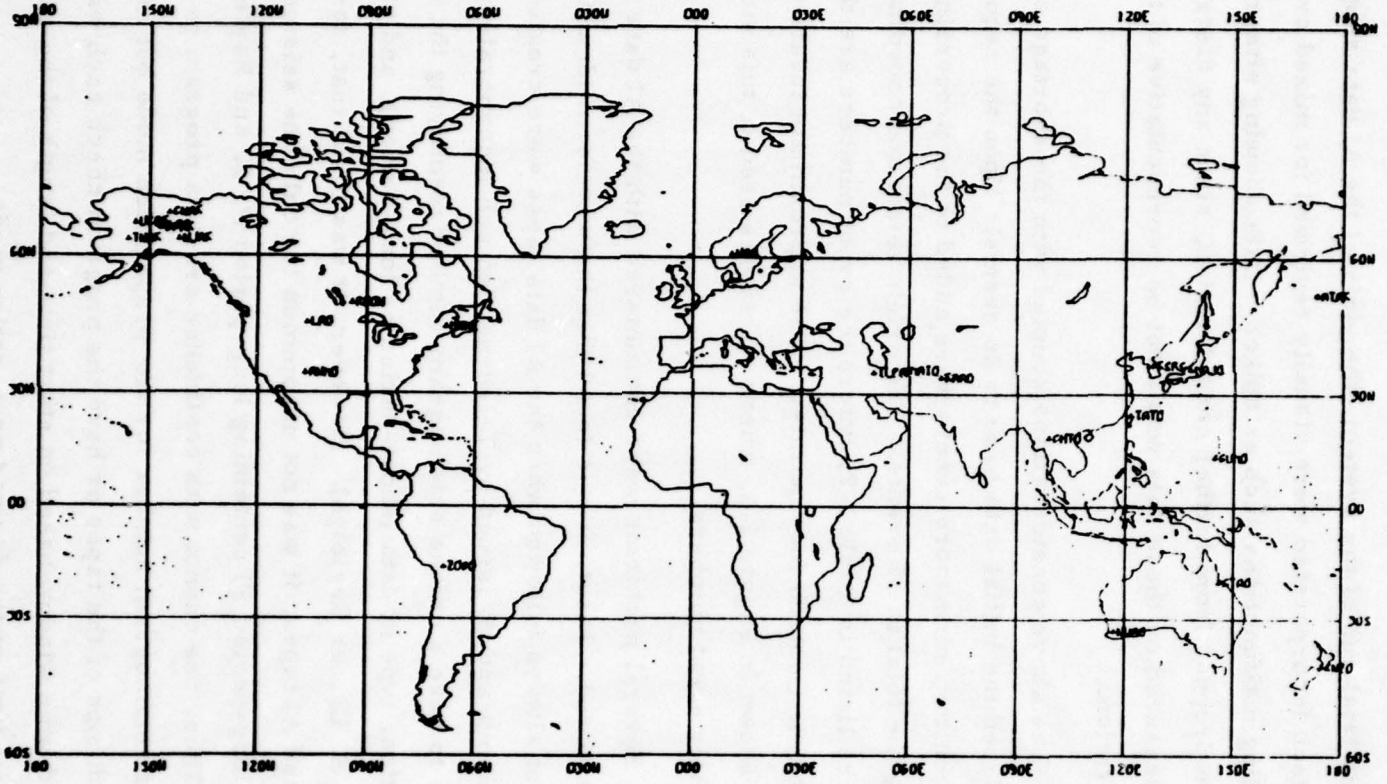

FIGURE I-2

LOCATIONS OF STATIONS

Since it is desirable to have as clean a data set as possible before making the trial run of the system, the plots of the AI data supplied by Teledyne Geotech Incorporated were visually reviewed for mixed events and station recording malfunctions such as spikes. Data showing either of these problems were dropped from further consideration, since any discrimination parameters measured on these data would not be representative of the event under consideration.

The above considerations coupled with the shortage of time available, reduced the initial data base to 26 events. Upon the request of the contract monitor, nine more events were added to the processing data base, bringing the total to 35 events. The origin times and coordinates of these events are listed in Table I-2, where the event numbers are those assigned by Teledyne Geotech Incorporated. The approximate locations of all 87 events are shown in Figure I-3, where the events used in this study are indicated by their event numbers.

Several problems were encountered with the AI data when processing was initiated. First, it was found that the waveform identification scheme was not always followed when the AI data tapes were created. According to a memorandum issued by Teledyne Geotech Incorporated, each waveform was to have a unique seismogram number identifying the event, recording station, type of data (short-period or long-period), and propagation mode (P, S, Lg, or Rayleigh). However, it was found that, for more recently created AI tapes, it was not uncommon for only one seismogram (identified as long-period P) containing long-period P, S, and Rayleigh to be on the tape. Thus, one cannot with confidence create a program to search on the basis of seismogram number for one propagation mode but must either check header dumps of the tapes or have the program check each waveform for the desired time window based on start time and length of the edit and expected arrival time of the desired propagation mode.

TABLE I-2

EVENT PARAMETERS

Event Number	Date (Mo/Da/Yr)	Origin Time (Hr:Min:Sec)	Latitude (^{o}N)	Longitude (^{o}E)	Tectonic Class
1	07/26/77	16:59:59.9	69.4	90.4	I
3	11/01/77	03:54:24.0	55.3	130.8	A
7	11/04/77	23:54:51.5	30.7	81.3	A
14	07/30/77	01:56:59.9	49.7	78.2	I
16	08/17/77	20:00:00.7	50.9	111.0	A
17	08/17/77	04:26:59.8	49.8	78.2	I
18	08/20/77	22:00:00.6	64.1	99.8	I
19	09/01/77	03:00:00.0	73.3	54.3	I
20	09/05/77	03:03:00.2	50.1	78.9	I
21	09/10/77	16:00:00.5	57.2	106.8	A
22	09/30/77	07:00:00.0	48.0	48.0	I
30	11/18/77	05:20:10	33.0	89.0	A
34	11/18/77	15:10:10	28.0	90.0	A
35	11/18/77	17:23:25	33.0	89.0	A
36	10/16/77	20:03:35	48.4	152.9	A
37	11/18/77	21:55:37.0	60.1	143.2	A
38	10/16/77	15:02:49	36.9	71.5	A
39	11/18/77	23:12:49	33.0	89.0	A
47	10/16/77	21:05:35	49.7	155.1	A
48	10/19/77	05:02:00	36.3	71.3	A
49	10/19/77	21:20:37	49.5	155.4	A
50	10/20/77	08:18:04	56.3	164.1	A
53	10/29/77	03:06:59.7	49.8	78.0	I
55	10/26/77	05:38:52.2	49.0	155.8	A
56	10/26/77	07:11:31.3	46.4	153.5	A
59	10/28/77	21:15:11.5	39.8	71.9	A
61	10/29/77	06:26:42.5	41.0	63.7	A
62	10/29/77	10:33:59.4	47.3	153.1	A
68	10/20/77	23:40:35	33.1	88.1	A
73	11/22/77	11:33:45	43.0	89.0	A
77	11/26/77	22:46:46	37.0	115.0	A
81	11/30/77	04:06:59	49.9	78.8	I
143	12/02/77	12:57:10	52.9	159.7	A
149	12/06/77	10:52:53	41.4	69.7	A
151	12/07/77	16:19:33	35.6	94.5	A

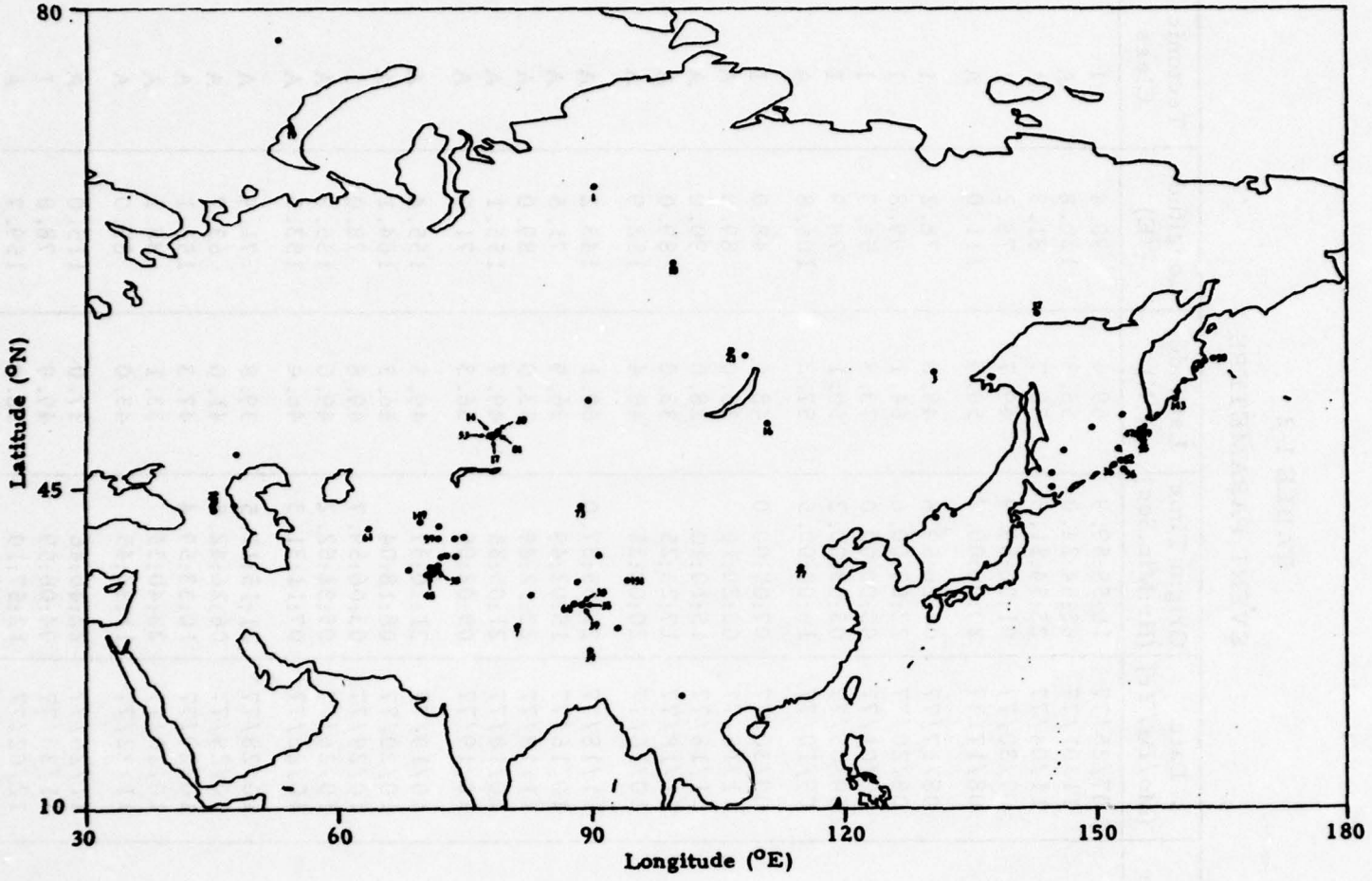

FIGURE I-3

LOCATIONS OF EVENTS

A second problem was that in no case was there a specific short-period Lg edit available from any of the SRO or ASRO stations. Although the short-period automatic detector installed at these stations must be held responsible in most cases for this lack of Lg data, one would expect Lg edits for some of the SRO-ASRO recorded events, since, as shown by Strauss and Weltman (1977), at some stations the automatic detector after being triggered will often stay on for long periods of time. Thus, one would expect there to be at least an occasional Lg edit for these stations on the AI tapes. This unfortunate lack of Lg edits also occurred for data recorded at the stations which continuously record short-period data. It was not uncommon to have a short-period P wave edit but no Lg edit where one would expect the data to have been available.

A surprising shortcoming of the AI data base is the absence of short-period S wave edits. Occasionally, an S wave can be found in the P wave edit when the station is near the event epicenter. However, no specific S wave edits were made during the completion of this data base. This lack of short-period S wave data, coupled with the scarcity of Lg data, seriously affects the quality of the event identification effort, since it minimizes the utility of the compressional-to-shear ratio type of discriminants which have been proven quite useful in the past (Booker and Mitronovas, 1964).

C. REPORT ORGANIZATION

The following sections of this report will discuss in detail the work carried out during the last year toward achieving the goals of the event identification task. Section II of this report presents a discussion of the theoretical background of event identification, followed by a description of the particular event identification methods used in this study. Included in the discussion of each method is the historical background of that method and an attempt to relate the method to the previously described theory. Section

III presents an in-depth examination of the signal identification parameter measurements program TISSPROG. Particular emphasis is placed on the flow of data through the sections of the program which measure the event identification parameters, since it is this portion of the program which has been developed this last year. Section IV presents a discussion of the analysis stage methodology of this research effort. In it is described the manner in which the network discriminant values are computed from the individual station discriminant values for each event. Following this is a description of the method of multivariate discrimination. Section V presents the actual analysis of the 35 AI events processed by this event identification system. Section VI presents the conclusions reached during the course of this research effort and recommendations for possible improvements in the methodology. Section VII lists the references cited in this report. Finally, Appendix A discusses the narrowband filter used in the measurement of several different event identification parameters.

SECTION II
THEORETICAL MOTIVATION

The purpose of this section is to provide a theoretical motivation for the discriminants used in this study. Much effort has been made in recent years to understand the earthquake and underground explosion source mechanisms, and to determine which features of the respective radiation fields may be used to characterize each type of seismic event. As a result of this research, several discriminants have evolved which prove to be quite useful in classifying seismic events either as earthquakes or as underground explosions.

A. THEORETICAL EARTHQUAKE AND UNDERGROUND EXPLOSION SOURCE MODELS

The underground explosion source has been described by Sharpe (1942) and others (Bishop, 1963; Toksöz et al., 1964; Carpenter, 1967; Liebermann and Pomeroy, 1969). A shock wave proceeds radially outward from the detonation point. In the region where this shock wave propagates, the peak stress levels greatly exceed the material strength of the surrounding medium, resulting in rapid dissipation of energy in the form of non-linear deformation (i. e. heating and fracture). At some distance from the detonation point, the stress levels associated with the shock front fall below the elastic limit of the medium, and reversible, infinitesimal strains prevail. At this point, energy is dissipated in the form of seismic radiation.

The transition boundary between the regions of non-linear and linear deformation is not well defined. However, it has been found useful to

represent this boundary schematically as a spherical surface, termed the 'equivalent cavity' (Sharpe, 1942). The radius of the equivalent cavity depends upon the size of the explosive charge and the material properties of the medium in which the charge is detonated (Bishop, 1963). Using far-field observations, it is possible to recover the pressure history only as it exists at this boundary (Toksöz et al., 1964; Liebermann and Pomeroy, 1969).

The earthquake source mechanism has been treated rather extensively in the seismic literature (substantial lists of references may be found on this subject in Brune, 1970; Hanks and Wyss, 1972; and Turnbull, 1976). One of the earliest descriptions of the earthquake source is the Elastic Theory of Fracture due to Reid (1911), based upon observations made after the San Francisco earthquake of 1906. According to the Elastic Rebound Theory, an earthquake occurs as the result of the accumulation of elastic stresses within a given region of the earth. These stresses slowly increase with time until they exceed the strength of the medium, at which point the accumulated stresses are relieved by fracture.

The rupture mechanism involved in the earthquake source was originally thought to be simple Coulomb fracture. However, consideration of shear strengths in the crust and upper mantle, and the rate of increase of overburden pressures with depth, indicates that Coulomb fracture is not a major contributing factor to the earthquake rupture mechanism at depths greater than 25 kilometers (Stacey, 1969).

Recent attempts to explain the physics of the rupture phenomenon have resulted in several fairly successful earthquake models. Steketee (1958) demonstrated the applicability of elastic dislocation theory to the earthquake source problem. In this case, rupture formation is initiated by the sudden application of stresses in an unstrained medium, equivalent to the instantaneous removal of stresses across a fault surface.

Dislocation models have been used successfully in several studies of the far-field radiation and static deformation caused by earthquakes (Chinnery, 1960, 1961; Knopoff and Gilbert, 1960; Burridge and Knopoff, 1964; Haskell, 1964; Berkhemer and Jacob, 1968). Additional studies (Aki, 1968; Haskell, 1969) have used dislocation models to explain near-source displacements. A successful earthquake dislocation model has been developed by Brune (1970). This model is derived by considering the effective stress available to accelerate opposing sides of the fault. Brune's model provides near- and far-field displacement-time functions and spectra for shear waves which agree reasonably well with observed earthquake spectra. In addition, Brune's model also provides a possible means for estimating the effective stress, stress drop, and source dimensions by comparison of observed seismic spectra to theoretical spectra obtained from the model. This technique has been used to estimate source parameters for several large earthquakes (Hanks and Wyss, 1972).

Attempts to explain the dynamics of the earthquake rupture mechanism have also led to the stress relaxation model of Archambeau (1968), where the rupture process is modeled in terms of a volume relaxation phenomenon. In this theory, the dynamical properties of the source are described in terms of the relaxation or readjustment of pre-existing stress fields. The initial shear stress field is taken to be the primary cause of rupture. Seismic effects are the result of the relaxation of this prestress shear field in the medium surrounding a region whose physical properties (rigidity in particular) have changed suddenly.

The tectonic source is viewed in terms of the release of potential strain energy from within a non-elastic zone in the medium. Within this non-linear rupture zone, stress release is achieved by flow, fracture, or phase change, so that strain energy within the volume is dissipated in the work of non-linear deformation.

This dynamic relaxation model requires that the stress field surrounding the rupture zone readjust to equilibrium in a fashion determined by the boundary conditions on the rupture surface once rupture is initiated. This readjustment is accomplished by seismic radiation wherever the medium is elastic.

Where the rupture process occurs instantaneously, the elastodynamic source model and the dislocation source model are equivalent (Snoke et al., 1975; Snoke, 1975). The spectral structure obtained using Archambeau's (1968) model for far-field displacement amplitudes differs from those obtained from other source models, in that the spectra obtained from the elastodynamic model exhibit peaks at long periods. Snoke (1975) asserts that these peaks are actually spurious, and are due to physically inadmissible applications of Archambeau's method of solution.

B. MOTIVATIONS FOR THE DISCRIMINANTS USED IN THIS STUDY

In order to classify seismic events of unknown origin either as earthquakes or as underground explosions, it is first necessary to establish a set of discriminant measurements on which the classification scheme may be based. These discriminants must be chosen to reflect the differences in the source characteristics for the two types of events. Also, because the discriminants are usually obtained from far-field seismic measurements and must be applied to events from tectonically different source regions, the discriminants must be chosen to be as insensitive as possible to variations introduced by differing travel paths and near-source environments.

Several discriminants have been developed in recent years which meet the above requirements to some degree. Each is based upon one (or a combination) of various observable features of the far-field radiation fields. Some of the characteristic differences between the radiation fields of the two

types of events which have been found to be useful in seismic discrimination are:

- Differences in partitioning of radiated energy at the source into shear wave and compressional wave radiation.
- Differences in the level of surface wave excitation for a given m_b.
- Differences in source complexities as indicated by varying amounts of energy present in the P-wave codas.
- Differences in the spectral characteristics of the radiation fields of each type of event.

The earthquake source models (i.e., the dislocation source model and Archambeau's (1968) elastodynamic source model) mentioned earlier in this section may be described in terms of a shear failure along a plane. In terms of first motions, the radiation field observed from an earthquake source is equivalent to that which would be observed by replacing the earthquake source by an equivalent point double-couple (Chinnery, 1960; Burridge and Knopoff, 1964). This has also been verified by several large-scale observational studies (Hodgson and Stevens, 1964; Stevens, 1969).

On the other hand, the underground explosion source as described by Sharpe (1942) and Carpenter (1967) may be represented in terms of an impulsive, radially symmetric point dilatational source. A significant difference between the double-couple source and the dilatational source is in the amount of energy partitioned into compressional and shear wave radiation at the source. From symmetry considerations, the dilatational source corresponding to an underground explosion generates only compressional waves in a homogeneous and isotropic medium (Von Seggern, 1972). Shear (SV) bodywaves and Rayleigh surface waves are also observed in the explosion radiation field, due to

mode conversions along the travel path and the presence of a free surface boundary. However, except for the effects of non-linear mode conversions and near-receiver scattering, no significant horizontally polarized shear bodywave or Love surface wave components should be observed in the explosion signature.

In contrast to theoretical expectations, significant horizontally polarized shear wave components have been observed in the radiation fields of some explosions. Archambeau and Sammis (1970), and Archambeau (1972) have suggested a mechanism to explain this phenomenon, where the anomalous SH component may be contributed by a combination of stress relaxation accompanying the creation of a fracture zone in a prestressed medium, and by weak zones and faulting in the immediate vicinity of the detonation point. The latter mechanism leads to secondary ruptures with definite fault symmetries. These mechanisms have been studied by Archambeau and Sammis to obtain estimates for the source parameters of the Bilby underground explosion. Similar results have been obtained by Toksöz et al. (1971), where the explosive source is modeled in terms of a composite dilatational and double-couple point source. The strength of the double-couple component with respect to the dilatational contribution is found to increase with increasing strength of the surrounding medium. Moreover, the orientation of radiation pattern from the double-couple has been found to be in general agreement with regional faulting trends, which supports the hypothesis that the observed SH wave component is due to explosion induced tectonic strain release.

An automatic spectral fitting procedure which determines a minimum least squares combined dilatational explosion source and double-couple earthquake source was developed by Tsai (1972). Since Tsai's method was established, a few studies have been done by several authors (Tsai 1972a, 1972b; Tsai and Shen, 1972; Turnbull et al., 1973, 1974, 1975; Sun, 1976, 1977; Hsiao, 1978) using this method. All of these studies have been aimed

toward the better understanding and utilization of the long-period teleseismic surface waves for source characterization and possibly for source discrimination. Turnbull (1971, 1972) extended the double-couple source, which is a direct result of the work of Ben-Menahem and Harkrider (1964) and Harkrider (1970), to higher order multipolar source. Alexander and Turnbull (1973) also combined the fundamental and first higher mode Rayleigh and Love wave spectra as a function of source parameter variation in order to investigate the possibility of obtaining a more precise surface wave magnitude measurement. From the examination of the observed Rayleigh and Love wave amplitude spectra of twenty-seven presumed underground nuclear explosions, Sun (1977) found that the seismic sources of those explosions have various degrees of double-couple component in addition to the explosive source. Therefore, a combined source, which consists of a point explosive source and a point double-couple source, has been used by Sun (1977) to model the explosive source and by Hsiao (1978) to model both explosive source and earthquake source. The results indicate that the estimates of dip angle of nine explosions most likely occur between 40° to 50°. This kind of consistency might imply that the explosion can induce structure rupture along the planes of maximum shear stress which usually are oriented around 45°. The results also show the lack of a dilatational component in long-period explosion surface waves, random strike and deeper focus which suggests that the double-couple source of explosions may be associated with large dislocations on a fracture zone surrounding the source.

Another explanation for the observed SH and Love wave components in some explosions is given by Viecelli (1973), which attributes these components to a spalling phenomenon. This is supported by Von Seggern's (1973) observations of events at the Amchitka Test Site. Briefly, Von Seggern found that in situ stress measurements yielded a residual stress level too low to account for the observed SH component in terms of a tectonic release

mechanism. Moreover, delays in the Rayleigh wave arrival as predicted by Viecelli (1973) for a spalling source were observed.

C. REGIONAL PHASE RATIO DISCRIMINANTS

The theoretical difference between earthquakes and explosions in the relative amounts of energy partitioned into compressional and shear wave radiation has been used in short-period, regional discrimination studies by Booker and Mitronovas (1964) and Bell (1978). In both cases discriminants were constructed by taking the ratio of energy in a compressional wave velocity window to the energy in shear and short-period surface wave (Lg) velocity windows. Although the propagation mechanism for the Lg phase is not fully understood, several explanations have been advanced which suggest that the phase is related to shear wave propagation across a continental structure.

The Lg phase is a short-period (approximately 0.5 to 6.0 seconds), large amplitude, emergent arrival which is confined almost entirely to continental travel paths, with an average source-receiver velocity of about 3.5 km/sec (Ewing et al., 1957; Landers, 1978). The Lg phase is most pronounced on the transverse component; however, it is also recorded on the vertical and radial components to some extent. Ewing et al. (1957), and Herrin and Richmond (1960) suggest that Lg is actually a guided shear wave, traveling in the upper portion of the continental crust. More recent studies (Knopoff et al., 1973; Panza and Calcagnile, 1975; Isacks and Stephens, 1975) suggest that Lg may be identified with higher-mode Love wave propagation, which does not require a low velocity channel in the Earth's crust. Landers (1978) attributes the vertical part of Lg to higher-mode Rayleigh waves and scattering near the receiver. In each case, however, the excitation of Lg is directly coupled to the partitioning of energy into shear wave radiation at the source, suggesting its usefulness in a seismic discrimination effort.

Of the various phase energy ratios studied by Booker and Mitronovas (1964) and Bell (1978), the most powerful (in a seismic discrimination context) were found to be:

- The ratio of energy in the Pg window (v (average velocity) = 6.9 km/sec - 4.9 km/sec) to the energy in the Lg window (v = 3.6 km/sec - 3.2 km/sec).
- The ratio of energy in the Pg window to the energy in a shear bodywave window (4.9 km/sec - 3.6 km/sec).
- The ratio of energy in a window containing Pn and Pg (v = first arrival - 4.6 km/sec) to the energy in a window containing shear bodywaves and Lg (v = 4.6 km/sec - 2.0 km/sec).

These discriminants were applied to a set of 20 North American earthquakes and 27 Nevada Test Site underground explosions. Threshold F-statistics were obtained which support the hypothesis that the earthquake and explosion group means for these discriminants were unequal at the 99 percent confidence level in all three cases (Bell, 1978).

Where short-period S and Lg data are available, regional discriminants based upon the difference in energy partitioning are used. However, instead of using ratios of total energy as did previous studies, the discriminants are constructed by taking the difference between magnitude measurements for the P, S, and Lg phases. The phase magnitudes are based upon broadband amplitude-period ratio measurements, and are scaled to m_b according to the following magnitude formulas:

$$m_{Pn} = 3.82 + 2.00 \log\Delta + \log(A/T) \text{ (Evernden, 1967)} \quad \text{(II-1)}$$

$$m_{Sn} = 3.79 + 1.80 \log\Delta + \log (A/T) \quad \text{(Fitch et al., 1978)}$$

$$m_{Lg} = 3.30 + 1.66 \log\Delta + \log (A/T) \quad \text{(Nuttli, 1973)}$$

After evaluating the magnitudes, the discriminants Δm_1 and Δm_2 are formed, where

$$\Delta m_1 = m_{Sn} - m_{Pn}$$

$$\Delta m_2 = m_{Lg} - m_{Pn}$$

It may be seen that these discriminants are analogous, in a formal sense, to the teleseismic $M_s - m_b$ discriminant.

The magnitude formulas for Pn, Sn and Lg are based upon the observed attenuation characteristics of Eastern North America, and have also been found to be applicable to many Eurasian events (Nuttli, 1973; Fitch et al., 1978). Because of the complex structure of tectonically active regions such as those found in the Western United States and Kuriles-Kamchatka, the magnitude formulas may be unreliable when applied to events from these areas. Magnitude formulas which apply to tectonically active and rift zones could be developed for a properly regionalized data base. However, the event data base used in the present study contains too few events to adequately represent each source region, thus it was felt that greater harm would be done by attempting to regionalize this data base than by considering it in toto.

D. THE TELESEISMIC $M_s - m_b$ DISCRIMINANT

In addition to being more efficient in generating shear body-waves, the shearing source corresponding to an earthquake is also a more efficient generator of surface waves than the dilatational explosive source (Douglas et al., 1971; Gilbert, 1973). This forms the basis for the $M_s - m_b$

discriminant introduced by Press et al. (1963), which has proven to be one of the most effective teleseismic discriminants available.

In addition to measuring the difference in the relative excitation of bodywave and surface wave radiation, the $M_s - m_b$ discriminant also reflects differences in the relative amounts of high and low frequency energy generated by the seismic source. A general feature of theoretical far-field displacement spectra for explosive, shear dislocation and stress relaxation sources is the characteristic roll-off in the spectra of bodywaves and surface waves at frequencies above some critical corner frequency which varies inversely with the source dimension (Hanks and Wyss, 1972; Aki, 1967).

Above the corner frequency, the displacement spectrum must decrease at least as quickly as $\omega^{-1.5}$ to ensure bounding of the energy integral. Aki (1967) discusses two statistical source models, one where the amplitude spectrum decays as ω^{-2} at high frequencies, and another due to Haskell (1966), which decays as ω^{-3}. Geller (1976) has also proposed a model where fault width, as well as length, and the direction of propagation are explicitly taken into account, resulting in different average spectra for bodywaves and surface waves. Above the corner frequency for width the average spectrum decays as ω^{-3}. In the region between the corner frequencies for length and width, the spectrum begins to decay as ω^{-2}, and below the corner frequency for length, the average spectrum is essentially flat.

For each of the representations described above, the corner frequencies decrease with increasing magnitude. This tends to segment the theoretical M_s versus m_b line, where the slope of the line varies according to whether M_s, m_b or both M_s and m_b are measured above or below the theoretical corner frequency. For $M_s > 6.5$, the slope found by Aki for ω^{-2} model closely follows the Gutenberg and Richter (1956) M_s versus m_b line, but diverges for $M_s < 6.5$.

Liebermann and Pomeroy (1969) utilized Aki's (1967) theoretical scaling relations for earthquakes, and a scaling relation for explosions where magnitude scales as the common logarithm of the cavity radius. For M_s and m_b measurements at 20 seconds and 1 second period, respectively, the dependence of M_s and m_b upon source dimension for earthquakes is given by Liebermann and Pomeroy (1969):

$$M_s \sim \begin{cases} \log L + \text{constant} & M_s > 6.5 \\ 2 \log L + \text{constant} & 3.5 < M_s < 6.5 \\ 3 \log L + \text{constant} & M_s < 3.5 \end{cases}$$

$$m_b \sim \begin{cases} \log L + \text{constant} & M_s > 3.0 \\ 2 \log L + \text{constant} & M_s < 3.0 \end{cases}$$

where

L is the fault length.

Similarly, for explosions,

$$\left.\begin{aligned} M_s &\sim 3 \log a + \text{constant} \\ m_b &\sim 3 \log a + \text{constant} \end{aligned}\right\} \quad m_b < 6.0$$

where

a is the radius of the effective cavity.

The results for M_s and m_b may be combined to give:

Earthquakes:

$$M_s = m_b + \text{constant} \qquad M_s > 6.5$$

$$M_s = 2m_b + \text{constant} \qquad 3.5 < M_s < 6.5$$

$$M_s = 1.5m_b + \text{constant} \qquad M_s < 3.5$$

Explosions:

$$M_s = m_b + \text{constant} \qquad m_b < 6.0 .$$

Thus, for $M_s > 3.5$ the earthquake and explosion populations diverge, and for $M_s < 3.5$, the two populations appear to merge.

These theoretical results indicate that larger earthquakes tend to excite lower frequencies more efficiently than higher frequencies, thus enhancing the $M_s - m_b$ discriminant for $3.5 < M_s < 6.5$. Clearly, additional data for low magnitude events are required to establish the behavior of $M_s - m_b$ at low magnitudes and the validity of Aki's theoretical scaling law.

Many studies have been conducted to evaluate the effectiveness of the $M_s - m_b$ discriminant involving numerous events from many different source regions (Thirlaway, 1968; SIPRI, 1968; Basham, 1969; Liebermann and Pomeroy, 1969; Capon et al., 1969; Evernden, 1969; Evernden and Filson, 1971; Marshall and Basham, 1972; Peppin and McEvilly, 1974; and Evernden, 1975; to name just a few). $M_s - m_b$ has been found to reliably separate earthquakes and underground explosions for m_b values as low as 4.75 (Evernden, 1969) to 5.00 (Thirlaway, 1968; SIPRI, 1968).

Estimates of bodywave and surface wave magnitudes may be influenced by factors which are not specifically source related. These factors tend to introduce scatter and bias into the magnitude measurements and tend to reduce the effectiveness of $M_s - m_b$ in the context of a world-wide discrimination scheme. Considerable research has been directed toward identifying sources of magnitude bias and removing or minimizing this bias where possible.

One source of error occurs where differing attenuation characteristics for various source-receiver paths are not accounted for. Consistent magnitude differences have been found, for example, for teleseismic events measured in the western United States and for those measured in the eastern United States (Evernden and Clark, 1970; Booth et al., 1974; Der, 1977). Liebermann and Pomeroy (1969) and Basham (1969) also note

systematic differences in the $M_s - m_b$ relations (i.e., the least squares $M_s - m_b$ lines) for events in the western United States as compared to those in Aleution-Kamchatka area, southern Algeria, central Asia, and Novaya Zemlya. For these regions the observed shift in the $M_s - m_b$ lines has been found to range from 0.3 to 0.5 magnitude units (Evernden and Filson, 1971; Solomon, 1972).

Regional dependence of $M_s - m_b$ has been explained in terms of differing levels of anelastic attenuation associated with each of the source regions under consideration. This suggests the need for consideration of $M_s - m_b$ on a regional, rather than global, basis (Liebermann and Pomeroy, 1969; Evernden and Filson, 1971; Marshall and Basham, 1972). In addition, Der (1977) suggests that a world-wide map of Q (or t*) values be compiled which would allow for correction of Q variations under both source and receiver.

Source depth also influences surface wave excitation, as noted by Evernden (1975). In general, deeper earthquakes result in less surface wave excitation relative to those occuring at shallow depths. Several methods have been studied for estimating source depth, such as the application of cepstral analysis and matched filter techniques to depth phases (Page, 1976) and by fitting source models to surface waves (Sun, 1976, 1977; and Hsiao, 1978). Such techniques might be employed in a screening process (Basham and Anglin, 1973; Bell, 1978) to quickly identify events as natural earthquakes which occur at depths greater than a few tens of kilometers, or which occur at sea or other areas where bomb emplacement is highly impractical.

E. COMPLEXITY

The underlying concept of the teleseismic P wave complexity discriminant is that the explosive source may be represented as a transient disturbance with a very short rise time (Liebermann and Pomeroy, 1969).

As a result, the first arrival consists of a short-period P wave with little trailing coda. In comparison, an earthquake is also represented as a transient phenomenon; however, the earthquake has a finite time duration as the disturbance propagates along the fault. This finite time duration tends to produce a significant coda following the initial P wave arrival. An example of this is shown in Figure II-1, where the upper trace is an eastern Kazakh underground nuclear explosion and the lower trace is an earthquake from the same region.

The complexity discriminant consists of measurements of the energy in the P wave coda taken at teleseismic distances. Complexity measurements are generally not made at regional distances because the presence of closely arriving crustal phases (i. e., Pn, Pg, and P*) make the signatures of both earthquakes and explosions appear complex. The conventional complexity measurement is the inverse ratio of the P wave energy in the first 5 seconds after the initial P wave arrival to the energy in the following 30 seconds (Evernden, 1969; Lambert et al., 1970). These time windows are not invariant, as demonstrated by Anglin (1971), who found that gates from 0 to 2 seconds and 2 to 35 seconds were optimum for measuring complexity on Eurasian data as recorded at the Yellowknife array (YKA) in Canada.

F. VARIABLE FREQUENCY MAGNITUDE METHODS

Variable frequency magnitude methods have been applied to short-period teleseismic P waves to discriminate explosions from earthquakes. Bache et al. (1975) thoroughly evaluated a short-period variable frequency magnitude discriminant described by Savino and Archambeau (1974), Bache et al. (1974), and Archambeau et al. (1974). Their results indicated operating characteristics similar to the M_s versus m_b discriminant. Their method is to measure the amplitude of filtered signals and to treat each pair of high and low frequency magnitude measurements as a bi-variate statistic. If a

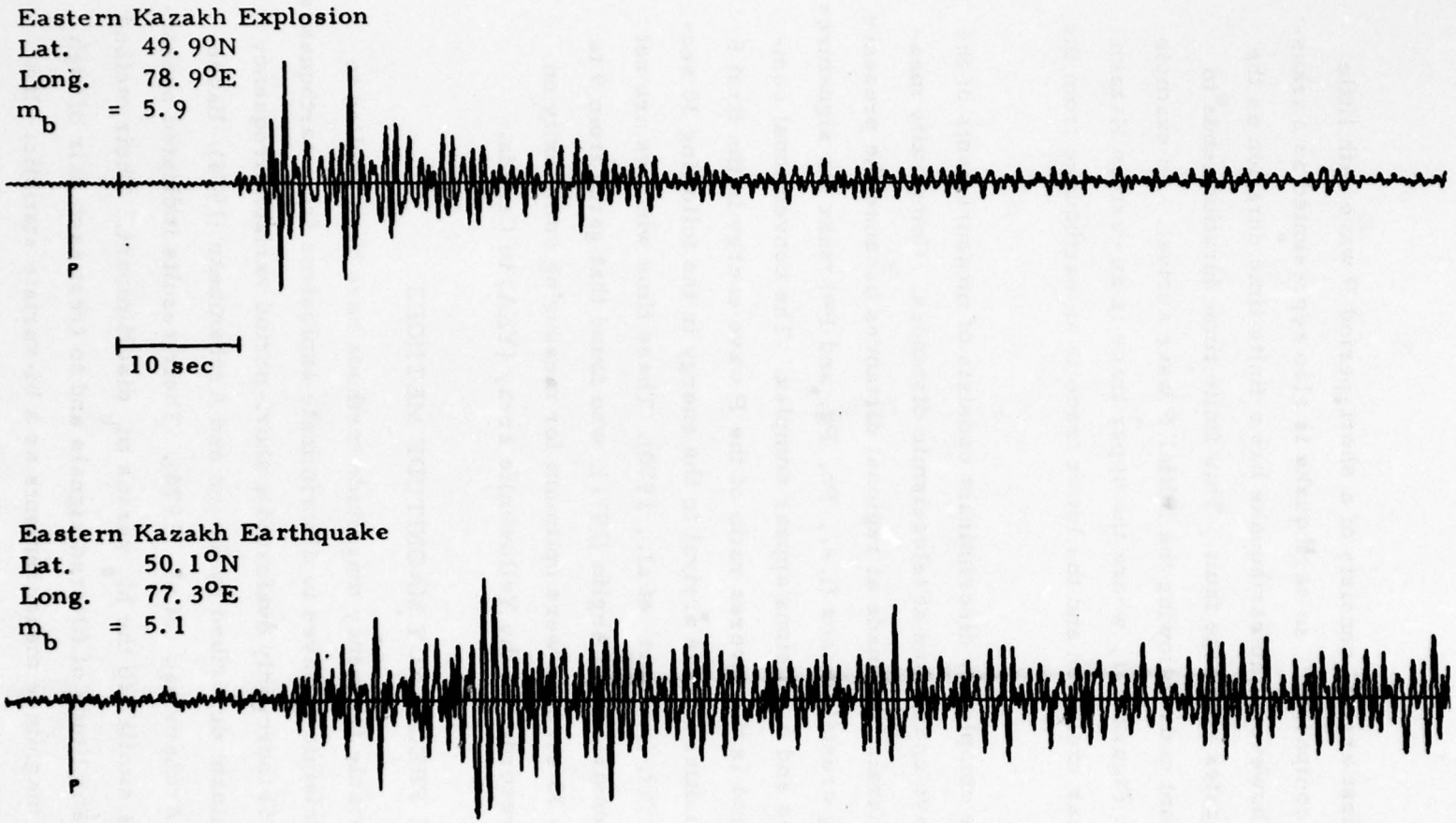

FIGURE II-1

P CODA FOR EASTERN KAZAKH EXPLOSION AND EARTHQUAKE
AS RECORDED AT MAIO

trend line is drawn through the earthquake population, then the distance of explosion coordinates from the earthquake trend line is approximately three quarters of a magnitude unit. The explosions are well separated from earthquakes by enhanced high frequency energy and by less low frequency energy. The effect of both of these changes is more normal displacement of the explosion points from the earthquake trendline.

Sax (1976) extended the variable frequency magnitude method to multivariate analysis of low and high frequency magnitude measurements and to the measured slope of the magnitude spectrum. The measurements of magnitudes at each frequency were reduced to a single variable which is independent of event size. This was done by subtracting from each high or low frequency magnitude measurement the average magnitude in the band between 1 Hz and 1.75 Hz. The resultant low frequency and high frequency magnitude and roll-off measurements were treated as single ten-dimensional vector measurements. A scalar mean and standard deviation was computed for each element of the vector to represent a 'normal' population of shallow earthquakes. To compute a discriminant 'z' vector, each unknown event vector measurement of magnitude and roll-off was reduced to a unit normal statistic by subtracting the mean and dividing by the standard deviation of the 'normal' earthquake population. The final step was to determine one or more mean z-discriminant vectors which point to explosion populations. In that way, each unknown z-discriminant vector is projected in the direction of vectors pointing toward known explosion populations. The results indicated excellent separation of NTS presumed explosions, eastern Kazakh presumed explosions, and shallow earthquakes. The vectors pointing toward NTS and eastern Kazakh presumed explosions were nearly orthogonal.

G. INSTANTANEOUS PHASE AND FREQUENCY MEASUREMENTS

The theoretical result that earthquakes tend, in general, to excite lower frequency radiation more efficiently than explosions from the same source region forms the basis for the mean instantaneous frequency discriminant. The mean instantaneous frequency has been studied in conjunction with the mean phase standard deviation by Unger (1978a). Used as a two-variate discriminant these parameters were found to significantly separate NORSAR single site recordings of Eurasian earthquakes and Russian presumed underground explosions.

It has been demonstrated that the presence of early secondary arrivals such as pP can be determined from rapid changes in the time series of instantaneous amplitude, phase, and frequency (Farnbach, 1975; Unger, 1976). The number of secondary arrivals may be quantized by measuring a regression analysis residue of the instantaneous phase time series, as described in Section III of this report, and by Unger (1978a). This residue is termed the phase standard deviation.

By plotting a measure of mean instantaneous frequency against the mean phase standard deviation for the first two seconds immediately following the P wave onset, Unger (1978a) found significant separation between populations of Russian presumed underground explosions, Eurasian earthquakes, and Nevada Test Site (NTS) underground explosions. Relative to the Eurasian earthquakes, the Russian presumed explosions exhibited both a higher dominant frequency and a greater number of early secondary signals as indicated by a larger mean phase standard deviation. In contrast, the NTS events showed near-monochromatic, low frequency waveforms, suggesting a lack of clearly defined early multiple signals.

The mechanism whereby Russian presumed explosions might exhibit more early multiple arrivals than Eurasian earthquakes or NTS explosions is not well understood. However, for the same data base, identical event classifications were independently obtained by Sax (1976).

SECTION III
MEASUREMENT OF EVENT IDENTIFICATION PARAMETERS

A. OVERVIEW OF THE MEASUREMENT PROGRAM

The purpose of this section is to describe the manner in which the various event identification parameters are measured on the data recorded at the individual stations. The program which performs these measurements, called TISSPROG, is described by Schmidt and Wilson (1978). This discussion will concentrate on those aspects of the program which deal with the event identification problem.

The concept underlying the creation of this program is that it is more efficient to make one computer run which will measure all desired event identification parameters than to run a series of programs each of which measures one parameter or a group of related parameters. The one-run approach minimizes the amount of time required to prepare for the computer run as well as the actual amount of computer time used. As an additional benefit, the one-run approach produces an output containing all desired measurements. Thus, the analyst is not required to spend time assembling the results of multiple computer runs before proceeding with his analysis. In the most general sense, the operation of the program is to compute necessary event parameters such as travel times, determine the type of measurements to be made for each input waveform, make these measurements, save the results in a manner suitable to the needs of the analyst, and repeat the procedure for the next selected event.

In order to minimize the amount of information to be input by the analyst, a number of parameters have been built into the program. These

parameters are:

- Station coordinates
- Station names (four-letter designators)
- Teleseismic P, S, LQ, and LR travel time equations
- Station tectonic classification - active, inactive, or rift
- Short-period noise magnitudes for the SRO and ASRO stations
- Short-period and long-period detection thresholds
- Veith and Clawson (1972) P factors for bodywave magnitude computation
- System response corrections
- Corner frequencies of short-period and long-period filters
- Empirical dispersion curve.

The purpose of each of these built-in parameters will be described in the course of this section.

The generalized flow of the event identification parameter measurement program is shown in Figure III-1. The basic parameters input to the program are date, origin time, and coordinates of the event (input parameter card) and station number, seismogram number, data type (SP or LP), channel number, type of waveform (P, S, or LR), and resample rate (seismogram cards), where one seismogram card is required for each waveform edit on the Area of Interest (AI) digital magnetic tape.

After opening and positioning the input AI tape and the output event waveform tape and discriminant tape, the program reads the event parameter card and the first seismogram card. (Other parameters such as depth and bodywave magnitude, if available, can be entered via the event

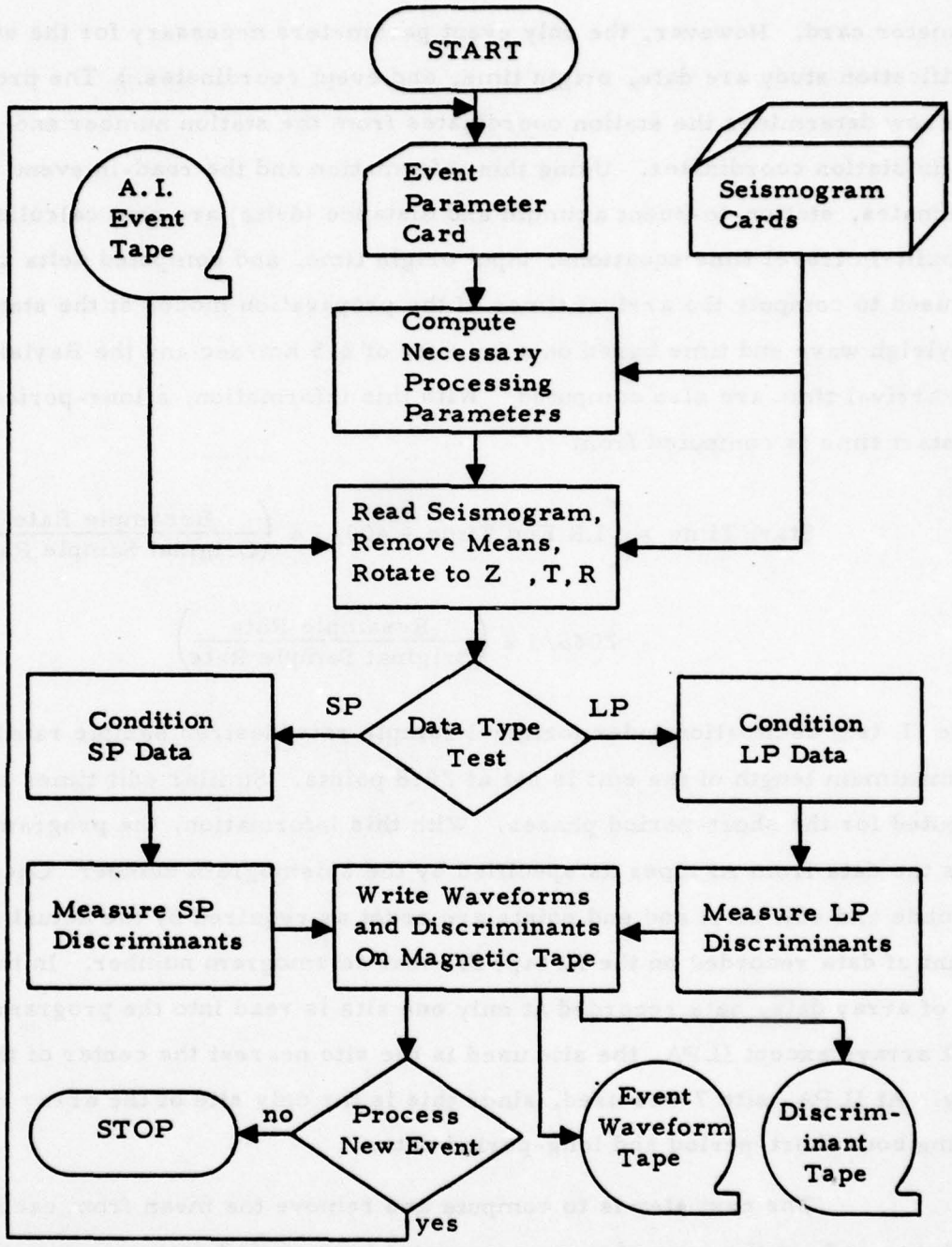

FIGURE III-1

GENERALIZED FLOW DIAGRAM OF THE EVENT IDENTIFICATION PARAMETER MEASUREMENT PROGRAM

parameter card. However, the only event parameters necessary for the event identification study are date, origin time, and event coordinates.) The program now determines the station coordinates from the station number and built-in station coordinates. Using this information and the read-in event coordinates, station-to-event azimuth and distance (delta) are next calculated. The built-in travel time equations, input origin time, and computed delta are then used to compute the arrival times of the propagation modes at the station. A Rayleigh wave end time based on a velocity of 2.5 km/sec and the Rayleigh wave arrival time are also computed. With this information, a long-period edit start time is computed from

$$\text{Start Time} = \left[\text{LR End Time} + 400/J * \left(\frac{\text{Resample Rate}}{\text{Original Sample Rate}}\right)\right] - 2048/J * \left(\frac{\text{Resample Rate}}{\text{Original Sample Rate}}\right)$$

where J is a decimation index (original sample rate/desired sample rate). The maximum length of the edit is set at 2048 points. Similar edit times are computed for the short-period phases. With this information, the program reads the data from AI tapes as specified by the seismogram number. Checks are made and edit start and end points are reset as required by the actual amount of data recorded on the AI tape for that seismogram number. In the case of array data, data recorded at only one site is read into the program. At all arrays except ILPA, the site used is the site nearest the center of the array. At ILPA, site 7 was used, since this is the only site of the array recording both short-period and long-period data.

The next step is to compute and remove the mean from each data trace and, in the case of three component long-period data, to rotate the data from its recorded vertical, north, east configuration to a vertical, transverse, radial configuration as determined by the computed azimuth. At this

point, the data are ready for the measurement stages of the program. The program therefore tests the input data type flag and directs the program flow toward the short-period or long-period data measuring algorithms as appropriate.

B. SHORT-PERIOD EVENT MEASUREMENT

The short-period discriminant measurement phase of TISSPROG proceeds as illustrated in Figure III-2. The short-period discriminant measurements are directed by a supervisory routine (subroutine SPEED), which directs control to each of the various discriminant measurement and data manipulation routines as required. In the case of magnitude measurements, only log (A/T) or log A values are calculated in SPEED. These values are then placed in the event header for magnitude calculation in subroutine FINISH.

1. Signal Processing Prior to Discriminant Measurements: Filtering, Signal Detection, Instrument Response Removal, and Edit Compression

The first step in the short-period discriminant measurement phase is to bandpass filter the input raw data trace over a broadband frequency range. This tends to subdue high frequency spikes (i. e., artifacts due to the instrumentation) and high frequency components in the data to avoid aliasing. Because the frequency interval is fairly broadband, a rectangular boxcar filter is used without risk of severe ringing problems. In the case of data sampled at 20 Hz, the filter cutoffs are 0. 3 Hz to 9. 9 Hz; where the data are sampled at 10 Hz, the filter cutoffs are set at 0. 3 Hz and 4. 9 Hz.

After the raw data trace has been filtered, the next step consists of running the automatic short-period signal detector described by Unger (1978a). The procedure for detecting and timing the onset of short-period signals is illustrated in Figure III-3. Over a previously specified

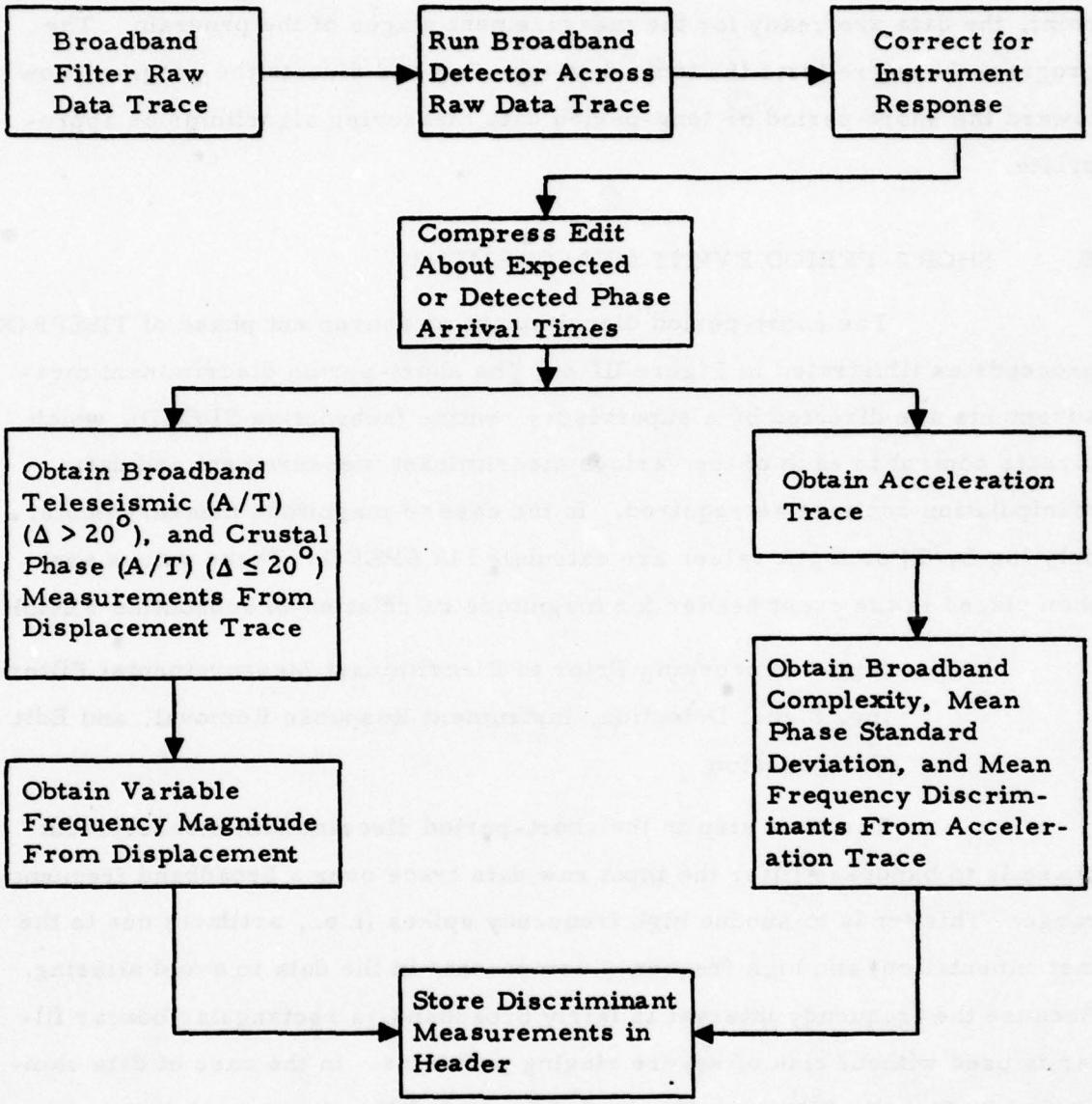

FIGURE III-2

SHORT-PERIOD DISCRIMINANT MEASUREMENT LOGIC FLOW

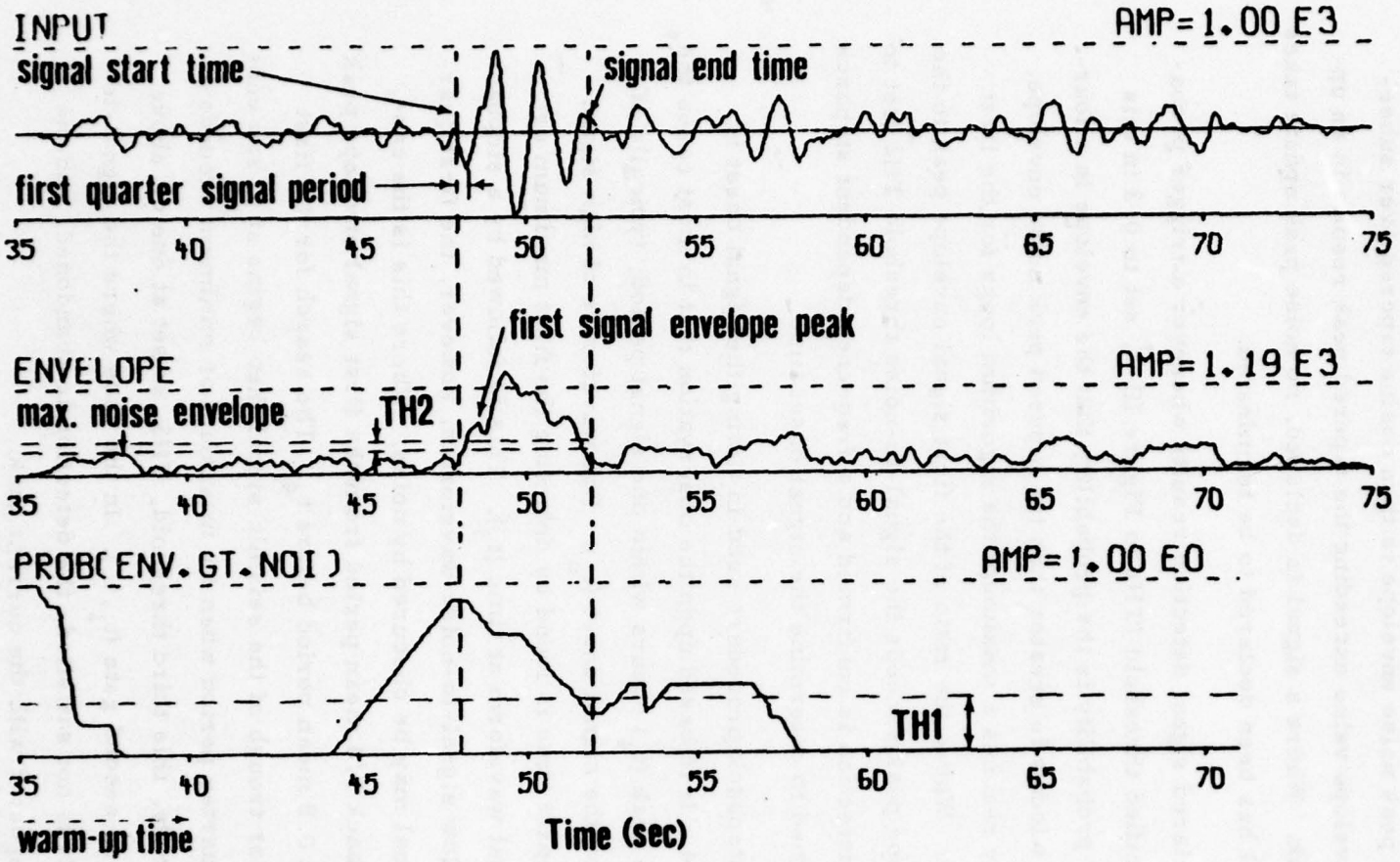

FIGURE III-3

SP SIGNAL DETECTION AND TIMING (Unger, 1978a)

warm-up time (10 seconds for events in this study), the peak noise envelope is established. The peak noise envelope is then cosine tapered over subsequent points. An envelope value exceeding the tapered peak results in an update in the noise peak. Where a signal is declared, no noise peak update takes place until the signal has been declared to be terminated.

A declared signal detection results whenever a trigger probability exceeds a specified threshold (TH1 in Figure III-3, set to 0.3 in this study). The trigger probability is the probability that the envelope in a four-second leading time window is greater than the tapered peak noise envelope. When this probability reaches a maximum the algorithm looks for the first signal envelope peak. Where the ratio of the first signal envelope peak to the tapered noise envelope peak exceeds the signal-to-noise threshold TH2 (set to 6.0 dB), the signal detection is confirmed and a frequency dependent stepback procedure is performed to determine the signal onset time.

The stepback procedure used in timing the signal onset is shown in Figure III-4. It is based upon the observation that in most cases the first signal envelope peak (t_4) occurs within one signal period, typically at about 3/4 period after the signal onset (t_o). For waveforms of high signal-to-noise ratio, the onset time is found by detecting the first maximum or minimum of the signal waveform at time (t_3). This is followed by a stepback of 1/4 period. For low signal-to-noise waveforms, however, the first quarter period of the signal may be obscured by noise. Where this is the case, the algorithm steps back 3/4 mean period from the first signal envelope peak (t_4) to the point t_2 at 0.8 mean period before t_4. The search for the first quarter period peak or trough of the seismic signal then begins at t_2 and ends as a detected first quarter period when its maximum or minimum exceeds a threshold. In this study, this third threshold, TH3, is set at one dB above the peak noise in a one second gate (t_1, t_2). In the case where the signal-to-noise threshold (TH2) is not satisfied, the detection is abandoned, and the noise peak value is updated with the current peak.

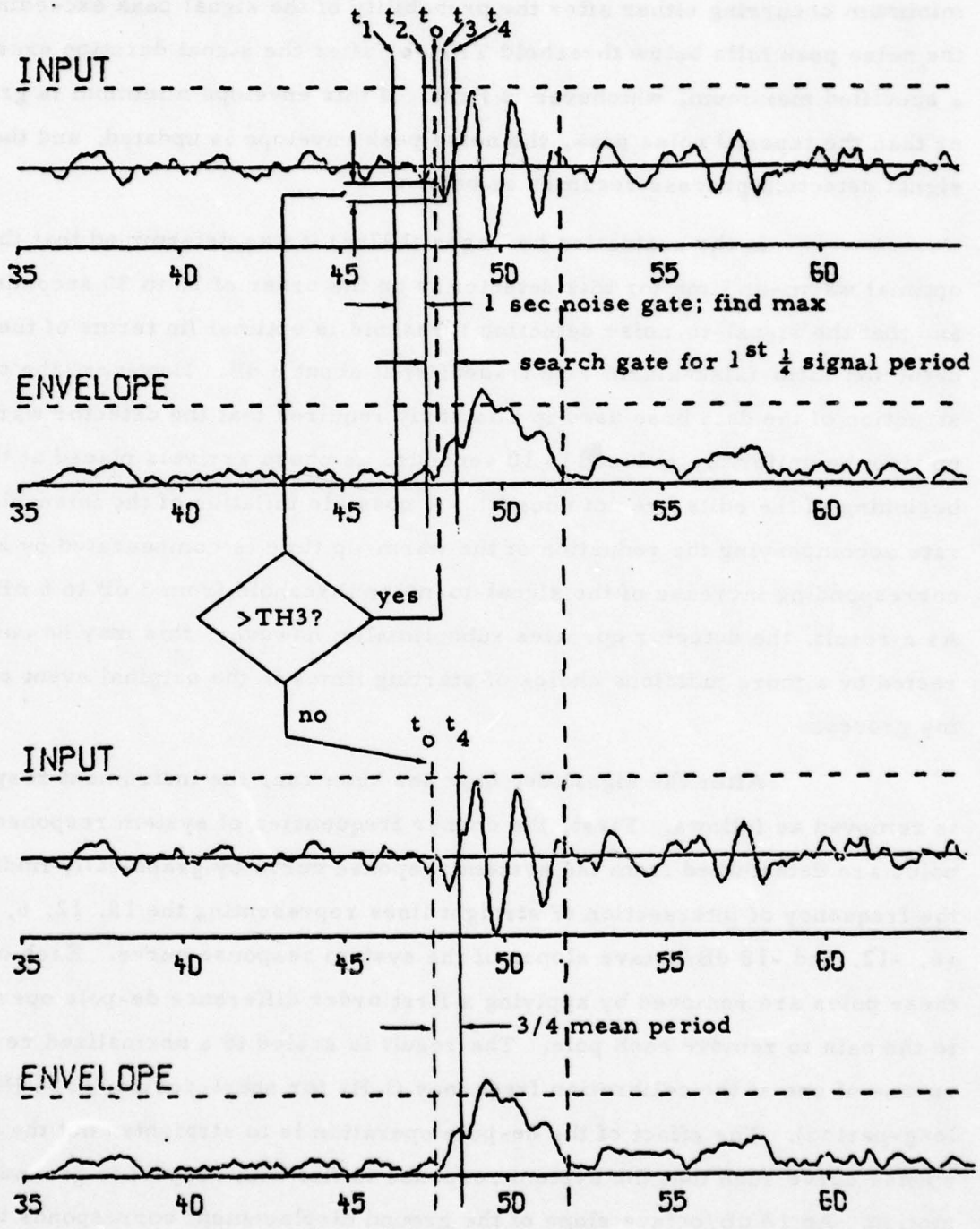

FIGURE III-4

STEPBACK PROCEDURE IN SP SIGNAL TIMING (Unger, 1978a)

The signal end time is taken as the moment of the first envelope minimum occurring either after the probability of the signal peak exceeding the noise peak falls below threshold THl, or after the signal duration exceeds a specified maximum, whichever is first. If this envelope minimum is greater than the tapered noise peak, the noise peak envelope is updated, and the signal detection process resumes as before.

In the evaluation by Unger (1978a) it was determined that the optimal warm-up time for this detector is on the order of 20 to 30 seconds, and that the signal-to-noise detection threshold is optimal (in terms of the detection ratio-false-alarm rate tradeoffs) at about 3 dB. However, the construction of the data base used in this study requires that the detector warm-up time be uniformly reduced to 10 seconds, as phase arrivals placed at the beginning of the edits are not unusual. A possible inflation of the false-alarm rate accompanying the reduction of the warm-up time is compensated by a corresponding increase of the signal-to-noise threshold from 3 dB to 6 dB. As a result, the detector operates suboptimally; however, this may be corrected by a more judicious choice of starting times in the original event editing process.

After the signal detector has been run, the instrument response is removed as follows. First, the corner frequencies of system response poles are determined from the system response curve by graphically finding the frequency of intersection of straight lines representing the 18, 12, 6, 0, -6, -12, and -18 dB/octave slopes of the system response curve. Each of these poles are removed by applying a first order difference de-pole operator to the data to remove each pole. The result is scaled to a normalized response of one at the calibration frequency (1 Hz for short-period, 0.04 Hz for long-period). The effect of the de-pole operation is to straighten out the response curve such that the system response is flat with respect to ground motion. An 18 dB/octave slope of the ground displacement corresponds to a

flat response to the first derivative of acceleration; a 12 dB/octave slope, to acceleration; a 6 dB/octave slope, to velocity; and a flat or 0 dB/octave slope, to displacement. Next, a set of narrowband filters are used to integrate the de-poled data in such a way as to yield a flat ground displacement response. Prior to application of the narrowband filters the de-poled data are bandpass filtered. For short-period data, the filter limits are between 0.16 Hz, the low -6 dB point of the first narrowband filter (centered at 0.3 Hz) and a frequency just below Nyquist frequency. For long-period data the limits are between 0.010 and 0.117 Hz. Integration of the data trace is approximated by narrowband filtering the data and summing the scaled results. The number of filters used depends on which poles have been removed from the data, that is on the slope of the de-poled data. For example, if the de-poled data has a slope of 18 dB/octave, which corresponds to the first derivative of acceleration, three integrations, therefore, three filters, would be necessary in order to correct the data to ground displacement. For short-period data, the first and lowest filter is centered at a $\log_{10}$ frequency of -0.7 and subsequent filters are spaced at increasing $\log_{10}$ frequencies in 0.2 increments. The effective bandwidth, the width between the -6 dB points, of the filters are 0.452 times the center frequency which allows the -6 dB points of the filters to just overlap. The filtered data are scaled to be one at 1 Hz. For long-period data the filters start with a $\log_{10}$ center frequency of -1.70 and subsequent filters are centered at even intervals of 0.10 in log frequency. The effective bandwidth is 0.222 times the center frequency. This again allows the -6 dB points to overlap. The filtered data are scaled to be one at 0.04 Hz. In both cases, the resultant scaled output for all the filters is then summed and added to the broadband filtered data which has had poles put in at each of the high -6 dB points of the filters. A pole, $1/|1-z|$, is approximated by $1/|1-\alpha z|$ where z is the delay operator $e^{-i\omega t}$ and α is the reflection coefficient. The poling operation is also scaled to be one at the previously stated frequencies for short- and long-period data.

In summary, the first order real poles and zeros used to represent the system response by fitting the amplitude response curve are removed by stable inverse operators with a normalized response of one at the calibration frequencies. To avoid round-off errors in the inverse of the zeros $(1-z)^N$ (6N dB/octave response), the low frequency response is synthesized by adding appropriately scaled narrowband filters which were demonstrated to pass the signal without seriously distorting the amplitude of signals. Frequencies above the bank of low frequency filters are flattened by inverting $(1-\alpha z)^N$ which has a stable inverse. The corner of the inverse $(1-\alpha z)^{-N}$ was designed to coincide with the corner of the highest frequency narrowband filter. The total inverse was obtained by adding the high-pass inverse output to the properly scaled narrowband filter outputs. The total inverse was designed to be accurate to approximately 0.1 magnitude units. This method was designed to avoid the large drift-errors commonly associated with the N-fold (N usually 3) integrations of the data required to derive ground displacements. Although the method appeared to work satisfactorily with the few examples examined, more data needs to be examined to verify this method since it is a critical step in obtaining accurate frequency dependent magnitude measurements.

In order to avoid storage of unnecessary amounts of noise data on the output event tapes and to facilitate analyst checking of automatic detections, it was found desirable to compress the short-period edit lengths. In the case of P and S wave edits, the edit length is shortened to 51.2 seconds. For those events where the short-period broadband detector is triggered, the edit is centered on the detected phase arrival time. For non-detected events, the edit is centered about the expected phase arrival time, determined by a linear fit to the Jeffreys-Bullen travel time curves in the distance range of interest. In the case of Lg edits, where the short-period broadband detector does not trigger, the edit is centered about the point corresponding to an

average source-receiver velocity of 3.6 km/sec. Edit compressions for both detections and non-detections are illustrated schematically in Figure III-5.

During the edit compression, several checks are performed to ensure that the proposed compressed edit is at least partially contained within the original edit. This allows for a limited amount of recovery in the event that insufficient data are supplied on the original edit tapes by further shortening the compressed edit. For events where the broadband detector is triggered, at least 10 seconds of data must be available before, and 25.6 seconds of data must be available after the detected phase arrival time. Where no detection occurs, at least 25.6 seconds of data must be available beginning at the expected phase arrival time.

In the event that fitting a compressed edit is not possible, the event in question is flagged unavailable, and processing skips to the next event.

After edit compression is completed, certain locations in the event header pertaining to edit status (*i.e.*, the edit start time, edit length, and detected phase arrival time) are updated. This is the last step of the edit compression.

2. Measurement of Broadband Complexity, Mean Phase Standard Deviation and Maximum Mean Frequency

Acceleration data are obtained by differentiating the displacement trace. At this point, a broadband complexity discriminant is obtained for teleseismic events (delta > 20 degrees). The complexity is computed as the ratio of the area under the complex envelope in the first 10 seconds immediately after signal onset to the area under the envelope in the first 5 seconds. This measure is used instead of the standard definition given in Section II in order to minimize path scattering effects which appear for longer time windows, and to reduce the bias arising from the inclusion of large

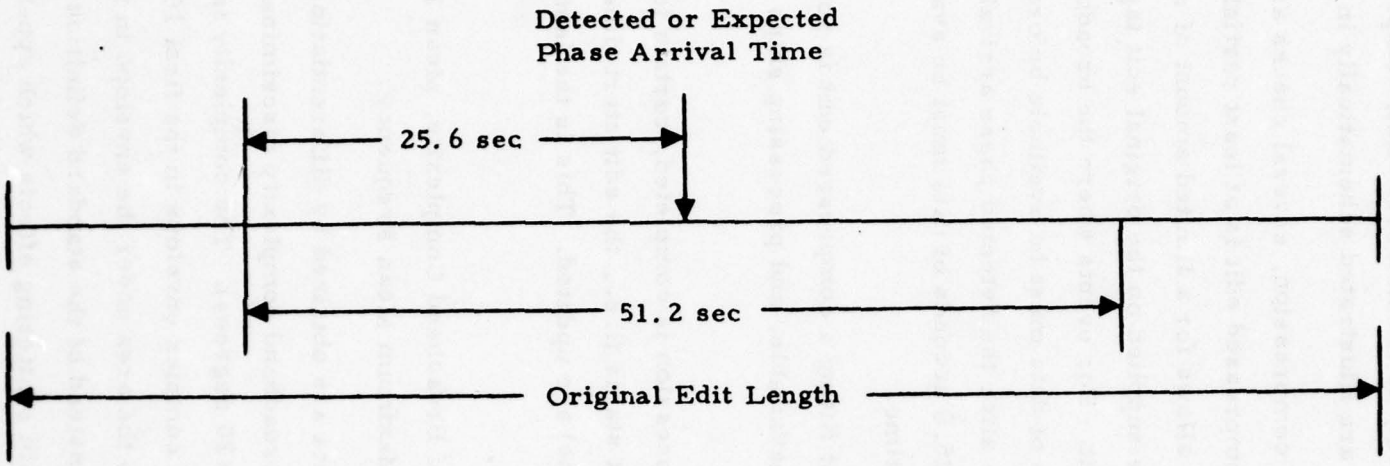

FIGURE III-5

SCHEMATIC ILLUSTRATION OF SHORT-PERIOD EDIT COMPRESSION

noise contributions, especially for smaller events. Two additional discriminants, maximum mean frequency and mean phase standard deviation are also measured from the acceleration trace. These discriminants are discussed in some detail by Unger (1978a), and in Section II.

Both the maximum mean frequency and the mean phase standard deviation are obtained from the quadratic regression estimate of the continuous instantaneous phase. An arbitrary time signal, x(t), may be written in terms of its envelope, $E_x(t)$, and its unwrapped instantaneous phase, $\phi_x(t)$, as (Whalen, 1971):

$$x(t) = E_x(t) \cos \phi_x(t) \qquad \text{(III-1)}$$

where

$$E_x(t) = (x^2(t) + \hat{x}^2(t))^{\frac{1}{2}}$$

$$\phi_x(t) = \tan^{-1} \hat{x}(t)/x(t) .$$

Here, $\hat{x}(t)$ is the Hilbert transform of $x(t)$, given by

$$\hat{x}(t) = PV \int_{-\infty}^{\infty} \frac{x(\tau)}{\pi(t-\tau)} \, d\tau ,$$

where

'PV' denotes the Cauchy principal value.

To obtain the maximum mean frequency and mean phase standard deviation, a quadratic regression is performed to fit the instantaneous phase with a quadratic polynomial within a window of given length (Unger, 1978a):

$$\hat{\phi}_x(t, \tau) = a_o(t) + a_1(t)\tau + a_2(t)\tau^2$$

where

t is the window start time

τ is the time relative to the start of the window

$\hat{\phi}_x(t, \tau)$ is the estimated instantaneous phase at time τ for the window starting at time t

$a_o(t), a_1(t), a_2(t)$ are the regression coefficients for the window beginning at time t.

In the regression process, $\hat{\phi}_x(t)$ is fit to the unwrapped instantaneous phase, $\phi_x(t, \tau)$, under a minimum mean-squared error criterion. The window is then stepped ahead one sample and a new regression is performed. A 4 second window is used in this study. The phase standard deviation for each window is given by:

$$\sigma_\phi(t) = \left\{ \sum_{i=1}^{L} \left[\phi(t, \tau_i) - \hat{\phi}(t, \tau_i) \right]^2 / (L-3) \right\}^{\frac{1}{2}} ,$$

where L is the length of the window in samples. The time variant mean phase is defined as the regressed phase, evaluated at the center of each window ($\tau = L/2$):

$$\bar{\phi}_x(t + L/2) \triangleq \hat{\phi}_x(t, L/2) = a_o(t) + a_1(t) L/2 + a_2(t) L^2/4. \quad \text{(III-2)}$$

The time variant mean frequency is then found by differentiating equation (III-2) with respect to τ, and evaluating at $\tau = L/2$:

$$\bar{f}(t + L/2) = \left[a_1(t) + L a_2(t) \right] / 2\pi.$$

The broadband complexity, mean frequency, and mean phase standard deviation are only obtained if the broadband signal detector is triggered. Where no detection is declared, the measurement of these quantities is bypassed and a null operation flag is set for that particular event-station combination.

3. Short-Period Magnitude Measurements

Several short-period magnitude estimates are obtained in the course of short-period event processing. For teleseismic events ($\Delta > 20^{\circ}$), a broadband m_b and several variable frequency magnitudes (VFM) are calculated. These are scaled using the Veith and Clawson (1972) P-factors. In addition, where data are available for regional events, crustal Pn, Sn, and Lg magnitudes are calculated according to the following formulas:

$$\left.\begin{aligned} m_{Pn} &= 3.82 + 2.00 \log\Delta + \log (A/T) \quad \text{(Evernden, 1967)} \\ m_{Sn} &= 3.79 + 1.80 \log\Delta + \log (A/T) \quad \text{(Fitch et al., 1978)} \\ m_{Lg} &= 3.30 + 1.66 \log\Delta + \log (A/T) \quad \text{(Nuttli, 1973).} \end{aligned}\right\} \text{(III-3)}$$

The logic flow for the broadband amplitude and period measurement is shown in Figure III-6. The first step consists of several quality control checks concerning the availability of a short-period edit and the consistency of the desired measurements with available data. For example, checks are made to ensure that regional phase measurements are not performed on teleseismic data, and that the supplied data falls, at least partially, within the following velocity windows:

Pn	:	8.3 km/sec - 5.0 km/sec
Sn	:	5.0 km/sec - 3.8 km/sec
Lg	:	3.8 km/sec - 2.4 km/sec
Teleseismic P:		15.0 km/sec - 8.0 km/sec.

If these checks are not passed, control returns to the supervisory routine.

If the checks are passed, a 5 percent cosine taper is applied to the beginning and end of the data series. The series is then broadband

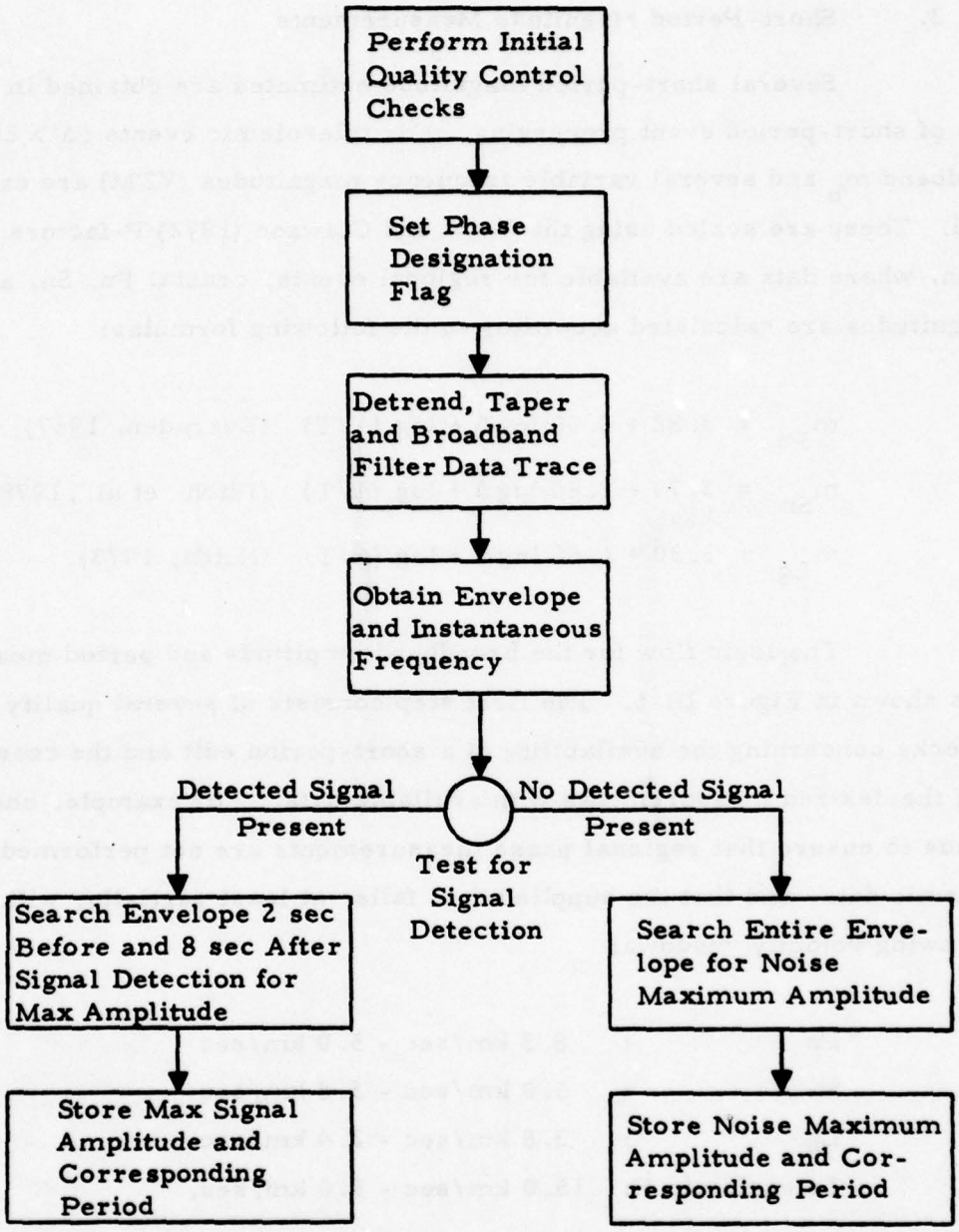

FIGURE III-6

BROADBAND SHORT-PERIOD (A/T) MEASUREMENT LOGIC FLOW

filtered between 0.3 Hz and one-half the Nyquist frequency. Broadband filtering is performed by an eighth order Butterworth filter.

After the data trace has been filtered, the signal envelope and instantaneous frequency are generated. The signal envelope is given in equation (III-1), where the Hilbert transform is calculated in the frequency domain using the relation:

$$\hat{x}(f) = -i \, \mathrm{sgnf} \, x(f) \ ,$$

where sgnf is the 'signum' operator defined by

$$\mathrm{sgnf} = \begin{cases} 1 & f > 0 \\ 0 & f = 0 \\ -1 & f < 0 \ . \end{cases}$$

The instantaneous frequency is obtained by evaluating the derivative of the instantaneous phase in closed form from equation (III-3):

$$x(t) = E_x(t) \cos \phi_x(t)$$

where

$$\phi_x(t) = \tan^{-1} \hat{x}(t)/x(t) \ .$$

Since the instantaneous frequency f(t) is related to the instantaneous phase by

$$\phi_x(t) = 2\pi \int f(t)dt,$$

then

$$\frac{d}{dt}\left(\phi_x(t)\right) = 2\pi f(t) .$$

Substituting the expression for $\phi_x(t)$ given in equation (III-1) and differentiating with respect to t :

$$\frac{d}{dt}\left(\phi_x(t)\right) = \frac{d}{dt}\left(\tan^{-1} \hat{x}(t)/x(t)\right)$$

$$= \frac{x(t)\frac{d\hat{x}(t)}{dt} - \hat{x}(t)\frac{dx(t)}{dt}}{E_x^2(t)} = 2\pi f(t). \qquad \text{(III-4)}$$

The expression in equation (III-4) has the advantage that it may be calculated without first unwrapping the instantaneous phase. A difference operator is used to approximate $dx(t)/dt$ and $d\hat{x}(t)/dt$.

After the envelope and instantaneous phase have been obtained the envelope is searched for the maximum amplitude of signal or noise. Whether it is signal or noise is determined by whether the broadband detector was triggered or not. If the detector was not triggered, the entire envelope is searched for a noise peak, $\log_{10} A_{max}/T$ is calculated where A_{max} is the maximum of the noise envelope and T is the corresponding period determined from the instantaneous frequency, and this value is stored in the event header. Where the detector was triggered the envelope is searched in a 10 second gate, beginning 2 seconds before the detected signal onset time. Again, $\log_{10} A_{max}/T$ is calculated for the signal peak, and this value is stored in the event header. The $\log A_{max}/T$ values are later scaled to teleseismic or regional crustal phase magnitudes using the formulas given in equation (III-3).

In addition to the broadband magnitudes, short-period variable frequency magnitudes (VFM) are also generated. The VFM measurement logic flow is illustrated in Figure III-7.

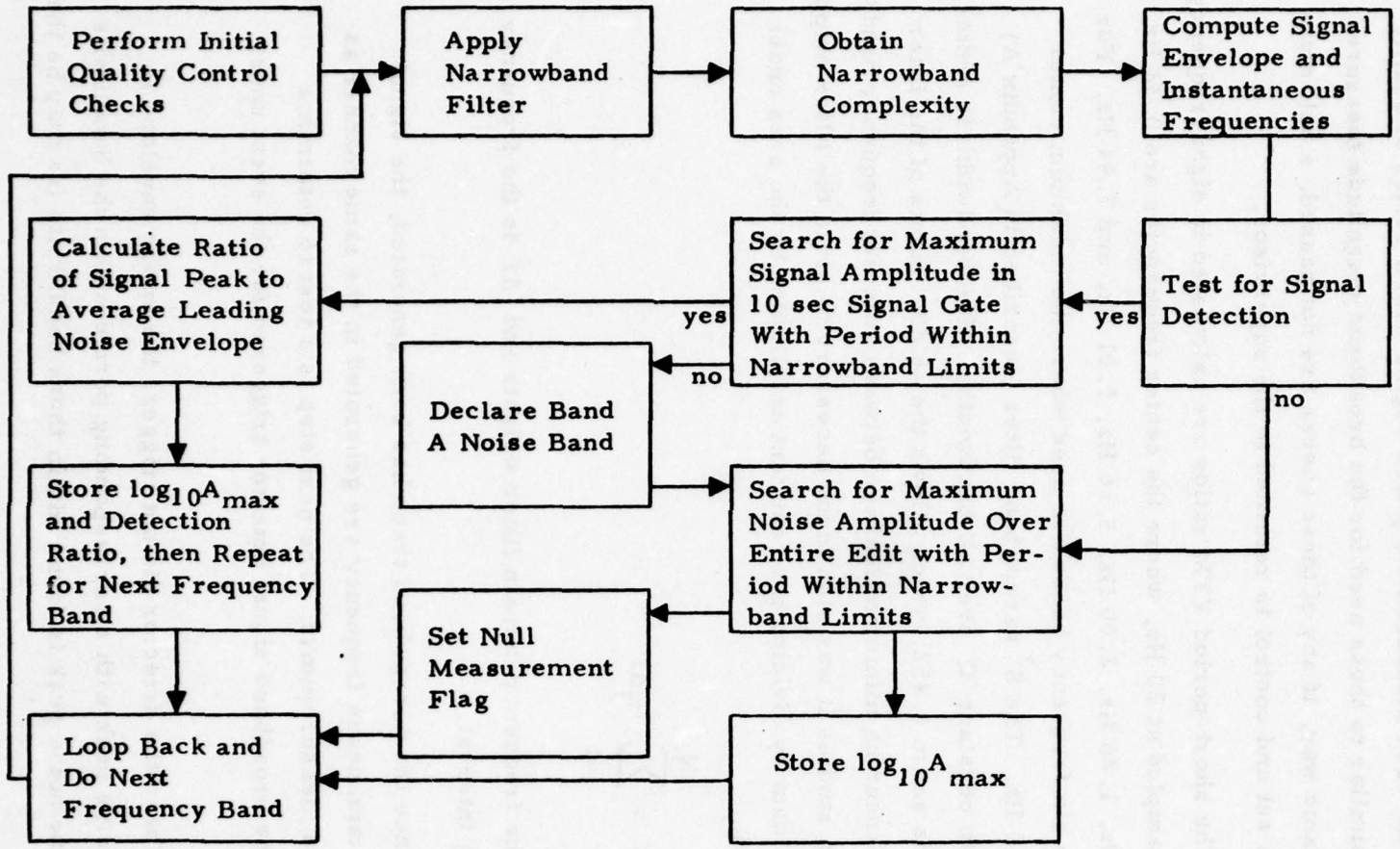

FIGURE III-7

SHORT-PERIOD VARIABLE FREQUENCY MAGNITUDE (VFM) MEASUREMENT LOGIC FLOW

The VFM measurement phase begins with a series of quality control checks similar to those used for the broadband magnitude measurements. In the same way, if any of these checks are not passed, a null measurement flag is set and control is returned to the supervisor.

The short-period VFM ratios are calculated in eight frequency bands for data sampled at 20 Hz, where the center frequencies are 0.32 Hz, 0.50 Hz, 0.79 Hz, 1.26 Hz, 2.00 Hz, 3.16 Hz, 5.01 Hz, and 7.94 Hz. For 10 Hz data, only six frequency bands are used where the maximum center frequency is 3.16 Hz. The S^3 narrowband filter (described in Appendix A) is used, scaled to constant Q over all bandwidths. The bandwidth to center frequency ratio is set to 0.452, which allows the -6 dB points of the filter to just overlap, ensuring minimum leakage between adjacent frequency bands. From calibration studies it was also found necessary to scale the filter output for short-period data by dividing the resultant amplitudes by the area under the filter, given by

$$W = \sum_{j=1}^{N} H_j \Delta f$$

where H_j are the frequency domain filter weights and Δf is the frequency domain sampling interval.

Once the narrowband trace has been generated, the signal envelope and instantaneous frequency are generated in the same manner as for the broadband measurements. The next step is a test to determine whether or not the broadband signal detector triggered for the event under consideration.

Where the detector did not trigger, the entire envelope is searched for a noise peak with a corresponding period within the bandlimits of the filter. If no noise peak is found within those bandlimits (as may be the

case, due to leakage of strong peaks from adjacent frequency bands) a null measurement flag is set and processing continues with the next frequency band.

If a noise peak with a corresponding period within the filter bandlimits is found, $\log(A_{max})$ is calculated where A_{max} is the maximum noise amplitude. This value is then stored in the event header, flagged as a noise measurement.

Where the broadband signal detector did trigger, the envelope is searched for a maximum in a 10 second window starting 2 seconds prior to the signal onset time. If no signal peak with a corresponding period within the filter bandpass is found, the frequency band is declared a noise band and a noise measurement is attempted as described previously. If a signal peak is found, then a detection ratio is calculated for that frequency band by taking the ratio of the peak signal envelope to the average noise envelope in whatever leading noise window is available. The $\log_{10}(A_{max})$ for the signal peak is then calculated and stored in the event header, together with the detection ratio, and processing proceeds to the next frequency band.

As in the case of the broadband magnitude measurements, the $\log_{10}(A_{max})$ values for the VFM are scaled to magnitude using the formulas given in equation (III-3). An additional threshold test is employed for each frequency band, where the signal envelope peak to average noise envelope ratio is tested. The purpose of this test is to avoid indiscriminant signal declarations in frequency bands which are dominated by noise. In order to maintain signal status, the signal envelope peak must exceed the average noise envelope by at least 10 dB. Otherwise, the measurement in that band is treated as noise.

In addition to measuring magnitudes in the narrow frequency bands, a narrowband complexity measurement is also made in each frequency

band. This measurement is only made when the broadband detector is triggered, and is carried out in a manner similar to that used in obtaining the broadband complexity.

C. LONG-PERIOD EVENT MEASUREMENTS

The long-period discriminant processing segment of TISSPROG consists of two parts. The first part involves removal of the instrument response, which is identical to the procedure used to correct for the instrument response for short-period data. The second part consists of the timing of the long-period phases and the measurement of the long-period VFM. This is illustrated schematically in Figure III-8.

Because no long-period signal detector is available to operate reliably on long-period data without a priori specified dispersion data and because the events in the test data base may exhibit vastly different dispersion characteristics as a result of the numerous different travel paths to various stations, an alternate method of long-period signal timing and detection is needed. To deal with this problem, broad-region dispersion models composed by Unger (1978b) are used. These models are based upon group velocity data obtained by Sun (1977). The group velocity data consist of recordings at a variety of stations of eastern Kazakh (EKZ) and Nevada Test Site (NTS) presumed nuclear explosions. For these events, it is possible to define an exponentially modulated group velocity window for any frequency of interest, as shown in Figure III-9 for NTS events and Figure III-10 for EKZ events. Although the group velocity windows are of necessity quite broad, they do prove to be useful in timing the long-period Love and Rayleigh phases.

Because most events in the test data base originate in the Asian continent, and to minimize the problem of running off the ends of the supplied long-period edits, the eastern Kazakh timing function is used in this study.

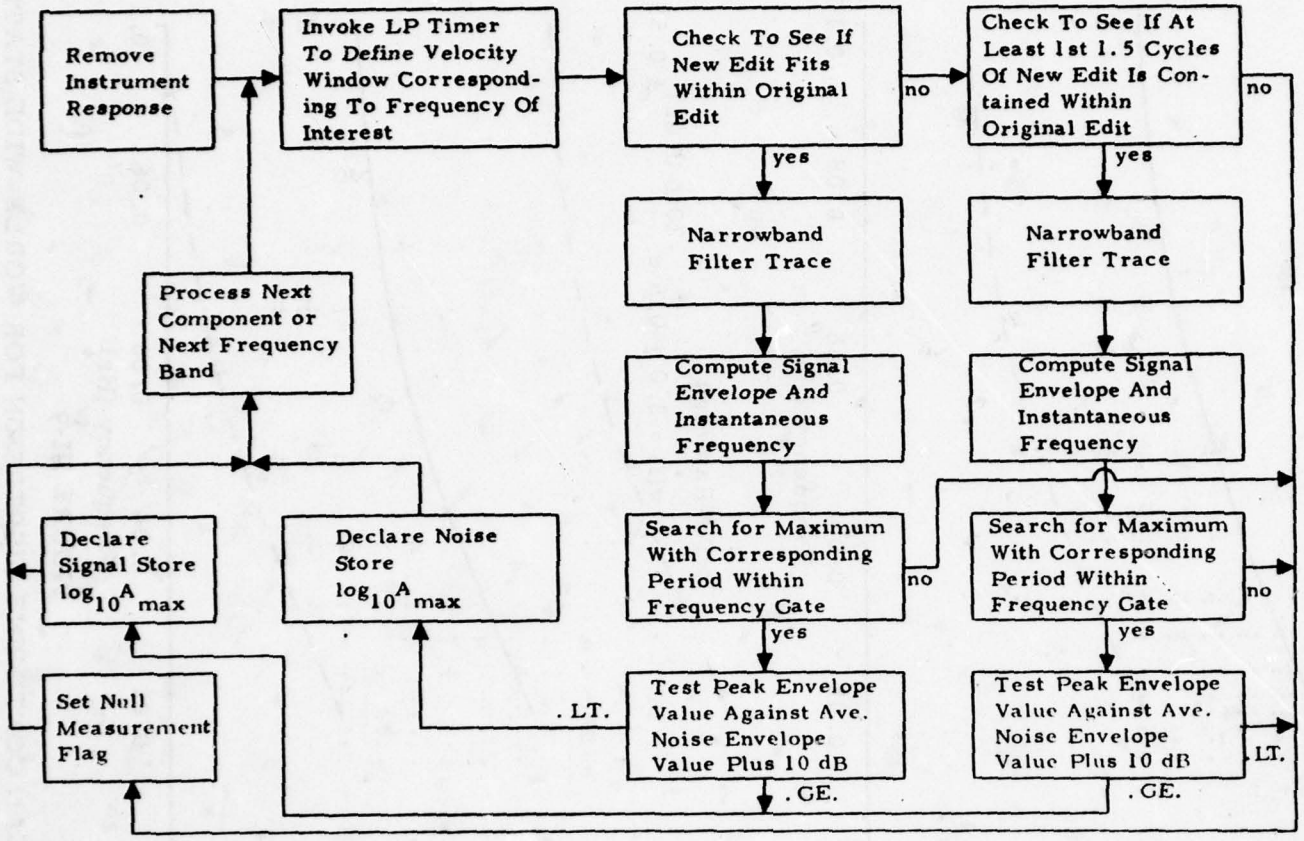

FIGURE III-8

LONG-PERIOD VARIABLE FREQUENCY MAGNITUDE MEASUREMENT LOGIC FLOW

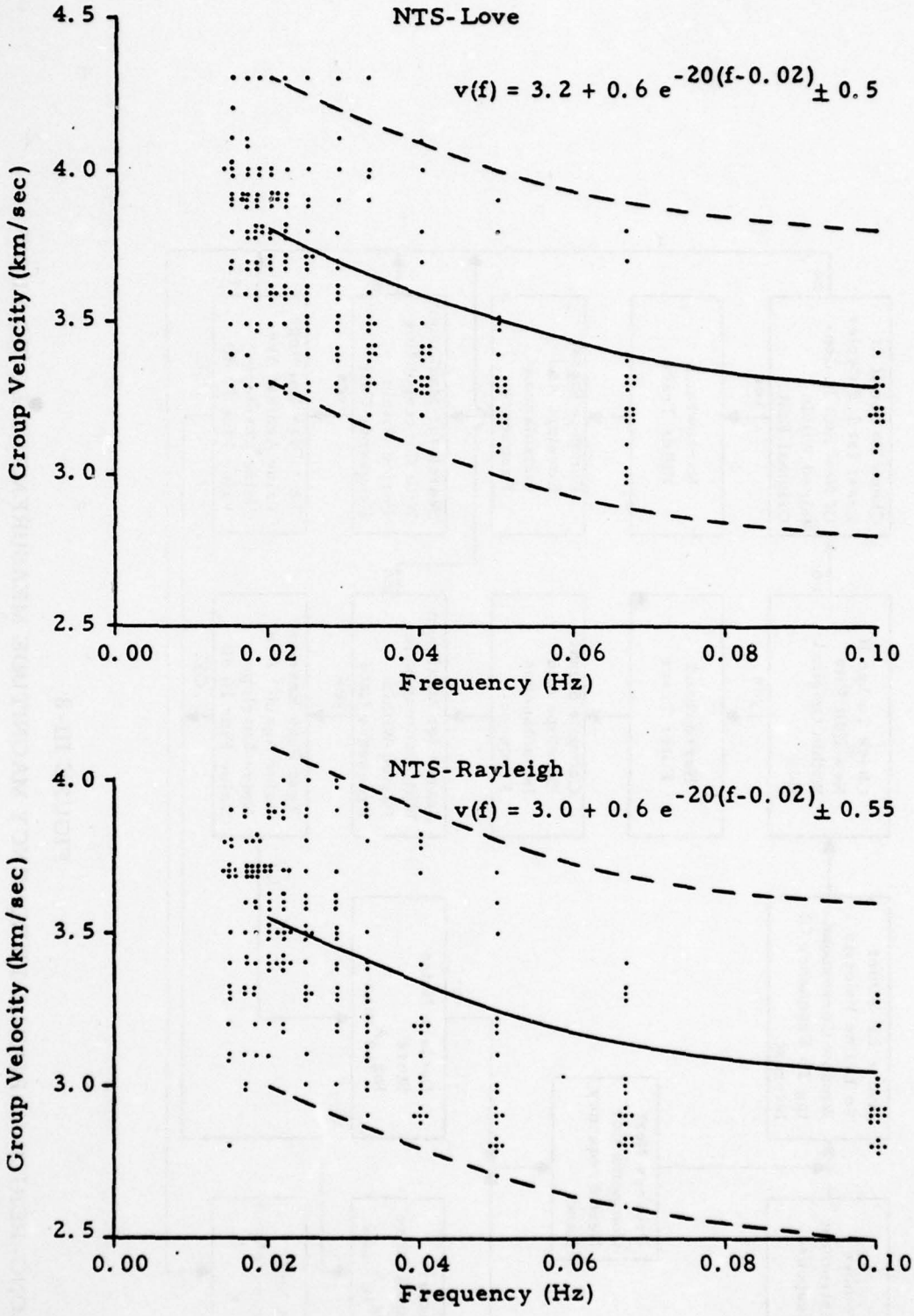

FIGURE III-9

NORTH AMERICAN CONTINENT DISPERSION FOR WORLD-WIDE STATIONS
(Unger, 1978b)

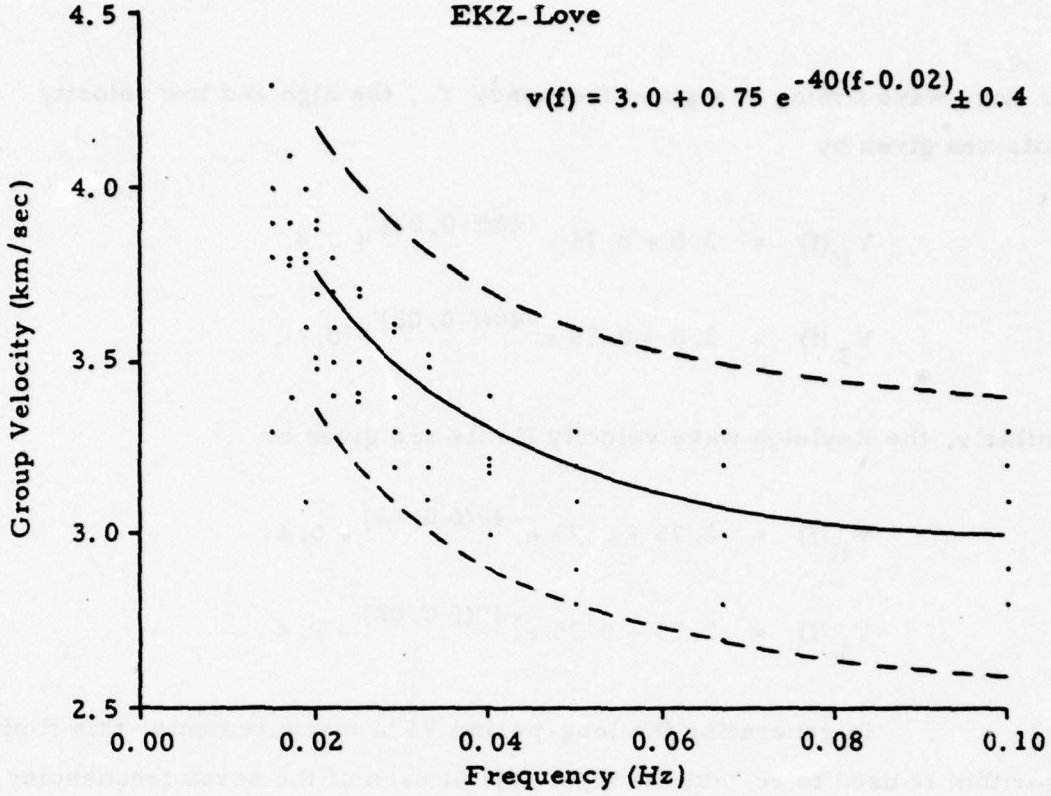

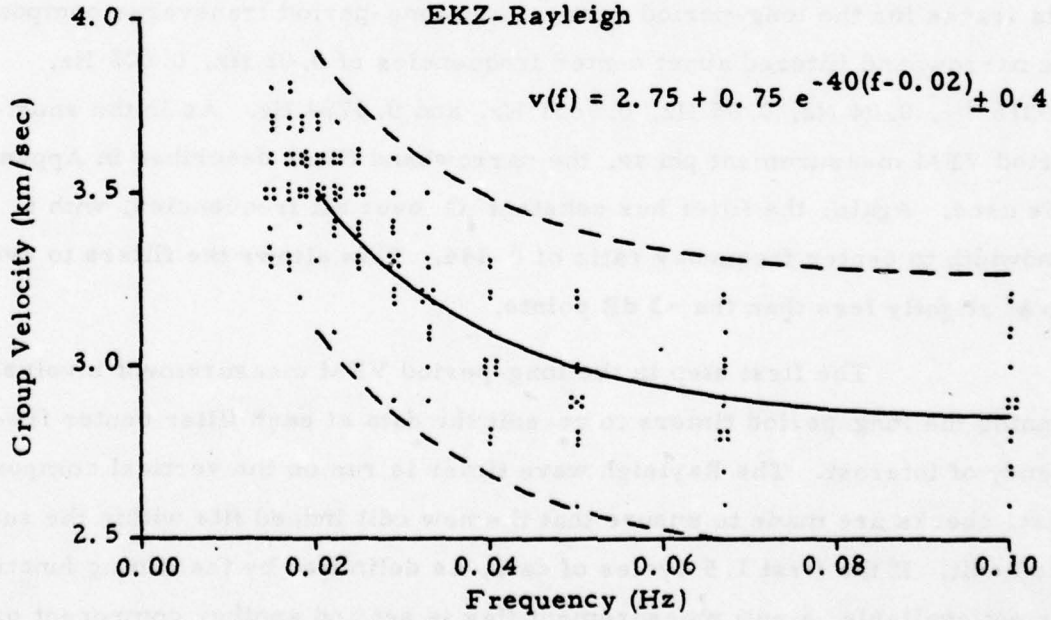

FIGURE III-10

ASIAN CONTINENT DISPERSION FOR WORLD-WIDE STATIONS
(Unger, 1978b)

For Love wave timing at a given frequency f , the high and low velocity limits are given by

$$V_H(f) = 3.0 + 0.75\, e^{-40(f-0.02)} + 0.4$$

$$V_L(f) = 3.0 + 0.75\, e^{-40(f-0.02)} - 0.4 .$$

Similarly, the Rayleigh wave velocity limits are given by

$$V_H(f) = 2.75 + 0.75\, e^{-40(f-0.02)} + 0.4$$

$$V_L(f) = 2.75 + 0.75\, e^{-40(f-0.02)} - 0.4 .$$

In generating the long-period VFM measurements, this timing algorithm is used to re-edit the input data at each of the seven frequencies of interest. In a manner similar to the short-period VFM measurements, the data traces for the long-period vertical and long-period transverse components are narrowband filtered about center frequencies of 0.02 Hz, 0.025 Hz, 0.0316 Hz, 0.04 Hz, 0.05 Hz, 0.0631 Hz, and 0.0794 Hz. As in the short-period VFM measurement phase, the narrowband filter described in Appendix A is used. Again, the filter has constant Q over all frequencies, with a bandwidth to center frequency ratio of 0.444. This allows the filters to overlap at slightly less than the -3 dB points.

The first step in the long-period VFM measurement involves running the long-period timers to re-edit the data at each filter center frequency of interest. The Rayleigh wave timer is run on the vertical component. Next, checks are made to ensure that the new edit indeed fits within the supplied edit. If the first 1.5 cycles of data, as delimited by the timing function, are not available, a null measurement flag is set and another component or

another frequency band is processed. If the first 1.5 cycles of data or more are available, the trace is re-edited with up to 400 seconds of leading noise included, and then narrowband filtered, and the signal envelope and instantaneous frequency are computed in a manner identical to that used in the short-period VFM measurement phase.

The next step consists of a search for the peak in the signal envelope (not including the leading noise portion) with a corresponding period within $\frac{1}{2}$ the bandwidth either side of the center frequency. Where no signal peak is found, a null measurement flag is set and processing proceeds to the next component or next frequency band. Where a signal peak is found, a detection ratio of the signal envelope peak to the average noise envelope is formed. This ratio is then tested against a 10 dB threshold. Where the detection ratio exceeds the threshold, a signal is declared, and $\log_{10}(A_{max})$ is computed, where A_{max} is the peak signal amplitude. This value is placed in the event header and is later scaled to magnitude.

For edits wholly contained within the supplied signal edits, where the detection ratio fails to exceed the threshold, the measurement is declared noise and $\log_{10}(A_{max})$ is computed and placed in the event header, where A_{max} is now the peak noise amplitude. In the case of short edits (i.e., edits not wholly contained within the supplied signal edit), a null measurement flag is set and processing proceeds to the next component or next frequency band. The reason this is done instead of declaring a noise measurement is to avoid the possibility of declaring a noise measurement for a given event where a large signal would have been present had the entire edit been obtained. This eliminates the possibility of assigning a low noise estimate to what would have been a large detected signal had the edit been complete.

In addition to the individual VFM magnitudes, an analogue to a broadband M_s is developed by taking the maximum of the long-period

vertical VFM measurements. This is then incorporated into the standard $M_s - m_b$ discriminant.

The formulas used in scaling long-period log(A/T) to magnitude are given by Nuttli and Kim (1975) for Eurasian earthquakes and explosions:

$$M_s = \log_{10}(A/T) + 0.89 \log_{10}\Delta + 1.34 \qquad \Delta < 10^\circ$$

$$M_s = \log_{10}(A/T) + 1.07 \log_{10}\Delta + 1.16 \qquad 10^\circ \leq \Delta \leq 25^\circ$$

$$M_s = \log_{10}(A/T) + 1.66 \log_{10}\Delta + 0.34 \qquad \Delta > 25^\circ \ .$$

D. EXAMPLES OF SHORT-PERIOD AND LONG-PERIOD EVENT MEASUREMENT

In this subsection, two examples are presented which illustrate the typical processing of short-period and long-period records. The event processed is an earthquake which occurred in eastern Russia:

Date	:	1 November 1977
Origin time	:	03:54:24
Latitude	:	55.3°N
Longitude	:	130.8°E
m_b (NEIS)	:	4.5
Depth (NEIS):		33 km.

The short-period data used here were recorded at Bluff, Alaska (BFAK). The long-period data were recorded at the ASRO site at Kabul, Afghanistan (KAAO).

1. Example of Short-Period Event Measurement

The computer output for the short-period event measurement example is shown in Figure III-11. The first step consists of reading the input seismogram card to identify the event to be processed (Figure III-11a). The data are fetched in segments of 128 points, decimated if desired, and the power within each segment is computed. After the data trace has been fetched, the broadband short-period detector is applied to the data as described in Subsection III-B. Next, the system response is removed as described in Subsection III-B (Figure III-11b). The edit is then compressed about the detected (broadband) phase arrival if the detector has triggered, or about the expected phase arrival if the detector has not triggered (Figure III-11c). A plot showing the original edit for this example, together with the detected phase arrival time and the 51.2 second compressed edit is shown in Figure III-12.

After edit compression has been completed, acceleration and displacement traces are generated. Measures of the broadband complexity, mean phase standard deviation, and mean instantaneous frequency are then obtained from the acceleration trace (Figure III-11d), as described in Subsection III-B. The broadband $\log_{10}(A/T)$ measurement is next (Figure III-11e) followed by the VFM $\log_{10}A$ and narrowband complexity measurements (Figure III-11f). The broadband $\log_{10}(A/T)$, the VFM $\log_{10}A$, and narrowband complexity are all measured from the displacement trace. Figure III-13 shows the narrowband filtered traces used in the VFM $\log_{10}A$ measurement process, together with plots of the corresponding envelopes and instantaneous frequencies. The final step in the short-period event processing is the organization of the measurements and other event information into the event header, which, together with the compressed data edit, is then written onto the output tape (Figure III-11g).

a.

```
>>>>>   PDE INFORMATION = PDEX 11  1 77  3 56 28  55.30 N 130.80 E 33.  4.50  0.0     KEI          <<<<<

                          REGION =                          QUALITY = 0   SUB-REGION = 656
   SIGNAL OVER-RIDE CARD =    11       1     77       4       20     58    2048
   QUALITY CHECK OVER-RIDE CARD =           500000.000      1000000.000      1500000.000       500000.000       1000000.000

.............................................................................................................

  SIGNAL HEADER SUMMARY FOR EVENT   55*656SP0003
         EDIT TIME = 16479 SECONDS OF DAY 77305
         EDIT LENGTH =  2048 POINTS
         EDIT LENGTH =    16 SEGMENTS
   INPUT SAMPLE RATE =  20.  PER SECOND
  OUTPUT SAMPLE RATE =  10.0 PER SECOND

.............................................................................................................
COMPUTED INDEX OF EDIT START POINT =      501
***** REQUEST EXCEEDED LIMITS OF SEISMOGRAM:  EDIT LENGTH REDUCED TO 1536 POINTS *****
INPUT STATION = BP09
COMPONENT 1 HAS BEEN FETCHED

    SIGNAL  POWER SUMMARY,SEGMENTS  1 TO 12
    SITE  COMP      SITE MEAN
     21    1        0.1770797


COMPONENT 1 SEGMENT POWERS

SEG  SITE 21
  1  3.6E 00
  2  4.9E 00
  3  8.9E 00
  4  2.0E 01
  5  5.2E 00
  6  4.3E 00
  7  5.5E 00
  8  3.9E 00
  9  4.3E 00
 10  6.6E 00
 11  5.6E 00
 12  2.4E 00
  DELTA FREQUENCY =     0.00488  HZ

        EVENT NAME = '55*656SP0003'
      STATION NUMBER = 55

               NUMBER OF POINTS IN RECORD =  1536

               SAMPLE RATE=10.00 HZ.
               SAMPLES TO SKIP=     0    SAMPLES TO PROCESS=  1536
               FREQ: CENTER= 1.00 LOW= 0.0 HIGH= 5.00

               AMPLITUDE PROBABILITY THRESHOLD =          0.30
               FIRST SIG. PEAK TO NOISE PEAK THRESHOLD =        6.00
               WARM-UP TIME =          10.00
               NOISE MAX. COSINE TAPER TIME CONSTANT =      180.00
               ESTIMATED SIGNAL DURATION =        60.00

               THRESHOLD TO FIND START TIME =   1.0

               INPUT WINDOW LENGTH IN POINTS =   40
**** SIGNAL START TIME= 34.40 SEC,  PEAK SNR= 10.0 DB,  SD= 1.0 + B-FACTOR
```

FIGURE III-11a

SHORT-PERIOD EVENT MEASUREMENT EXAMPLE SHOWING SHORT-PERIOD DATA EDIT AND BROADBAND SIGNAL DETECTION

b.

```
                NOTE:  ALL SPECTRAL CHECKS ARE ON FIRST COMPONENT OF DATA

        LOG(CP)=-0.70      CP= 0.200      AMPL.=          119.7     LOG AMPL.= 2.078
        LOG(CP)=-0.50      CP= 0.316      AMPL.=          248.0     LOG AMPL.= 2.394
        LOG(CP)=-0.30      CP= 0.501      AMPL.=          168.6     LOG AMPL.= 2.227
        LOG(CP)=-0.10      CP= 0.794      AMPL.=          202.1     LOG AMPL.= 2.306
        LOG(CP)= 0.10      CP= 1.259      AMPL.=          111.5     LOG AMPL.= 2.047
        LOG(CP)= 0.30      CP= 1.995      AMPL.=           30.1     LOG AMPL.= 1.478
        LOG(CP)= 0.50      CP= 3.162      AMPL.=           13.9     LOG AMPL.= 1.144
    0      0.0      1.000      0.800      0.100      0.605      0.809      1.000      1.607      0.395
    0      0.0      1.000      1.070      0.100      0.511      0.809      1.000      1.517      0.489
    0      0.0      1.000      2.700      0.100      0.181      0.809      1.000      1.165      0.817
    0      0.0      1.000      4.550      0.100      0.057      0.809      1.000      1.048      0.943
    0      0.0      1.000 .    6.370      0.100      0.018      0.809      1.000      1.015      0.982
    0      0.0      1.000      8.930      0.100      0.004      0.809      1.000      1.003      0.996
  DELTA FREQUENCY =    0.00488   HZ
    1      0.200    1.000      0.0        0.100      1.000      0.809      0.992      0.618      7.982
SUM=    0.098328   C=    0.199526   W=    0.090186
    1      0.251    1.000      0.251      0.100      0.854      0.809      0.988      0.590      4.848
    1      0.316    1.000      0.0        0.100      1.000      0.809      0.980      0.618      5.041
SUM=    0.155814   C=    0.316228   W=    0.142935
    1      0.398    1.000      0.398      0.100      0.779      0.809      0.969      0.589      3.203
    1      0.501    1.000      0.0        0.100      1.000      0.809      0.951      0.618      3.189
SUM=    0.246946   C=    0.501187   W=    0.226537
    1      0.631    1.000      0.631      0.100      0.673      0.809      0.922      0.603      2.175
                   SYSTEM RESPONSE HAS BEEN REMOVED
        LOG(CP)=-0.70      CP= 0.200      AMPL.=         7041.7     LOG AMPL.= 3.848
        LOG(CP)=-0.50      CP= 0.316      AMPL.=         4235.0     LOG AMPL.= 3.627
        LOG(CP)=-0.30      CP= 0.501      AMPL.=         1013.7     LOG AMPL.= 3.006
        LOG(CP)=-0.10      CP= 0.794      AMPL.=          285.4     LOG AMPL.= 2.456
        LOG(CP)= 0.10      CP= 1.259      AMPL.=           84.8     LOG AMPL.= 1.929
        LOG(CP)= 0.30      CP= 1.995      AMPL.=           14.5     LOG AMPL.= 1.161
        LOG(CP)= 0.50      CP= 3.162      AMPL.=            5.4     LOG AMPL.= 0.731
```

c.

```
.................................................................................................
            BEGIN EDIT COMPRESSION FOR EVENT 550456SP0003 ABOUT P PHASE
            DELTA =   39.09 DEGREES

            COMPRESSED EDIT LENGTH, SECONDS:  51.20
            VM & VL FOR START AND END OF COMPRESSED EDIT:    10.24    9.13
            START OF COMPRESSED EDIT:
                SECONDS INTO ORIGINAL EDIT:        8.80
                SECONDS INTO SUBSET:       33.80
            DETECTED PHASE ARRIVAL TIME:
                SECONDS INTO ORIGINAL EDIT:       34.40
                SECONDS INTO SUBSET:       59.40
            EXPECTED PHASE ARRIVAL TIME:
                SECONDS INTO ORIGINAL EDIT:       30.00
                SECONDS INTO SUBSET:       55.00
            PHASE ARRIVAL TIME CHOSEN:
                SECONDS INTO ORIGINAL EDIT:       34.40
                SECONDS INTO SUBSET:       59.40
            EDIT START PRECEDES PHASE ARRIVAL TIME BY  25.60 SECONDS
            THE FOLLOWING HEADER LOCATIONS HAVE BEEN CHANGED:
                28, 3, 15: EDIT LENGTHS IN SECS, POINTS, AND BYTES   51.20    512    2048
                5, 6, 7: EDIT START, HRS, MINS, AND SECS       6.00    1.00  270.00
                26, 27: EDIT START, SECS INTO DAY AND YEAR-DAY       18087      77305
                51: INDEX OF SIGNAL START RELATIVE TO EDIT START  257
            END EDIT COMPRESSION FOR EVENT 550456SP0003
.................................................................................................
```

FIGURE III-11b, c

SHORT-PERIOD EVENT MEASUREMENT EXAMPLE SHOWING (b) INSTRUMENT RESPONSE REMOVAL, AND (c) SHORT-PERIOD EDIT COMPRESSION

d.

```
EVENT NAME = '55*656SP0003'
STATION NUMBER = 55

          NUMBER OF POINTS IN RECORD =   512

          SAMPLE RATE=10.00 HZ.
          SAMPLES TO SKIP=     0    SAMPLES TO PROCESS=   512
          FREQ: CENTER= 1.00 LOW= 0.0 HIGH= 5.00

          AMPLITUDE PROBABILITY THRESHOLD =          0.30
          FIRST SIG. PEAK TO NOISE PEAK THRESHOLD =        6.00
          WARM-UP TIME =         10.00
          NOISE MAX. COSINE TAPER TIME CONSTANT =     100.00
          ESTIMATED SIGNAL DURATION =          60.00

          THRESHOLD TO FIND START TIME =   1.0

          INPUT WINDOW LENGTH IN POINTS =   40

          FIRST PT. OF SIGNAL GATE = 257

                                   COMPLEXITY FACTORS

          RATIO OF 0-10 SEC TO 0-5 SEC INTEGRATED SIGNAL TRACES  (TRAP. RULE)---    2.355E 00

          MEAN FRQ=  1.01 MEAN PHASE S.D.=  1.33

          MAX. MEAN FRQ=  1.01  MEAN PHASE S.D.=  1.33

          CHI-SQUARED DISCRIMINANT (MEAN) =     3.99

          CHI-SQUARED DISCRIMINANT (MAX) =     3.99

                ***********************************
```

e.

```
*****************************...BEGIN A/T MEASUREMENT FOR EVENT 55*656SP0003...*****************************

          VELOCITY WINDOW INFORMATION
              P PHASE VELOCITY LIMITS (HIGH, LOW)  15.00     8.00
              ACTUAL VELOCITY LIMITS USED (HIGH, LOW)  10.26    9.15
              NUMBER OF SAMPLES IN WINDOW  512, EXTENDED WITH ZEROS TO  512

          BROADBAND FILTER INFORMATION
              LOW FREQUENCY CUTOFF (-6DBA POINT)   0.30
              HIGH FREQUENCY CUTOFF (-6DBA POINT)   2.50
              CENTER FREQUENCY    0.87
              FILTER ORDER     8

          *** PLOT SET  16 ***

              A            LOG A/T          PERIOD (T)       VELOCITY        SECS. INTO EDIT
          132.645          1.615            3.222            9.607            28.60
*****************************....END A/T MEASUREMENT FOR EVENT 55*656SP0003....*****************************
```

FIGURE III-11d, e

SHORT-PERIOD EVENT MEASUREMENT EXAMPLE SHOWING (d) BROADBAND COMPLEXITY, MEAN INSTANTANEOUS FREQUENCY, MEAN PHASE STANDARD DEVIATION, AND (e) BROADBAND $LOG_{10}(A/T)$ MEASUREMENT

f.

```
SUM=   0.155853   C=    0.316228   W=    0.142935
                  FIRST PT. OF SIGNAL GATE = 257

                                        COMPLEXITY FACTORS
                  RATIO OF 0-10 SEC TO 0-5 SEC INTEGRATED SIGNAL TRACES  (TRAP. RULE)---    2.5338 00
                  ### PLOT SET  18 ###
                  DETECTION TIME =    25.60        PEAK-TO-NOISE AVE. ENV. RATIO, DB =   7.35
                  LENGTH OF NOISE SAMPLE, SECS =   23.10        # OF NOISE POINTS INCLDED IN NOISE ENV AVE =    191
                  PEAK=     506.08    PERIOD=  3.7 SEC    AT TIME=    33.5
                  LOG(AMPL.) = 2.70     FILTER CENTER PERIOD=  3.2
                  **********

SUM=   0.266855   C=    0.501187   W=    0.226537
                  FIRST PT. OF SIGNAL GATE = 257

                                        COMPLEXITY FACTORS
                  RATIO OF 0-10 SEC TO 0-5 SEC INTEGRATED SIGNAL TRACES  (TRAP. RULE)---    2.1228 00
                  ### PLOT SET  19 ###
                  DETECTION TIME =    25.60        PEAK-TO-NOISE AVE. ENV. RATIO, DB =  12.14
                  LENGTH OF NOISE SAMPLE, SECS =   23.10        # OF NOISE POINTS INCLDED IN NOISE ENV AVE =     40
                  PEAK=     128.21    PERIOD=  2.5 SEC    AT TIME=    30.8
                  LOG(AMPL.) = 2.11     FILTER CENTER PERIOD=  2.0
                  **********

SUM=   0.391338   C=    0.794328   W=    0.359036
                  FIRST PT. OF SIGNAL GATE = 257

                                        COMPLEXITY FACTORS
                  RATIO OF 0-10 SEC TO 0-5 SEC INTEGRATED SIGNAL TRACES  (TRAP. RULE)---    3.0548 00
                  ### PLOT SET  20 ###
                  DETECTION TIME =    25.60        PEAK-TO-NOISE AVE. ENV. RATIO, DB =  26.83
                  LENGTH OF NOISE SAMPLE, SECS =   23.10        # OF NOISE POINTS INCLDED IN NOISE ENV AVE =     16
                  PEAK=      49.28    PERIOD=  1.8 SEC    AT TIME=    31.5
                  LOG(AMPL.) = 1.69     FILTER CENTER PERIOD=  1.3
                  **********

SUM=   0.620261   C=    1.258925   W=    0.569036
                  FIRST PT. OF SIGNAL GATE = 257

                                        COMPLEXITY FACTORS
                  RATIO OF 0-10 SEC TO 0-5 SEC INTEGRATED SIGNAL TRACES  (TRAP. RULE)---    2.4028 00
                  ### PLOT SET  21 ###
                  DETECTION TIME =    25.60        PEAK-TO-NOISE AVE. ENV. RATIO, DB =  25.17
                  LENGTH OF NOISE SAMPLE, SECS =   23.10        # OF NOISE POINTS INCLDED IN NOISE ENV AVE =     52
                  PEAK=      13.63    PERIOD=  1.0 SEC    AT TIME=    26.2
                  LOG(AMPL.) = 1.13     FILTER CENTER PERIOD=  0.8
                  **********

SUM=   0.983150   C=    1.995262   W=    0.901858
                  FIRST PT. OF SIGNAL GATE = 257

                                        COMPLEXITY FACTORS
                  RATIO OF 0-10 SEC TO 0-5 SEC INTEGRATED SIGNAL TRACES  (TRAP. RULE)---    1.9018 00
                  ### PLOT SET  22 ###
                  DETECTION TIME =    25.60        PEAK-TO-NOISE AVE. ENV. RATIO, DB =  32.52
                  LENGTH OF NOISE SAMPLE, SECS =   23.10        # OF NOISE POINTS INCLDED IN NOISE ENV AVE =     39
                  PEAK=       0.58    PERIOD=  0.6 SEC    AT TIME=    29.2
                  LOG(AMPL.) =-0.26     FILTER CENTER PERIOD=  0.5
                  **********

SUM=   1.555866   C=    3.162275   W=    1.429348
                  FIRST PT. OF SIGNAL GATE = 257

                                        COMPLEXITY FACTORS
                  RATIO OF 0-10 SEC TO 0-5 SEC INTEGRATED SIGNAL TRACES  (TRAP. RULE)---    1.9988 00
                  ### PLOT SET  23 ###
                  DETECTION TIME =    25.60        PEAK-TO-NOISE AVE. ENV. RATIO, DB =   6.45
                  LENGTH OF NOISE SAMPLE, SECS =   23.10        # OF NOISE POINTS INCLDED IN NOISE ENV AVE =      1
                  PEAK=       0.02    PERIOD=  0.4 SEC    AT TIME=    28.4
                  LOG(AMPL.) =-1.68     FILTER CENTER PERIOD=  0.3
                  **********
```

FIGURE III-11f

SHORT-PERIOD EVENT MEASUREMENT EXAMPLE SHOWING VARIABLE FREQUENCY MAGNITUDE (VFM) LOG_{10} A MEASUREMENT AND NARROWBAND COMPLEXITIES

g.

```
                DISPLAY OF EVENT HEADER INFORMATION
NO SEISMOGRAM NUMBER
     1 COMPONENTS      DATA LENGTH:   512 POINTS
EVENT DESIGNATION:  550456SP0003   ARRAY NAME: SRO              DATA TYPE: GPH
DATA RECORD LENGTH:  2048 BYTES
     1 EDITED SITES
SIGNAL  PARTITION       TIME DOMAIN
SOURCE ROUTINE: SSPROG
DATA PRESENTATION:  PAW
ANALYZ CHANNELS PROCESSED:   1
NUMBER OF CHANNELS DELETED:  0
RE-SAMPLED EVERY   2.0 POINTS
DATA TIME:       14407 (SEC)    77305 (YRDAY)     -OR-  DATE 11/ 1/77   TIME  4. 1.27
DATA LENGTH:   51.2 SECONDS
SIGNAL STARTS AT POINT NO.      257
SOURCE TIME:     14066 (SEC)    77305 (YRDAY)     -OR-  DATE 11/ 1/77   TIME  3.54.26
CONFIDENCE OF SOURCE TIME (PDE CODE):
SOURCE AT LATITUDE  55.30 N.   LONGITUDE  130.80 E.   DEPTH  33.00 (KM.)
ACCORDING TO NEI      , M_B = 0.0   M_S = 0.0   TI ESTIMATED M_S = 0.0

TI ESTIMATED SIGNAL-TO-NOISE RATIO:   10.0 DB.
STD. DEV. OF RESIDUAL TIME:                STATIONS IN PDE REPORTING
REGION =                          SUB-REGION = 656     NORSAR QUALITY = 0
  P-TIME  P-TIME  S-TIME  S-TIME  LQ-TIME  LQ-TIME  LR-TIME  LR-TIME  LR
   SEC     YR-DAY   SEC     YR-DAY   SEC     YR-DAY   SEC     YR-DAY   LENGTH
  14509   77305   14694   77305   15094   77305   15185   77305    639
AZIMUTH  (STATION TO SOURCE):  -63.68    (PRIMARY BEAM DIRECTION):    0.0
DISTANCE (STATION TO SOURCE):   39.09 (DEG.)        -OR-          4338.70 (KM.)
          STATION ELEVATION:    0.0  KM.
   SEISMOMETER TYPE:              RECORDING TYPE:
TECTONIC CLASS CODE: AA
TELESEISMIC P PHASE LOG(A/T):  1.61  (PHASE ARRIVAL DETECTED 25.60 SECONDS AFTER EDIT START)
LOG(A/T) FROM FIRST ENVELOPE PEAK:  0.07
AVER SMOOTHED FREQUENCY:            1.07
MINIMUM MEAN SMOOTHED FREQUENCY:    1.01
MEAN PHASE STANDARD DEVIATION:      1.33
              VARIABLE FREQUENCY MEASUREMENTS
LOG OF CENTER FREQ.  LOG OF DISPLACEMENT  COMPLEXITY FOR CENTER FREQ.
      -0.40                 -1.10                 1.53
      -0.30                 -1.11                 1.51
      -0.10                 -1.04                 1.06
       0.00                 -1.03                 1.00
       0.10                 -1.12                 1.00
       0.20                 -1.20                 1.00
       0.30                 -1.24                 1.00
       0.50                 -1.44                 1.09

BROADBAND COMPLEXITY:  2.20      ENVELOPE COMPLEXITY:  2.35
MP(FROM FIRST 5 SEC. OF SIGNAL ON ACCELERATION TRACE): 6.34
SITE NUMBER 55      LATITUDE  64.77 N.   LONGITUDE -146.89 E.

HEADER RECORD WRITTEN ON OUTPUT TAPE ON UNIT 13
SHORT-PERIOD DATA WRITTEN ON OUTPUT TAPE
 NORMAL TERMINATION OF EVENT PROCESSING
```

FIGURE III-11g

SHORT-PERIOD EVENT MEASUREMENT EXAMPLE SHOWING INFORMATION CONTAINED IN SHORT-PERIOD EVENT HEADER

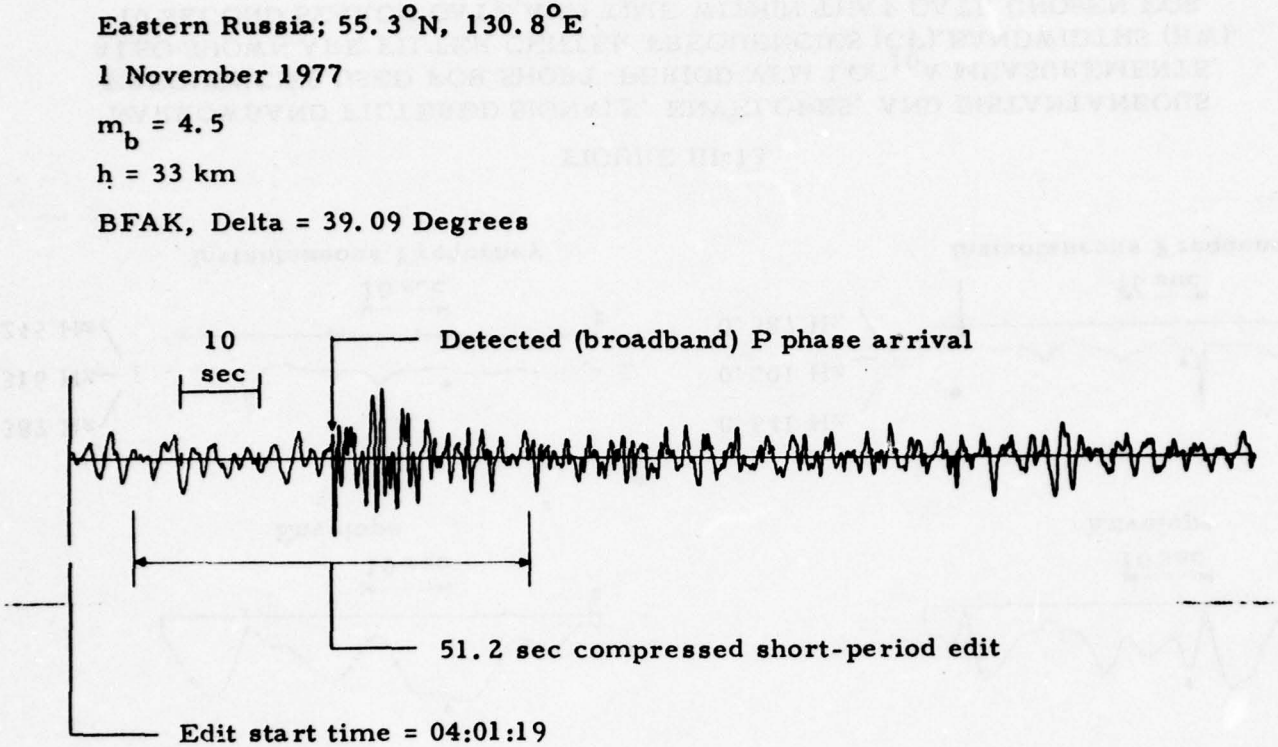

FIGURE III-12

RAW INPUT SHORT-PERIOD DATA TRACE SHOWING DETECTED P PHASE ARRIVAL AND 51.2 SEC COMPRESSED EDIT

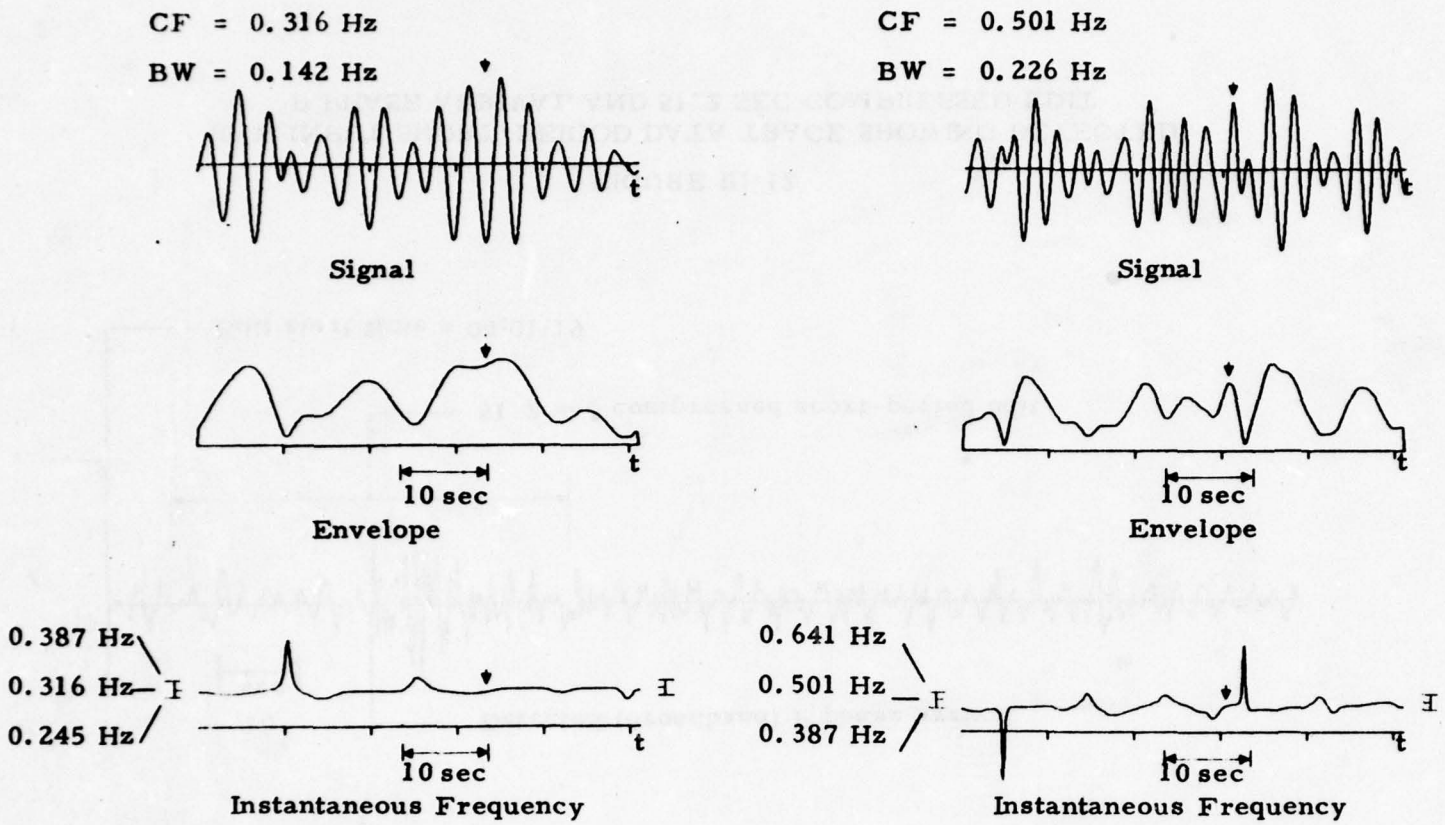

FIGURE III-13

NARROWBAND FILTERED SIGNALS, ENVELOPES, AND INSTANTANEOUS FREQUENCIES USED FOR SHORT-PERIOD VFM $LOG_{10}A$ MEASUREMENTS. ALSO SHOWN ARE FILTER CENTER FREQUENCIES (CF), BANDWIDTHS (BW), 10 SECOND SEARCH GATE, AND TIME WITHIN THAT GATE CHOSEN FOR $LOG_{10}A$ MEASUREMENTS (▼)
(PAGE 1 OF 3)

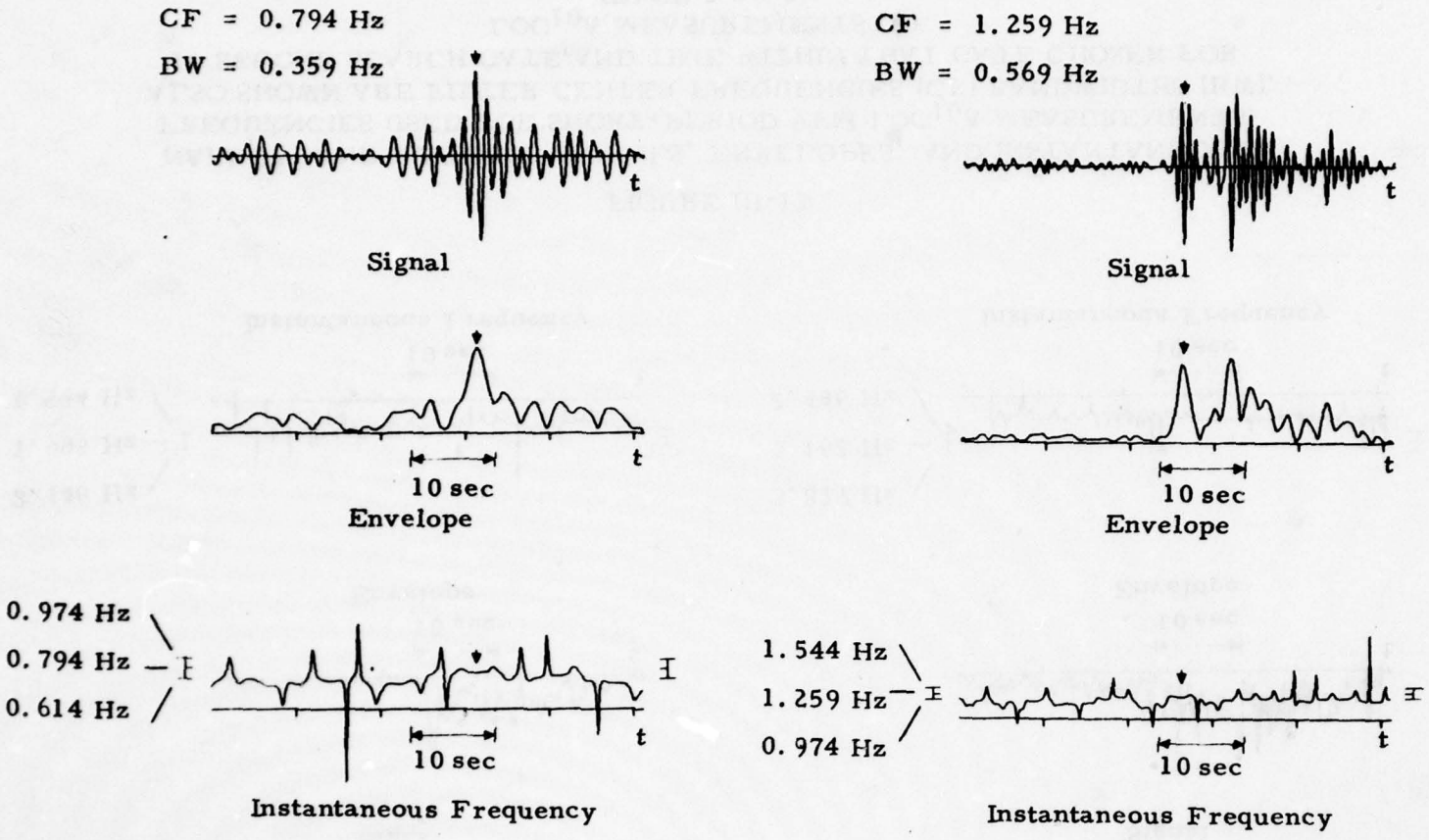

FIGURE III-13

NARROWBAND FILTERED SIGNALS, ENVELOPES, AND INSTANTANEOUS FREQUENCIES USED FOR SHORT-PERIOD VFM $LOG_{10}A$ MEASUREMENTS. ALSO SHOWN ARE FILTER CENTER FREQUENCIES (CF), BANDWIDTHS (BW), 10 SECOND SEARCH GATE, AND TIME WITHIN THAT GATE CHOSEN FOR $LOG_{10}A$ MEASUREMENTS (▼)
(PAGE 2 OF 3)

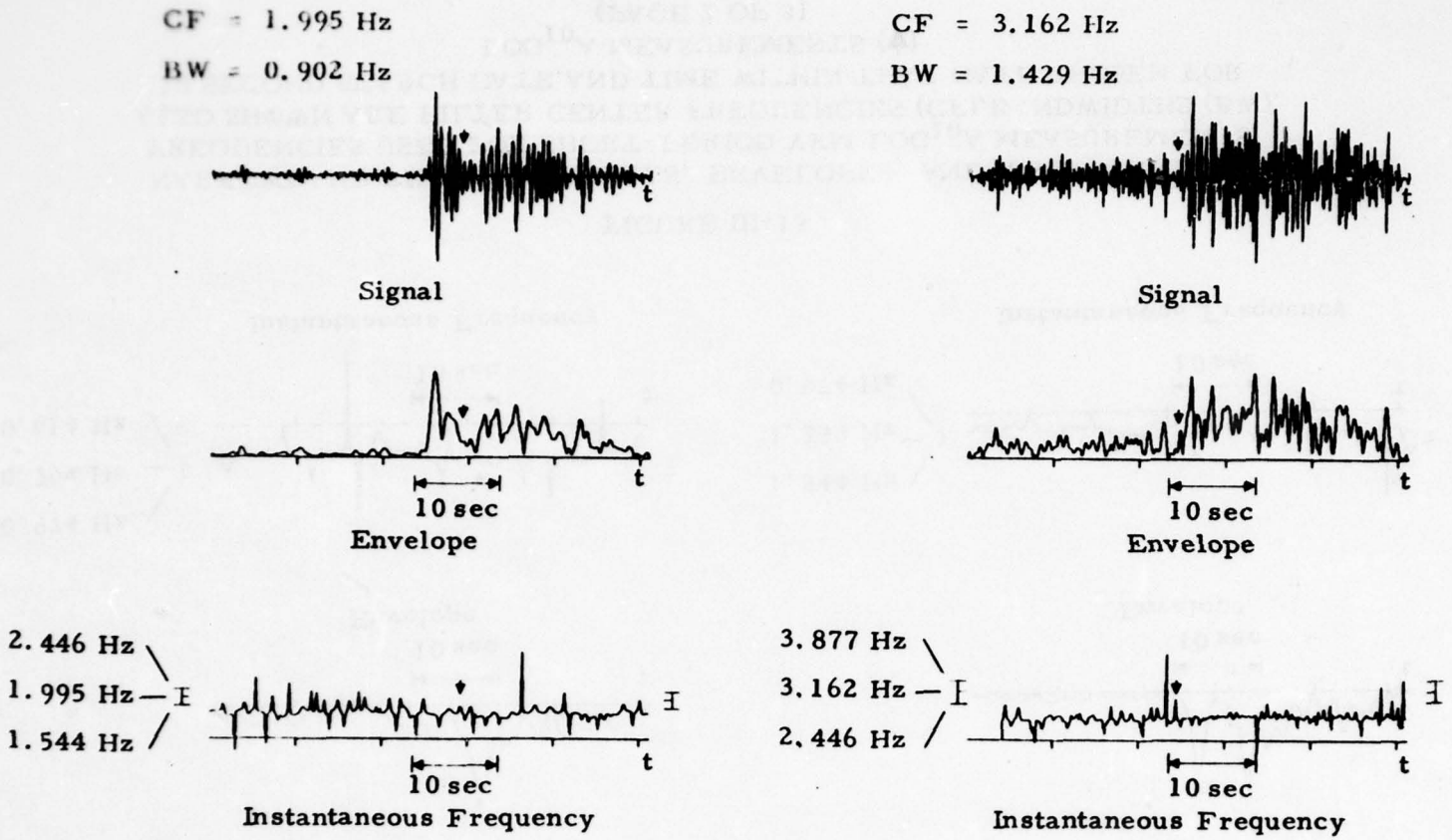

FIGURE III-13

NARROWBAND FILTERED SIGNALS, ENVELOPES, AND INSTANTANEOUS FREQUENCIES USED FOR SHORT-PERIOD VFM $LOG_{10}A$ MEASUREMENTS. ALSO SHOWN ARE FILTER CENTER FREQUENCIES (CF), BANDWIDTHS (BW), 10 SECOND SEARCH GATE, AND TIME WITHIN THAT GATE CHOSEN FOR $LOG_{10}A$ MEASUREMENTS (▼)
(PAGE 3 OF 3)

2. Example of Long-Period Event Measurement

The output for the long-period event measurement example is shown in Figure III-14. As in the case of the short-period example, the first step in the long-period event measurement process consists of reading the input seismogram card to identify the event to be processed (Figure III-14a). The three components of data are fetched in segments of 128 points, the data are rotated to the vertical, transverse, and radial configuration, and automated checks are made to determine whether the data contain evidence of clipping or uncorrectable spikes. Next, the instrument response is removed (Figure III-14b), and measurements of $\log_{10}A$ are made on the vertical and transverse components for long-period VFM computation (Figure III-14c). The narrowband filtered long-period traces and the corresponding envelopes and instantaneous frequencies are shown in Figure III-15. As in the short-period case, the final step in the long-period event processing is the organization of the long-period measurements and other event information into the event header, which, together with the three components of data, is then written onto the output tape (Figure III-14d).

a.

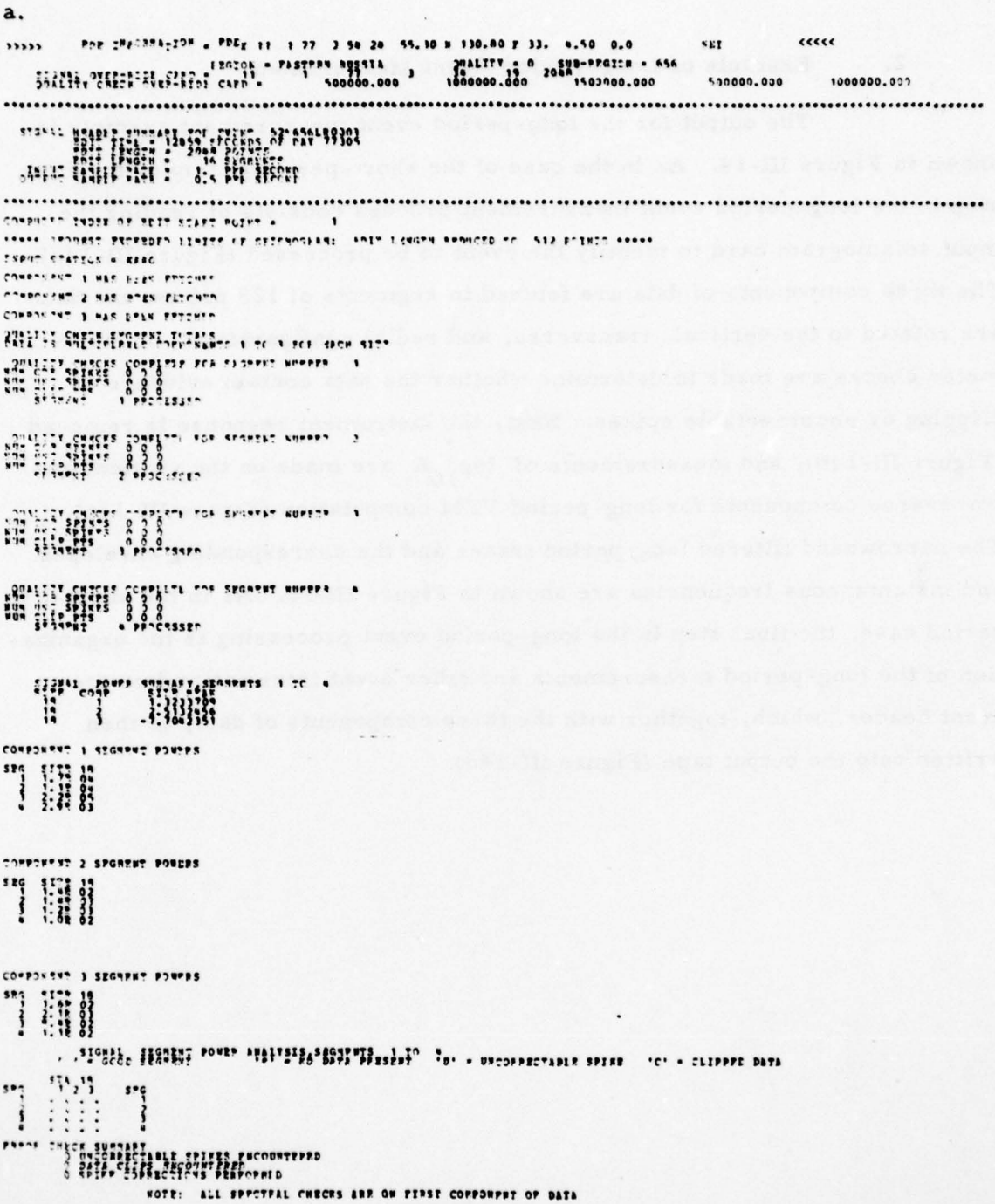

FIGURE III-14a

LONG-PERIOD EVENT MEASUREMENT EXAMPLE SHOWING LONG-PERIOD THREE COMPONENT DATA EDIT AND AUTOMATED QUALITY CHECKS

b.

```
            LOG(CP)=-1.70    CP= 0.020    AMPL.=          6776.5    LOG AMPL.= 3.831
            LOG(CP)=-1.60    CP= 0.025    AMPL.=          3262.0    LOG AMPL.= 3.513
            LOG(CP)=-1.50    CP= 0.032    AMPL.=          3448.2    LOG AMPL.= 3.538
            LOG(CP)=-1.40    CP= 0.040    AMPL.=          2566.8    LOG AMPL.= 3.409
            LOG(CP)=-1.30    CP= 0.050    AMPL.=          2493.7    LOG AMPL.= 3.397
            LOG(CP)=-1.20    CP= 0.063    AMPL.=           523.2    LOG AMPL.= 2.719
            LOG(CP)=-1.10    CP= 0.079    AMPL.=           163.6    LOG AMPL.= 2.214
        0     0.0      0.040     0.023     2.000     0.745     0.876     1.000     2.003     0.255
        0     0.0      0.040     0.032     2.000     0.666     0.876     1.000     1.902     0.334
        0     0.0      0.040     0.041     2.000     0.599     0.876     1.000     1.800     0.401
        0     0.0      0.040     0.050     2.000     0.533     0.876     1.000     1.690     0.467
        0     0.0      0.040     0.063     2.000     0.453     0.876     1.000     1.559     0.547
        0     0.0      0.040     0.023     2.000     0.745     0.876     1.000     2.003     0.255
        0     0.0      0.040     0.032     2.000     0.666     0.876     1.000     1.902     0.334
        0     0.0      0.040     0.041     2.000     0.599     0.876     1.000     1.800     0.401
        0     0.0      0.040     0.050     2.000     0.533     0.876     1.000     1.690     0.467
        0     0.0      0.040     0.063     2.000     0.453     0.876     1.000     1.559     0.547
        0     0.0      0.040     0.023     2.000     0.745     0.876     1.000     2.003     0.255
        0     0.0      0.040     0.032     2.000     0.666     0.876     1.000     1.902     0.334
        0     0.0      0.040     0.041     2.000     0.599     0.876     1.000     1.800     0.401
        0     0.0      0.040     0.050     2.000     0.533     0.876     1.000     1.690     0.467
        0     0.0      0.040     0.063     2.000     0.453     0.876     1.000     1.559     0.547
        1     0.020    0.040     0.0       2.000     1.000     0.876     0.969     0.497     3.999
SUM=    0.004767    C=    0.019953    W=    0.004390
        1     0.022    0.040     0.022     2.000     0.755     0.876     0.961     0.497     2.093
        1     0.025    0.040     0.0       2.000     1.000     0.876     0.951     0.497     3.181
SUM=    0.006018    C=    0.025119    W=    0.005526
        1     0.028    0.040     0.028     2.000     0.702     0.876     0.938     0.512     2.303
        1     0.020    0.040     0.0       2.000     1.000     0.876     0.969     0.497     3.999
SUM=    0.004767    C=    0.019953    W=    0.004390
        1     0.022    0.040     0.022     2.000     0.755     0.876     0.961     0.497     2.093
        1     0.025    0.040     0.0       2.000     1.000     0.876     0.951     0.497     3.181
SUM=    0.006018    C=    0.025119    W=    0.005526
        1     0.028    0.040     0.028     2.000     0.702     0.876     0.938     0.512     2.303
        1     0.020    0.040     0.0       2.000     1.000     0.876     0.969     0.497     3.999
SUM=    0.004767    C=    0.019953    W=    0.004390
        1     0.022    0.040     0.022     2.000     0.755     0.876     0.961     0.497     2.093
        1     0.025    0.040     0.0       2.000     1.000     0.876     0.951     0.497     3.181
SUM=    0.006018    C=    0.025119    W=    0.005526
        1     0.028    0.040     0.028     2.000     0.702     0.876     0.938     0.512     2.303
                   SYSTEM RESPONSE HAS BEEN REMOVED
            LOG(CP)=-1.70    CP= 0.020    AMPL.=          7509.9    LOG AMPL.= 3.876
            LOG(CP)=-1.60    CP= 0.025    AMPL.=          3926.2    LOG AMPL.= 3.594
            LOG(CP)=-1.50    CP= 0.032    AMPL.=          3711.0    LOG AMPL.= 3.569
            LOG(CP)=-1.40    CP= 0.040    AMPL.=          2373.8    LOG AMPL.= 3.375
            LOG(CP)=-1.30    CP= 0.050    AMPL.=          3448.5    LOG AMPL.= 3.538
            LOG(CP)=-1.20    CP= 0.063    AMPL.=           697.5    LOG AMPL.= 2.844
            LOG(CP)=-1.10    CP= 0.079    AMPL.=           668.0    LOG AMPL.= 2.825
```

FIGURE III-14b

LONG-PERIOD EVENT MEASUREMENT EXAMPLE SHOWING LONG-PERIOD SYSTEM RESPONSE REMOVAL

C.

```
                COMPONENT # =  1

                THE FREQUENCY RANGE 0.0200 TO 0.0200 HZ HAS VELOCITY LIMITS    2.85 TO 4.15 KM/SEC
                THE COMPRESSED EDIT HAS  371 NONZERO POINTS
                THE NEXT HIGHEST POWER OF TWO IS  512
                THE NEW EDIT STARTS     0 SECONDS INTO THE PRIMARY EDIT
                THERE ARE 174 SECONDS OF NOISE AT THE FRONT OF THE EDIT
                THE NEW EDIT STARTS     0 SECONDS INTO THE GEOTECH EDIT
SUM=     0.009671   C=    0.020000   W=    0.008800
                *** PLOT SET    1.000
          PEAK=     523.84    PERIOD= 50.2 SEC    AT TIME=    642.0

                LOG10 OF LP AMPLITUDE =  2.72          WITH PERIOD = 50.24 SEC            CENTER PERIOD = 50.00
                NOISE AVE ENV =    77.41          DETECTION RATIO IN DB =     16.61          # OF PTS IN NOISE AVE ENV =    35
        ************************************************************************

                COMPONENT # =  2

                THE FREQUENCY RANGE 0.0200 TO 0.0200 HZ HAS VELOCITY LIMITS    3.10 TO 4.40 KM/SEC
                THE COMPRESSED EDIT HAS  298 NONZERO POINTS
                THE NEXT HIGHEST POWER OF TWO IS  512
                THE NEW EDIT STARTS     0 SECONDS INTO THE PRIMARY EDIT
                THERE ARE 104 SECONDS OF NOISE AT THE FRONT OF THE EDIT
                THE NEW EDIT STARTS     0 SECONDS INTO THE GEOTECH EDIT
SUM=     0.009671   C=    0.020000   W=    0.008880
                *** PLOT SET    2.000
          PEAK=     127.07    PERIOD= 45.0 SEC    AT TIME=    386.0

                LOG10 OF LP AMPLITUDE =  2.10          WITH PERIOD = 45.01 SEC            CENTER PERIOD = 50.00
                NOISE AVE ENV =    7.92           DETECTION RATIO IN DB =     24.10          # OF PTS IN NOISE AVE ENV =    37
        ************************************************************************

                COMPONENT # =  1

                THE FREQUENCY RANGE 0.0250 TO 0.0250 HZ HAS VELOCITY LIMITS    2.71 TO 4.01 KM/SEC
                THE COMPRESSED EDIT HAS  416 NONZERO POINTS
                THE NEXT HIGHEST POWER OF TWO IS  512
                THE NEW EDIT STARTS     0 SECONDS INTO THE PRIMARY EDIT
                THERE ARE 216 SECONDS OF NOISE AT THE FRONT OF THE EDIT
                THE NEW EDIT STARTS     0 SECONDS INTO THE GEOTECH EDIT
SUM=     0.012094   C=    0.025000   W=    0.011100
                *** PLOT SET    3.000
          PEAK=     644.71    PERIOD= 42.7 SEC    AT TIME=    642.0

                LOG10 OF LP AMPLITUDE =  2.81          WITH PERIOD = 42.74 SEC            CENTER PERIOD = 40.00
                NOISE AVE ENV =    67.66          DETECTION RATIO IN DB =     19.58          # OF PTS IN NOISE AVE ENV =    23
        ************************************************************************

                COMPONENT # =  2

                THE FREQUENCY RANGE 0.0250 TO 0.0250 HZ HAS VELOCITY LIMITS    2.96 TO 4.26 KM/SEC
                THE COMPRESSED EDIT HAS  337 NONZERO POINTS
                THE NEXT HIGHEST POWER OF TWO IS  512
                THE NEW EDIT STARTS     0 SECONDS INTO THE PRIMARY EDIT
                THERE ARE 142 SECONDS OF NOISE AT THE FRONT OF THE EDIT
                THE NEW EDIT STARTS     0 SECONDS INTO THE GEOTECH EDIT
SUM=     0.012094   C=    0.025000   W=    0.011100
                *** PLOT SET    4.000
          PEAK=     171.92    PERIOD= 39.3 SEC    AT TIME=    632.0

                LOG10 OF LP AMPLITUDE =  2.24          WITH PERIOD = 39.30 SEC            CENTER PERIOD = 40.00
                NOISE AVE ENV =    9.00           DETECTION RATIO IN DB =     25.63          # OF PTS IN NOISE AVE ENV =    29
        ************************************************************************
```

FIGURE III-14c

LONG-PERIOD EVENT MEASUREMENT EXAMPLE SHOWING LONG-PERIOD VARIABLE FREQUENCY MAGNITUDE (VFM) $LOG_{10}A$ MEASUREMENTS ON VERTICAL (1) AND TRANSVERSE (2) COMPONENTS (PAGE 1 OF 4)

```
C.                COMPONENT # =  1

                  THE FREQUENCY RANGE 0.0316 TO 0.0316 HZ HAS VELOCITY LIMITS    2.57 TO 3.07 KM/SEC
                  THE COMPRESSED EDIT HAS  469 NONZERO POINTS
                  THE NEXT HIGHEST POWER OF TWO IS  512
                  THE NEW EDIT STARTS    0 SECONDS INTO THE PRIMARY EDIT
                  THERE ARE 264 SECONDS OF NOISE AT THE FRONT OF THE EDIT
                  THE NEW EDIT STARTS    0 SECONDS INTO THE GEOTECH EDIT

SUM=    0.015291  C=    0.031600   W=    0.010030
                  *** PLOT SET   5 ***
          PEAK=     657.50   PERIOD= 35.2 SEC    AT TIME=   630.0

                  LOG10 OF LP AMPLITUDE =  2.82          WITH PERIOD = 35.20 SEC          CENTER PERIOD = 31.65
                  NOISE AVE ENV =    38.95          DETECTION RATIO IN DB =    24.55          # OF PTS IN NOISE AVE ENV =   32
                **********************************************************************

                  COMPONENT # =  2

                  THE FREQUENCY RANGE 0.0316 TO 0.0316 HZ HAS VELOCITY LIMITS    2.82 TO 4.12 KM/SEC
                  THE COMPRESSED EDIT HAS  381 NONZERO POINTS
                  THE NEXT HIGHEST POWER OF TWO IS  512
                  THE NEW EDIT STARTS    0 SECONDS INTO THE PRIMARY EDIT
                  THERE ARE 184 SECONDS OF NOISE AT THE FRONT OF THE EDIT
                  THE NEW EDIT STARTS    0 SECONDS INTO THE GEOTECH EDIT

SUM=    0.015291  C=    0.031600   W=    0.010030
                  *** PLOT SET   6 ***
          PEAK=     201.69   PERIOD= 33.9 SEC    AT TIME=   456.0

                  LOG10 OF LP AMPLITUDE =  2.31          WITH PERIOD = 33.93 SEC          CENTER PERIOD = 31.65
                  NOISE AVE ENV =     7.95          DETECTION RATIO IN DB =    28.14          # OF PTS IN NOISE AVE ENV =   22
                **********************************************************************

                  COMPONENT # =  1

                  **FUNCTP: THIS IS A SHORT EDIT**
                  THE FREQUENCY RANGE 0.0400 TO 0.0400 HZ HAS VELOCITY LIMITS    2.47 TO 3.76 KM/SEC
                  THE COMPRESSED EDIT HAS  512 NONZERO POINTS
                  THE NEXT HIGHEST POWER OF TWO IS  512
                  THE NEW EDIT STARTS    0 SECONDS INTO THE PRIMARY EDIT
                  THERE ARE 312 SECONDS OF NOISE AT THE FRONT OF THE EDIT
                  THE NEW EDIT STARTS    0 SECONDS INTO THE GEOTECH EDIT

SUM=    0.019368  C=    0.040000   W=    0.017760
                  *** PLOT SET   7 ***
          PEAK=     142.24   PERIOD= 27.9 SEC    AT TIME=   618.0

                  LOG10 OF LP AMPLITUDE =  2.56          WITH PERIOD = 27.95 SEC          CENTER PERIOD = 25.00
                  NOISE AVE ENV =    33.79          DETECTION RATIO IN DB =    20.60          # OF PTS IN NOISE AVE ENV =   55
                **********************************************************************

                  COMPONENT # =  2

                  THE FREQUENCY RANGE 0.0400 TO 0.0400 HZ HAS VELOCITY LIMITS    2.69 TO 3.99 KM/SEC
                  THE COMPRESSED EDIT HAS  426 NONZERO POINTS
                  THE NEXT HIGHEST POWER OF TWO IS  512
                  THE NEW EDIT STARTS    0 SECONDS INTO THE PRIMARY EDIT
                  THERE ARE 226 SECONDS OF NOISE AT THE FRONT OF THE EDIT
                  THE NEW EDIT STARTS    0 SECONDS INTO THE GEOTECH EDIT

SUM=    0.019368  C=    0.040000   W=    0.017760
                  *** PLOT SET   8 ***
          PEAK=     169.22   PERIOD= 28.0 SEC    AT TIME=   468.0

                  LOG10 OF LP AMPLITUDE =  2.28          WITH PERIOD = 28.01 SEC          CENTER PERIOD = 25.00
                  NOISE AVE ENV =    11.17          DETECTION RATIO IN DB =    24.56          # OF PTS IN NOISE AVE ENV =   67
                **********************************************************************
```

FIGURE III-14c

LONG-PERIOD EVENT MEASUREMENT EXAMPLE SHOWING LONG-PERIOD VARIABLE FREQUENCY MAGNITUDE (VFM) $LOG_{10}A$ MEASUREMENTS ON VERTICAL (1) AND TRANSVERSE (2) COMPONENTS (PAGE 2 OF 4)

C.

```
COMPONENT # =  1

**NOTE: THIS IS A SHORT EDIT**
THE FREQUENCY RANGE 0.0500 TO 0.0500 HZ HAS VELOCITY LIMITS    2.47 TO 3.63 KM/SEC
THE COMPRESSED EDIT HAS  512 NONZERO POINTS
THE NEXT HIGHEST POWER OF TWO IS  512
THE NEW EDIT STARTS    0 SECONDS INTO THE PRIMARY EDIT
THERE ARE 354 SECONDS OF NOISE AT THE FRONT OF THE EDIT
THE NEW EDIT STARTS    0 SECONDS INTO THE GEOTECH EDIT

SUM=   0.324201   C=    0.050000   W=    0.022200
PEAK=  000 PLOT SET  9.000
       107.44   PERIOD= 21.7 SEC    AT TIME=   726.0

LOG10 OF LP AMPLITUDE =  2.03          WITH PERIOD = 21.65 SEC          CENTER PERIOD = 20.00
NOISE AVE ENV =   14.99          DETECTION RATIO IN DB =   15.09          # OF PTS IN NOISE AVE ENV =   26
**********

COMPONENT # =  2

THE FREQUENCY RANGE 0.0500 TO 0.0500 HZ HAS VELOCITY LIMITS    2.58 TO 3.88 KM/SEC
THE COMPRESSED EDIT HAS  467 NONZERO POINTS
THE NEXT HIGHEST POWER OF TWO IS  512
THE NEW EDIT STARTS    0 SECONDS INTO THE PRIMARY EDIT
THERE ARE 262 SECONDS OF NOISE AT THE FRONT OF THE EDIT
THE NEW EDIT STARTS    0 SECONDS INTO THE GEOTECH EDIT

SUM=   0.324201   C=    0.050000   W=    0.022200
PEAK=  000 PLOT SET  10.000
       140.54   PERIOD= 22.2 SEC    AT TIME=   524.0

LOG10 OF LP AMPLITUDE =  2.24          WITH PERIOD = 22.20 SEC          CENTER PERIOD = 20.00
NOISE AVE ENV =   12.74          DETECTION RATIO IN DB =   22.99          # OF PTS IN NOISE AVE ENV =   67
**********

COMPONENT # =  1

**NOTE: THIS IS A SHORT EDIT**
THE FREQUENCY RANGE 0.0631 TO 0.0631 HZ HAS VELOCITY LIMITS    2.47 TO 3.63 KM/SEC
THE COMPRESSED EDIT HAS  512 NONZERO POINTS
THE NEXT HIGHEST POWER OF TWO IS  512
THE NEW EDIT STARTS    0 SECONDS INTO THE PRIMARY EDIT
THERE ARE 392 SECONDS OF NOISE AT THE FRONT OF THE EDIT
THE NEW EDIT STARTS    0 SECONDS INTO THE GEOTECH EDIT

SUM=   0.330539   C=    0.063100   W=    0.028016
PEAK=  000 PLOT SET  11.000
       61.14   PERIOD= 17.7 SEC    AT TIME=   524.0

LOG10 OF LP AMPLITUDE =  1.72          WITH PERIOD = 17.70 SEC          CENTER PERIOD = 15.85
NOISE AVE ENV =    8.07          DETECTION RATIO IN DB =   16.17          # OF PTS IN NOISE AVE ENV =   39
**********

COMPONENT # =  2

THE FREQUENCY RANGE 0.0631 TO 0.0631 HZ HAS VELOCITY LIMITS    2.48 TO 3.78 KM/SEC
THE COMPRESSED EDIT HAS  504 NONZERO POINTS
THE NEXT HIGHEST POWER OF TWO IS  512
THE NEW EDIT STARTS    0 SECONDS INTO THE PRIMARY EDIT
THERE ARE 296 SECONDS OF NOISE AT THE FRONT OF THE EDIT
THE NEW EDIT STARTS    0 SECONDS INTO THE GEOTECH EDIT

SUM=   0.330539   C=    0.063100   W=    0.028016
PEAK=  000 PLOT SET  12.000
       82.19   PERIOD= 17.8 SEC    AT TIME=   586.0

LOG10 OF LP AMPLITUDE =  1.91          WITH PERIOD = 17.82 SEC          CENTER PERIOD = 15.85
NOISE AVE ENV =   13.03          DETECTION RATIO IN DB =   16.00          # OF PTS IN NOISE AVE ENV =   66
**********
```

FIGURE III-14c

LONG-PERIOD EVENT MEASUREMENT EXAMPLE SHOWING LONG-PERIOD VARIABLE FREQUENCY MAGNITUDE (VFM) $LOG_{10}A$ MEASUREMENTS ON VERTICAL (1) AND TRANSVERSE (2) COMPONENTS (PAGE 3 OF 4)

C.

```
COMPONENT # =  1

**NOTE: THIS IS A SHORT EDIT**
THE FREQUENCY RANGE 0.0794 TO 0.0794 HZ HAS VELOCITY LIMITS    2.47 TO 1.47 KM/SEC
THE COMPRESSED EDIT HAS  503 NONZERO POINTS
THE NEXT HIGHEST POWER OF TWO IS  512
THE NEW EDIT STARTS   18 SECONDS INTO THE PRIMARY EDIT
THERE ARE 400 SECONDS OF NOISE AT THE FRONT OF THE EDIT
THE NEW EDIT STARTS   18 SECONDS INTO THE GEOTECH EDIT

SUM=   0.038429   C=   0.079400   W=   0.035250
PEAK=      000 PLOT SET  13.000
          40.55   PERIOD= 13.4 SEC    AT TIME=   600.0

LOG10 OF LP AMPLITUDE =  1.61          WITH PERIOD = 13.44 SEC          CENTER PERIOD = 12.59
NOISE AVE ENV =    6.43          DETECTION RATIO IN DB =    16.00          # OF PTS IN NOISE AVE ENV =   14
**********************************************************************

COMPONENT # =  2

**NOTE: THIS IS A SHORT EDIT**
THE FREQUENCY RANGE 0.0794 TO 0.0794 HZ HAS VELOCITY LIMITS    2.47 TO 1.72 KM/SEC
THE COMPRESSED EDIT HAS  512 NONZERO POINTS
THE NEXT HIGHEST POWER OF TWO IS  512
THE NEW EDIT STARTS    0 SECONDS INTO THE PRIMARY EDIT
THERE ARE 318 SECONDS OF NOISE AT THE FRONT OF THE EDIT
THE NEW EDIT STARTS    0 SECONDS INTO THE GEOTECH EDIT

SUM=   0.038429   C=   0.079400   W=   0.035250
PEAK=      000 PLOT SET  18.000
          42.70   PERIOD= 14.1 SEC    AT TIME=   600.0

LOG10 OF LP AMPLITUDE =  1.63          WITH PERIOD = 14.15 SEC          CENTER PERIOD = 12.59
NOISE AVE ENV =    5.60          DETECTION RATIO IN DB =    17.65          # OF PTS IN NOISE AVE ENV =    6
**********************************************************************
```

FIGURE III-14c

LONG-PERIOD EVENT MEASUREMENT EXAMPLE SHOWING LONG-PERIOD VARIABLE FREQUENCY MAGNITUDE (VFM) $LOG_{10}A$ MEASUREMENTS ON VERTICAL (1) AND TRANSVERSE (2) COMPONENTS (PAGE 4 OF 4)

d.

```
                DISPLAY OF EVENT HEADER INFORMATION
NO SEISMOGRAM NUMBER
     3 COMPONENTS      DATA LENGTH:   512 POINTS
EVENT DESIGNATION:  52*656LR0003   ARRAY NAME: SRO              DATA TYPE: SPK
DATA RECORD LENGTH:  2048 BYTES
     1 EDITED SITES
SIGNAL  PARTITION       TIME DOMAIN
SOURCE ROUTINE: SSPPOG
DATA ORIENTATION:  RAW
[illegible] CHANNELS PROCESSED:   3
NUMBER OF CHANNELS DELETED:   0
RE-SAMPLED EVERY   2.0 POINTS
DATA TIME:       15130 (SEC)    77305 (YRDAY)     -OR-  DATE 11/ 1/77   TIME  4.12.10
DATA LENGTH: 1024.0 SECONDS
SIGNAL STARTS AT POINT NO.     -280
SOURCE TIME:     14864 (SEC)    77305 (YRDAY)     -OR-  DATE 11/ 1/77   TIME  3.58.24
CONFIDENCE OF SOURCE TIME (PDP CODE):
SOURCE AT LATITUDE  55.30 N.  LONGITUDE  130.80 E.   DEPTH  33.00 (KM.)
ACCORDING TO NEI      , N_R = 4.5   N_S = 0.0   TI ESTIMATED N_S = 0.0
TI ESTIMATED SIGNAL-TO-NOISE RATIO:    0.0 DB.
STD. DEV. OF RESIDUAL TIME:              STATIONS IN PDE REPORTING
REGION = EASTERN RUSSIA          SUB-REGION = 656     NORSAR QUALITY = 0
  P-TIME  P-DAY  S-TIME  S-DAY  LQ-TIME  LQ-DAY  LR-TIME  LR-DAY  LR
    SEC     YR     SEC     YR     SEC      YR      SEC      YR    LENGTH
   14972  77305   14979  77305   15263   77305    15344   77305    561
AZIMUTH  (STATION TO SOURCE):   61.72    (PRIMARY BEAM DIRECTION):    0.0
DISTANCE (STATION TO SOURCE):   46.53 (DEG.)        -OR-          5164.39 (KM.)
          STATION ELEVATION:    0.0  KM.
   SEISMOMETER TYPE:              RECORDING TYPE:
TECTONIC CLASS CODE: AB
LOG AMPLITUDES:  VERTICAL   TRANSVERSE
  10 SECOND        2.22        2.10
  11 SECOND        2.01        2.26
  12 SECOND        1.82        2.11
  13 SECOND        1.58        2.20
  14 SECOND        1.03        2.06
  15 SECOND        1.27        1.81
  16 SECOND        1.27        1.83
  LOG OF 18-22 SECOND A/T:     1.70
SITE NUMBER 52      LATITUDE  34.50 N.   LONGITUDE   69.00 E.

HEADER RECORD WRITTEN ON OUTPUT TAPE ON UNIT 13
COMPONENT  1  TRACE WRITTEN ON OUTPUT TAPE
COMPONENT  2  TRACE WRITTEN ON OUTPUT TAPE
COMPONENT  3  TRACE WRITTEN ON OUTPUT TAPE
```

FIGURE III-14d

LONG-PERIOD EVENT MEASUREMENT EXAMPLE SHOWING LONG-PERIOD EVENT HEADER INFORMATION

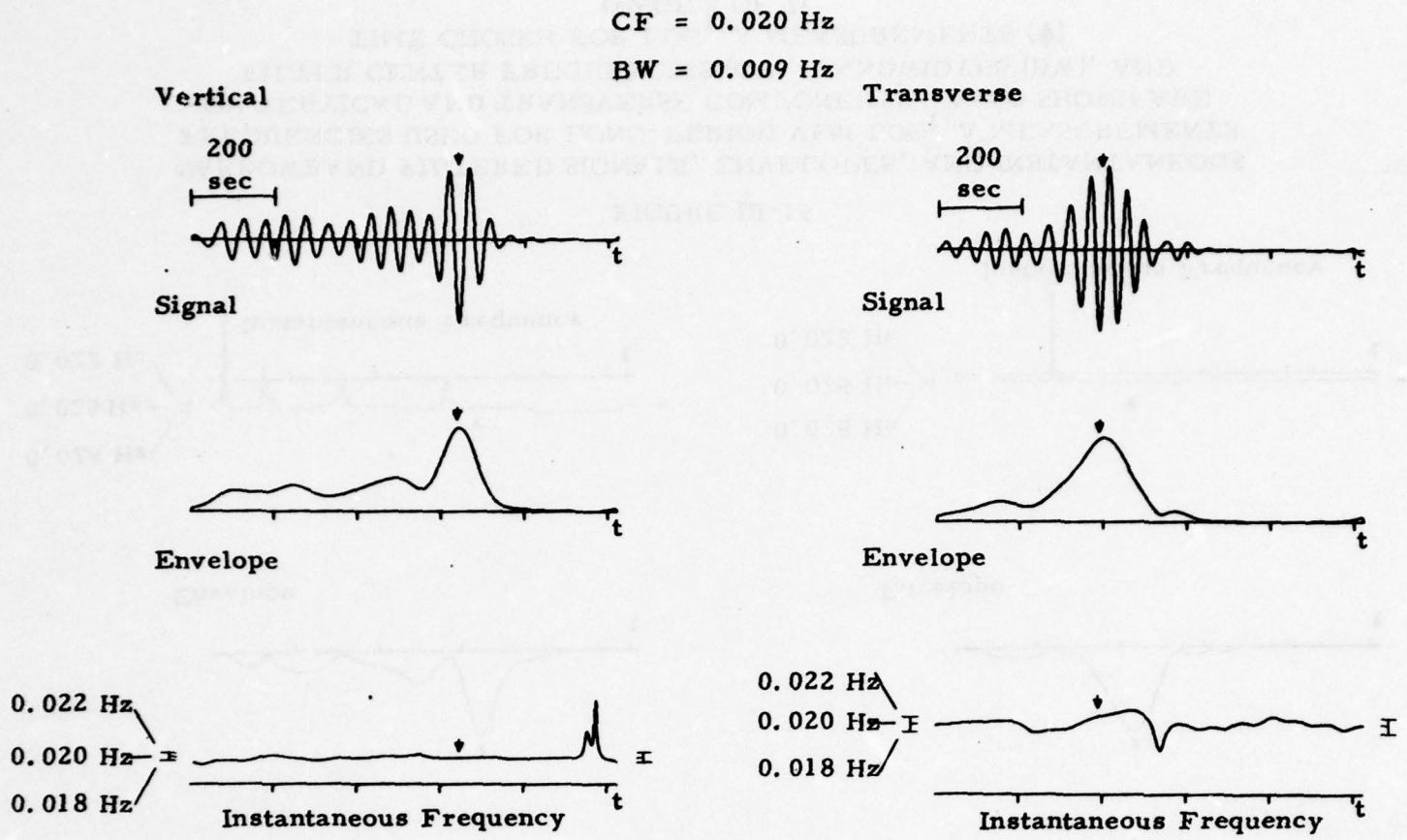

FIGURE III-15

NARROWBAND FILTERED SIGNALS, ENVELOPES, AND INSTANTANEOUS FREQUENCIES USED FOR LONG-PERIOD VFM $LOG_{10}A$ MEASUREMENTS ON VERTICAL AND TRANSVERSE COMPONENTS. ALSO SHOWN ARE FILTER CENTER FREQUENCIES (CF), BANDWIDTHS (BW), AND TIME CHOSEN FOR $LOG_{10}A$ MEASUREMENTS (▼)
(PAGE 1 OF 7)

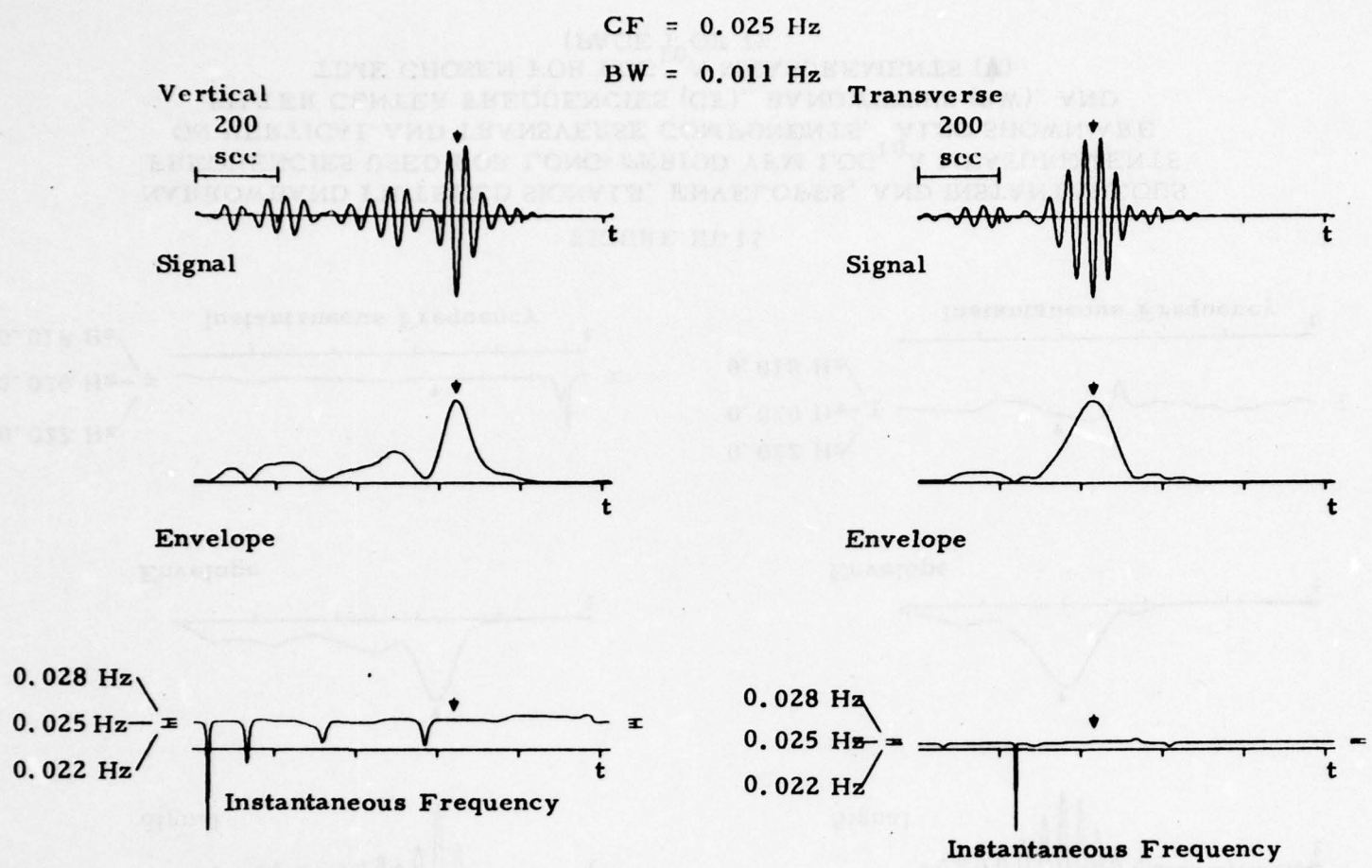

FIGURE III-15

NARROWBAND FILTERED SIGNALS, ENVELOPES, AND INSTANTANEOUS FREQUENCIES USED FOR LONG-PERIOD VFM $LOG_{10}A$ MEASUREMENTS ON VERTICAL AND TRANSVERSE COMPONENTS. ALSO SHOWN ARE FILTER CENTER FREQUENCIES (CF), BANDWIDTHS (BW), AND TIME CHOSEN FOR $LOG_{10}A$ MEASUREMENTS (▼)
(PAGE 2 OF 7)

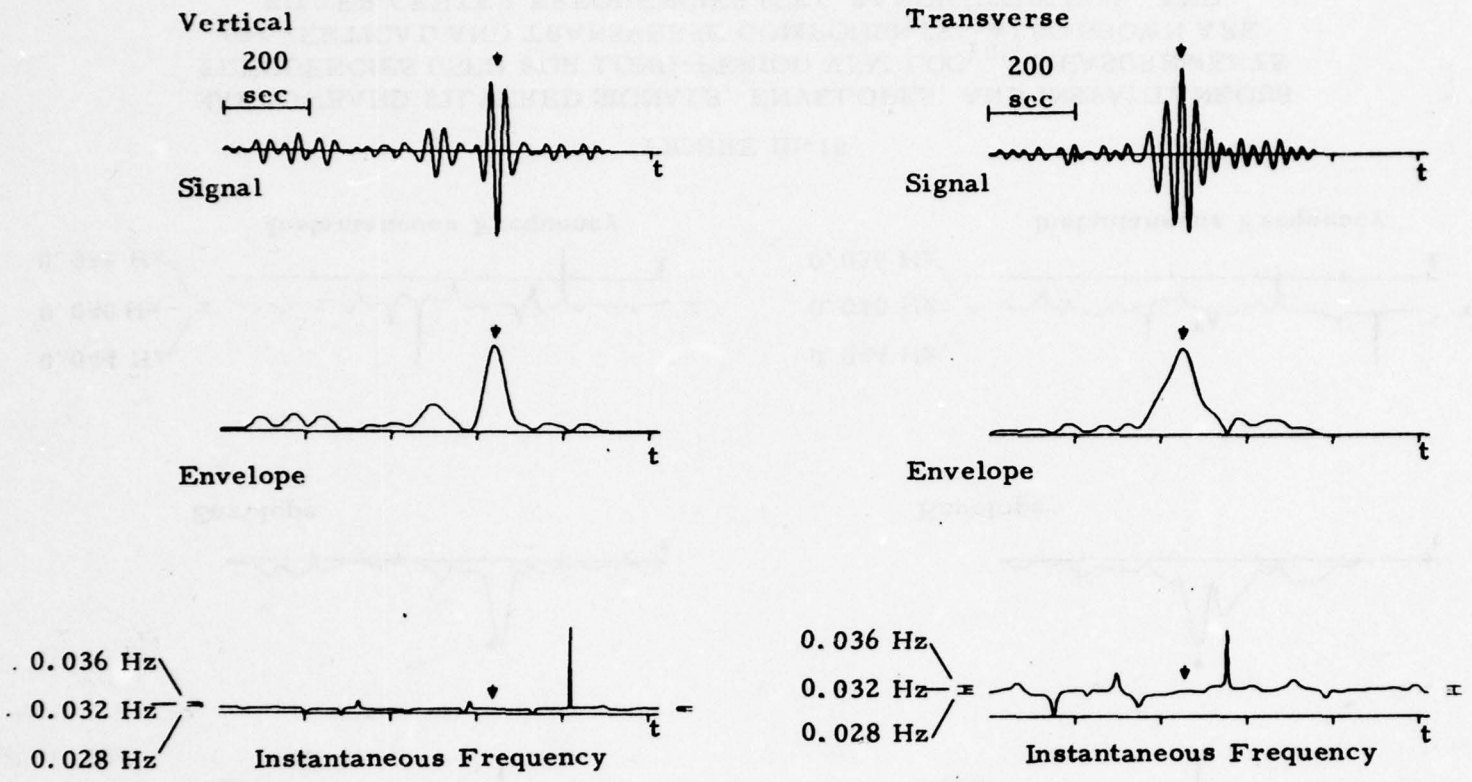

III-51

FIGURE III-15

NARROWBAND FILTERED SIGNALS, ENVELOPES, AND INSTANTANEOUS FREQUENCIES USED FOR LONG-PERIOD VFM $LOG_{10}A$ MEASUREMENTS ON VERTICAL AND TRANSVERSE COMPONENTS. ALSO SHOWN ARE FILTER CENTER FREQUENCIES (CF), BANDWIDTHS (BW), AND TIME CHOSEN FOR $LOG_{10}A$ MEASUREMENTS (▼)
(PAGE 3 OF 7)

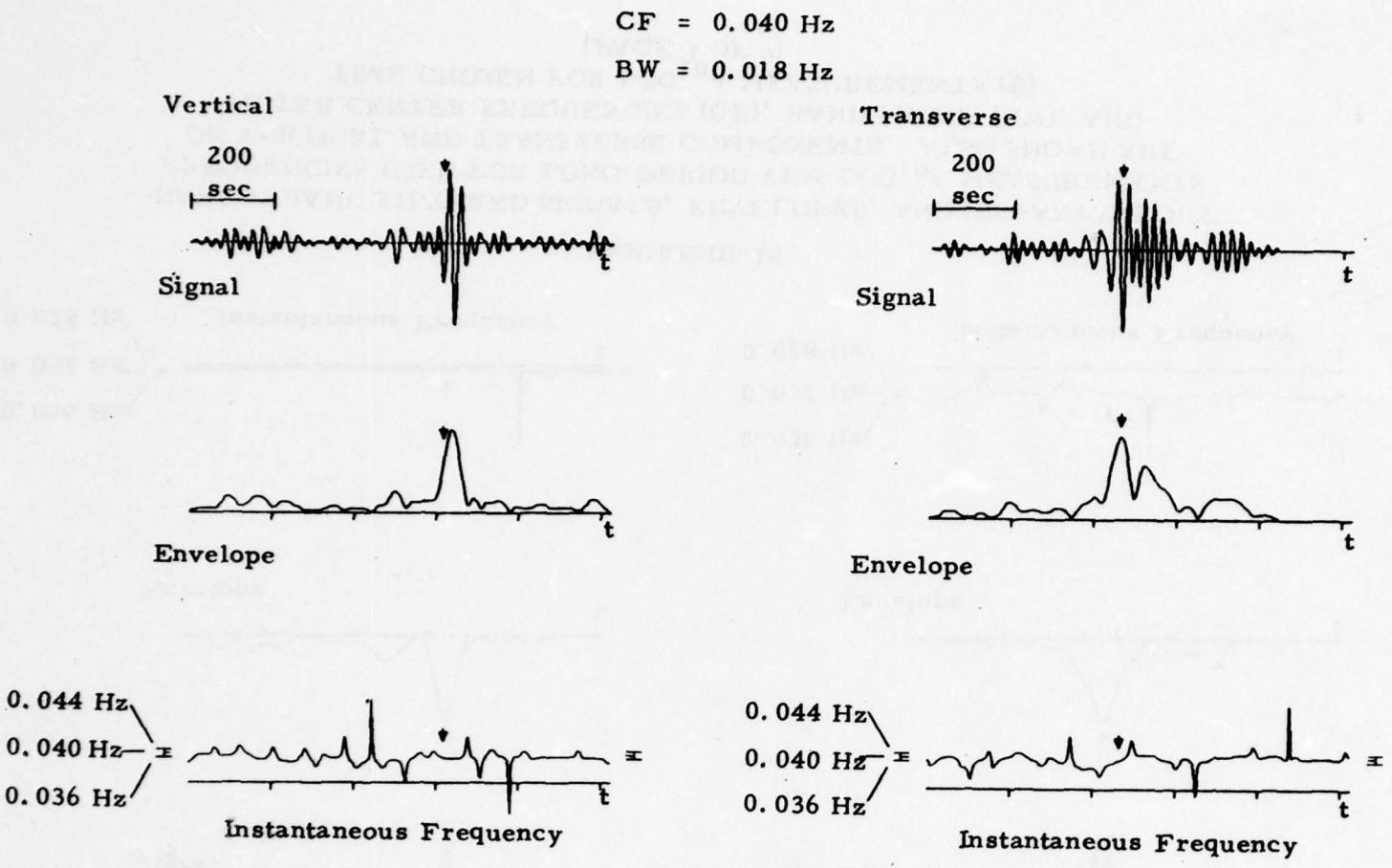

FIGURE III-15

NARROWBAND FILTERED SIGNALS, ENVELOPES, AND INSTANTANEOUS FREQUENCIES USED FOR LONG-PERIOD VFM $LOG_{10}A$ MEASUREMENTS ON VERTICAL AND TRANSVERSE COMPONENTS. ALSO SHOWN ARE FILTER CENTER FREQUENCIES (CF), BANDWIDTHS (BW), AND TIME CHOSEN FOR $LOG_{10}A$ MEASUREMENTS (▼)
(PAGE 4 OF 7)

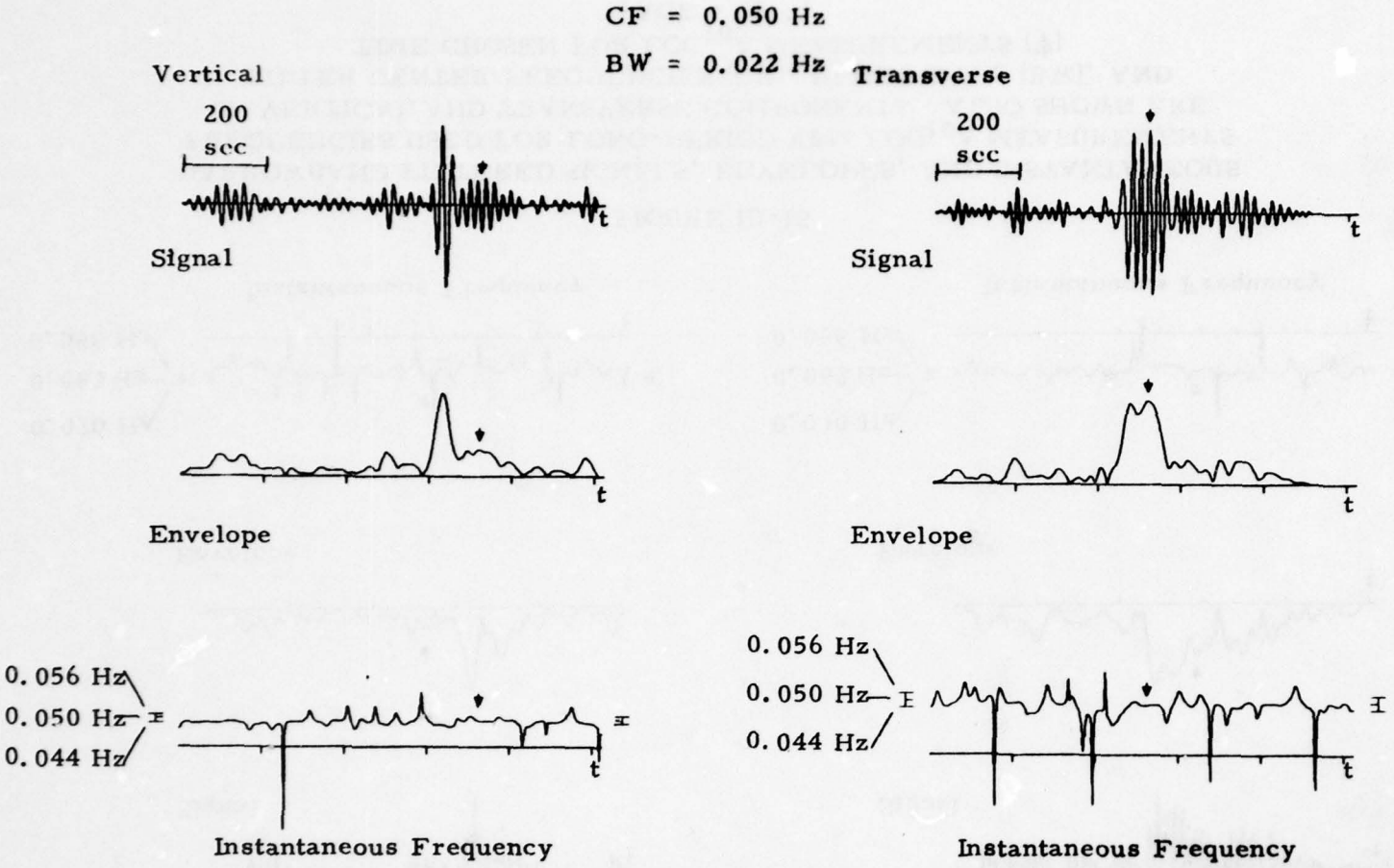

FIGURE III-15

NARROWBAND FILTERED SIGNALS, ENVELOPES, AND INSTANTANEOUS FREQUENCIES USED FOR LONG-PERIOD VFM $LOG_{10}A$ MEASUREMENTS ON VERTICAL AND TRANSVERSE COMPONENTS. ALSO SHOWN ARE FILTER CENTER FREQUENCIES (CF), BANDWIDTHS (BW), AND TIME CHOSEN FOR $LOG_{10}A$ MEASUREMENTS (▼)
(PAGE 5 OF 7)

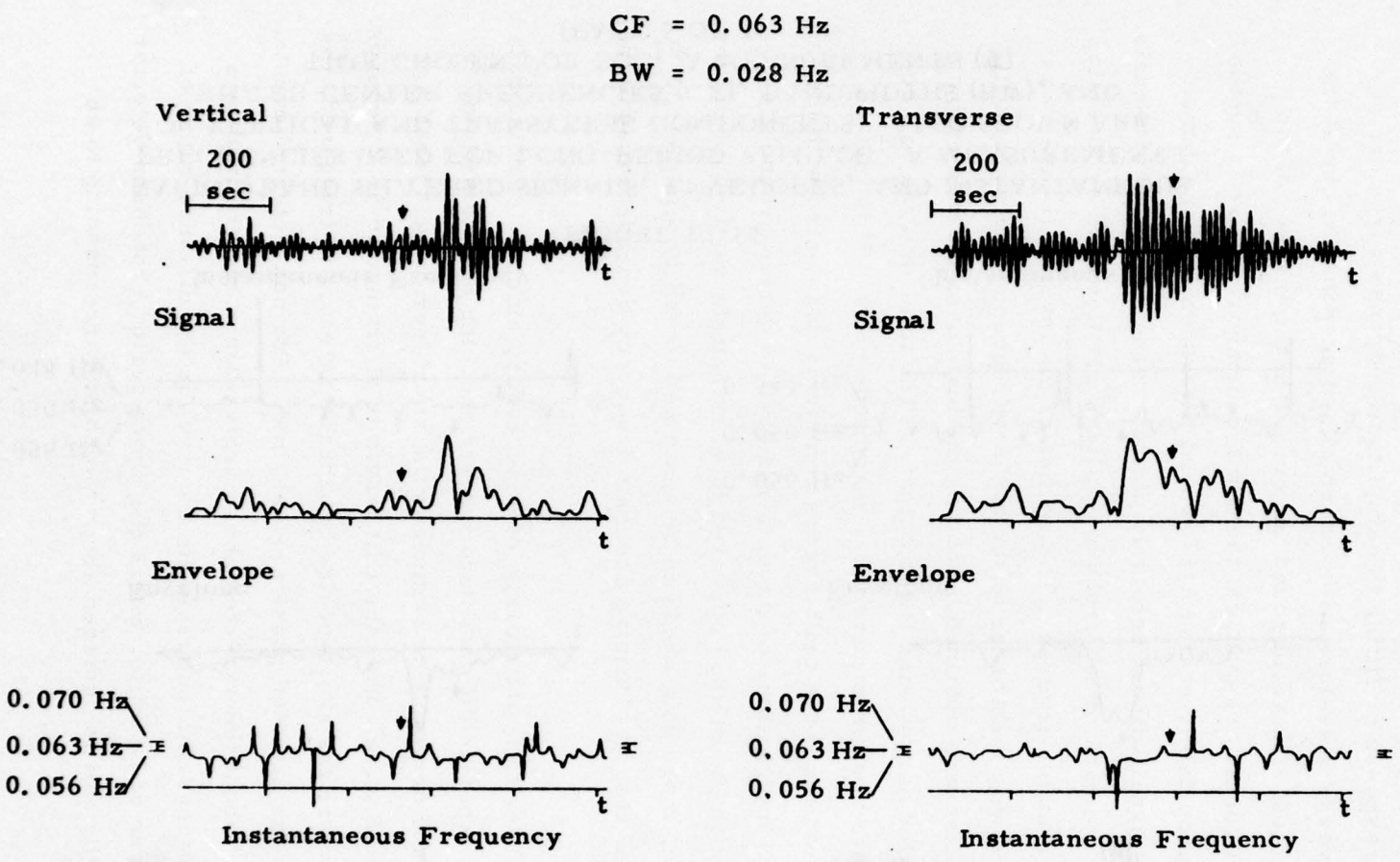

FIGURE III-15

NARROWBAND FILTERED SIGNALS, ENVELOPES, AND INSTANTANEOUS FREQUENCIES USED FOR LONG-PERIOD VFM $LOG_{10}A$ MEASUREMENTS ON VERTICAL AND TRANSVERSE COMPONENTS. ALSO SHOWN ARE FILTER CENTER FREQUENCIES (CF), BANDWIDTHS (BW), AND TIME CHOSEN FOR $LOG_{10}A$ MEASUREMENTS (▼)
(PAGE 6 OF 7)

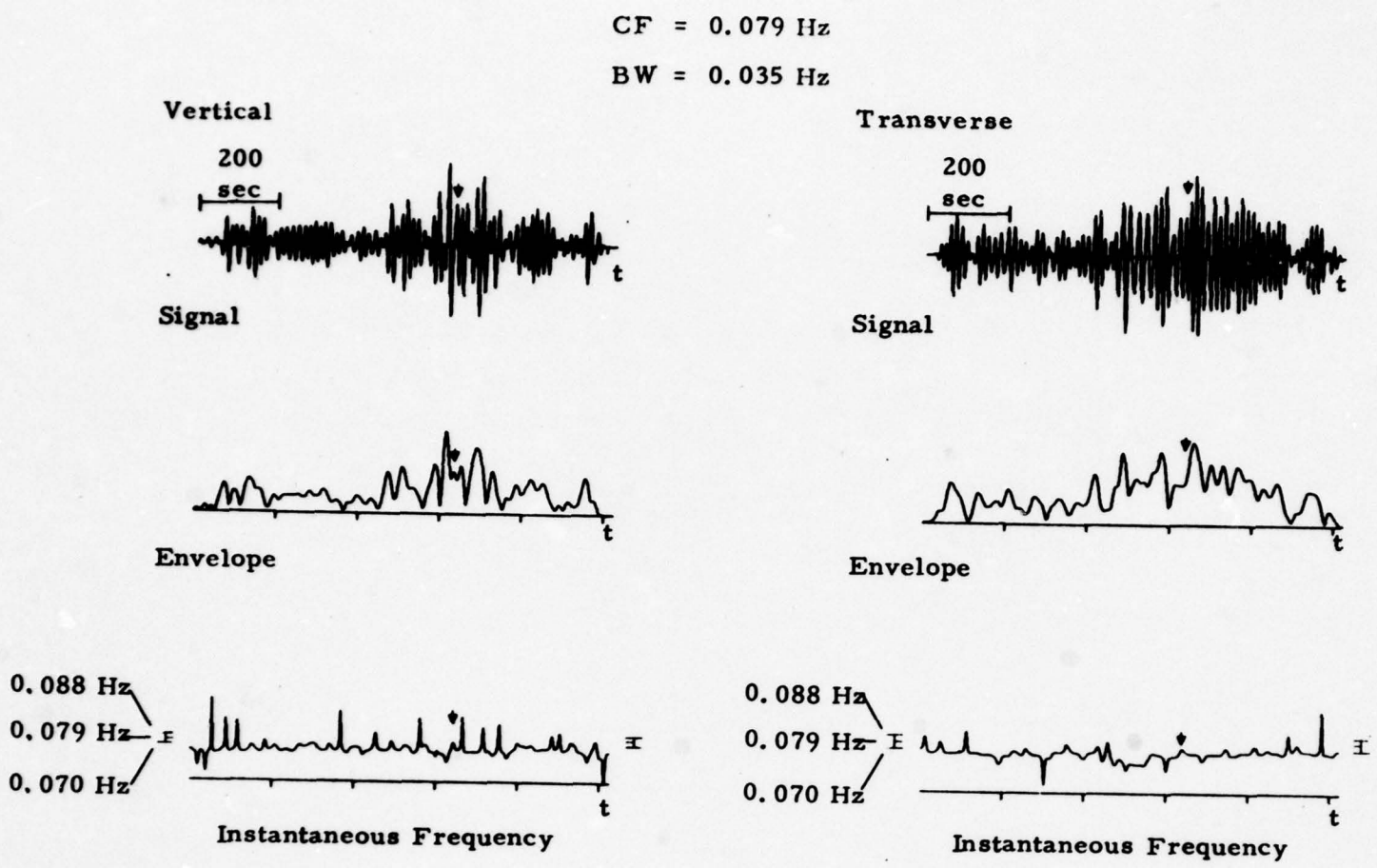

FIGURE III-15

NARROWBAND FILTERED SIGNALS, ENVELOPES, AND INSTANTANEOUS FREQUENCIES USED FOR LONG-PERIOD VFM $LOG_{10}A$ MEASUREMENTS ON VERTICAL AND TRANSVERSE COMPONENTS. ALSO SHOWN ARE FILTER CENTER FREQUENCIES (CF), BANDWIDTHS (BW), AND TIME CHOSEN FOR $LOG_{10}A$ MEASUREMENTS (▼)
(PAGE 7 OF 7)

SECTION IV

MULTIVARIATE DISCRIMINATION

The purpose of this section is to discuss a statistical process called Multivariate Discrimination, and techniques for applying that process to a large Event Discriminant Data Base (EDDB), in an effort to solve the event identification problem. The section begins with an overview presenting the methodology of applying multivariate discrimination to the event identification problem. It continues with a detailed description of the EDDB and its creation and maintenance as an integral part of the Extended Interactive Seismic Processing System (ISPSE) on the PDP-15/50 computer. In addition the analysis, implementation, and execution of a discrimination algorithm to yield event identifications are discussed. The algorithm is implemented by means of the Interactive Seismic Programming Language (ISPL) which facilitates access to the EDDB (Shaub et al., 1977). This section concludes with a series of figures illustrating a typical session on the Event Identification System.

A. OVERVIEW

The Event Identification System was created for the purpose of automatically generating signal waveform edits and measurements to provide a data base for calculating event discriminants and for classifying the type of event source indicated by the discriminant measurements. Since a ground rule of this task was to classify the event without prior knowledge of the discriminant characteristics of a particular source region, that is without any training data, the identification system was designed to adaptively isolate abnormal events and build up a class of such similar events as other events of similar discriminant pattern become available.

Past research has indicated that most discriminants are highly influenced by the tectonic region of the source. By reciprocity, it might be presumed they are also influenced by the tectonic region of the receiver since the source and receiver tectonics convey information on the crustal and upper mantle structure traversed by the raypaths. For example, both Sax (1976) and Unger (1978a) showed that the pattern of short-period discriminants were completely different for presumed explosion events from eastern Kazakh, which is a tectonically active mountainous region, and the Nevada Test Site, which is located in a rift zone. To take care of this situation in the event classification system, all signals of an event are characterized in the header by a class code to indicate the tectonic classification of the source and receiver. This can be used either to derive corrections to the signal measurements or to derive separate tectonic class population means and standard deviations of the discriminants derived from signals.

A provision is made in the system to visually inspect waveforms for the purpose of checking the automatic algorithms used to window and detect signals. As a result of the visual inspection, the data of an event can be prepared again to assure appropriate selection of windows and detection threshold. Also, based on selected manual runs of the signal measurements, the signal measurement files and detection status of the measurements can be edited. This quality control process is considered an important feature of the system.

The generation of event discriminants from magnitude measurements of signals observed at a set of stations is done by applying the method of Ringdal (1974). The method yields an unbiased maximum likelihood estimate of the mean magnitude from measurements of detected and non-detected signals. Other signal measurements are processed to obtain an event representation of the station discriminants derived from signal measurements. The resultant event discriminants are deposited as new data in the event

discriminant files. In case of changes in the methodology for computing a discriminant, old discriminant data can be retrieved, corrected, and re-deposited. The function process for classifying the event source is an adaptive part of the event identification system. The classification procedure is started by determining the average discriminant vector and its standard deviation for a set of 'normal' shallow earthquake events. Each unknown event is compared to the average earthquake discriminant vector. If the event is anomalous, it is compared to other anomalous events which are sub-divided into sets based on a measure of similarity. If it does not fit into any of the prior determined sets of anomalous events, it is held as a singular event until enough events are obtained to set up a new class of anomalous events. The discrimination capability is assessed by correlating the groupings with known or presumed earthquakes.

Figure IV-1 illustrates the event identification system as four function processes operating on common permanent disk files of seismic data. The files are accessed by any user of the system. The classification status of the events in the files evolve as more data are entered into the system and as the discriminant data files are subjected to more classification processing. The classification is objective given prescribed threshold criteria for declaring an event anomalous and for grouping anomalous events. The function which prepares discriminant data by automatically editing events and detecting signals is performed on the IBM 360/44 computer. The functions which generate event discriminants and classify the event sources are performed on the PDP-15/50 computer.

B. THE EVENT DISCRIMINANT DATA BASE

The structure, creation, and maintenance of the Event Discriminant Data Base (EDDB) is discussed in this subsection. The EDDB is resident on the ten megaword disk drive of the PDP-15/50 computer and is

FUNCTION PROCESS BLOCK DIAGRAM

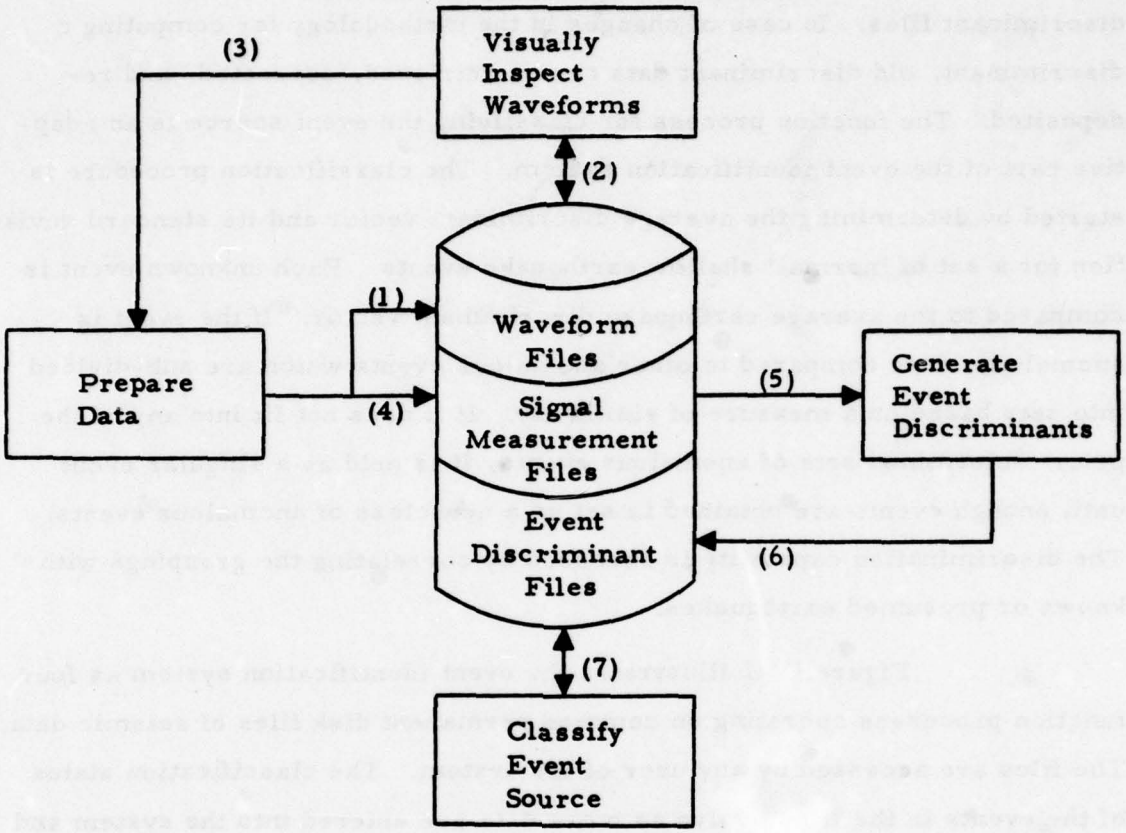

ACTIONS

(1) Deposit waveform edits on disk for visual inspection.

(2) Spot check the detection status of signals. Revise the detection status, if necessary.

(3) Spot check the signal edit windows. Re-prepare data, if necessary.

(4) Deposit automatically determined signal measurements into permanent seismic measurement files.

(5) Reduce signal measurements to a set of unbiased estimates of the event's discriminant vector.

(6) Deposit estimates of the event's discriminants into the event discriminant files.

(7) Classify the event type, if possible, otherwise update its process status and try again when more event data are available.

FIGURE IV-1

EVENT IDENTIFICATION SYSTEM

supported by the Extended Interactive Seismic Processing System (ISPSE) which executes on that machine (Shaub et al., 1977). The principal items comprising the EDDB are vectors of discriminant measurements obtained by preprocessing waveform data from various recording stations.

1. Description of the EDDB

The general organization of the Event Discriminant Data Base (EDDB) is shown in Figure IV-2. Note that it consists of four file types, namely:

- An Event Directory
- Raw Event Discriminant Data Files
- Averaged Event Discriminant Class Files
- A Class Directory File.

These files are physically compatible in that they are easily accessed via the DREAD and DWRIT statements featured by the Interactive Seismic Programming Language (ISPL). (Subsection IV-C-5, The Extended Interactive Seismic Processing System (ISPSE), Shaub et al., 1977.)

EDDB structure is based primarily on three attributes: event sequence number, station designation, and tectonic class code. When an event is recorded in the Event Directory it is assigned a sequence number. For each event so recorded, at the most fifty discriminant vector entries, corresponding to fifty reporting stations, reside in one or two Raw Event Discriminant Data Files. The Event Directory groups these entries by pointing to Raw Event Discriminant Data File locations holding discriminant vectors for stations belonging to the same tectonic class.

Currently, there are three tectonic classes in the EDDB; 'A'= active, 'I'=inactive, and 'R'=rift. Hence, the tectonic class code for an event with epicenter in an 'A' zone which is recorded at a station in an 'I' zone is 'AI'. Codes derived in this way are also called event-station class by class

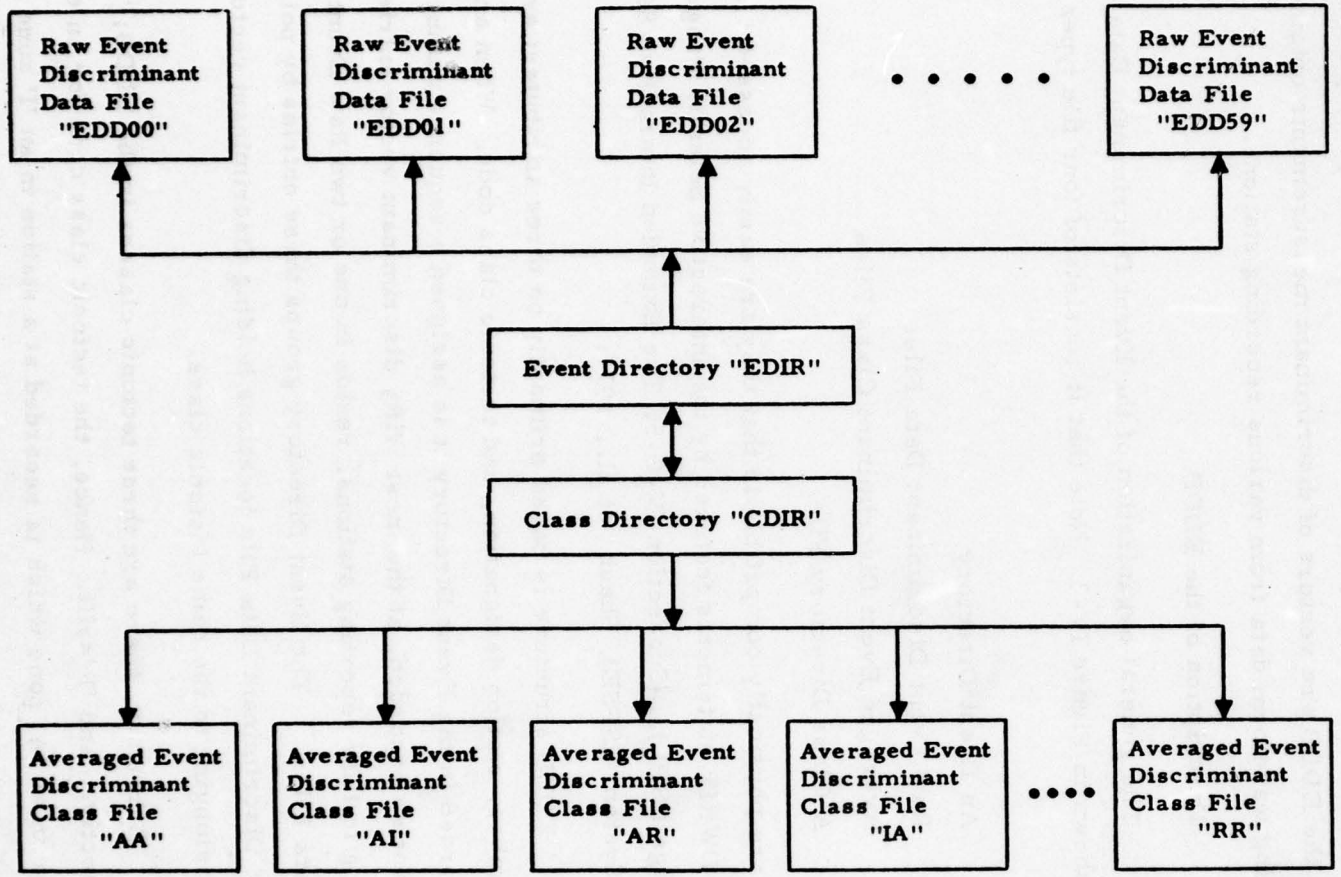

FIGURE IV-2

GENERAL ORGANIZATION OF EVENT DISCRIMINANT DATA BASE (EDDB)

codes and are the names given to the Averaged Event Discriminant Class Files. These files contain average discriminant vector entries, one per event, computed as an unbiased mean (Ringdal, 1975) of the discriminant vectors for all reporting stations belonging to the same tectonic class. Therefore, if an event is reported by stations spanning all three tectonic classes, it will appear in three Averaged Event Discriminant Class Files.

To unify the above concepts, consider the remaining EDDB file type, the Class Directory. The Class Directory is partitioned by the nine tectonic class codes. Within each partition, the corresponding Averaged Event Discriminant Class File name is recorded, together with a vector of Event Directory sequence numbers. This vector specifies which events belong to that file and their locations within the file.

With an overview of the EDDB structure in mind, detailed descriptions of the four file types noted will now be presented.

a. Event Directory

The structure of the Event Directory is shown in Figure IV-3. A representative entry to the Event Directory is comprised of attributes which may be defined as follows:

- Event Sequence Number - An integer J, $1 \leq J \leq 199$, assigned to an event when it is recorded in the Event Directory. For example, the fifth event recorded is assigned the event sequence number 5.
- Event Designation Number - The unique four digit number appearing as the last four characters of the TI alphanumeric event designation.
- Event Class Code - The tectonic class ('A', 'I', or 'R') of the zone in which the event's epicenter is located.

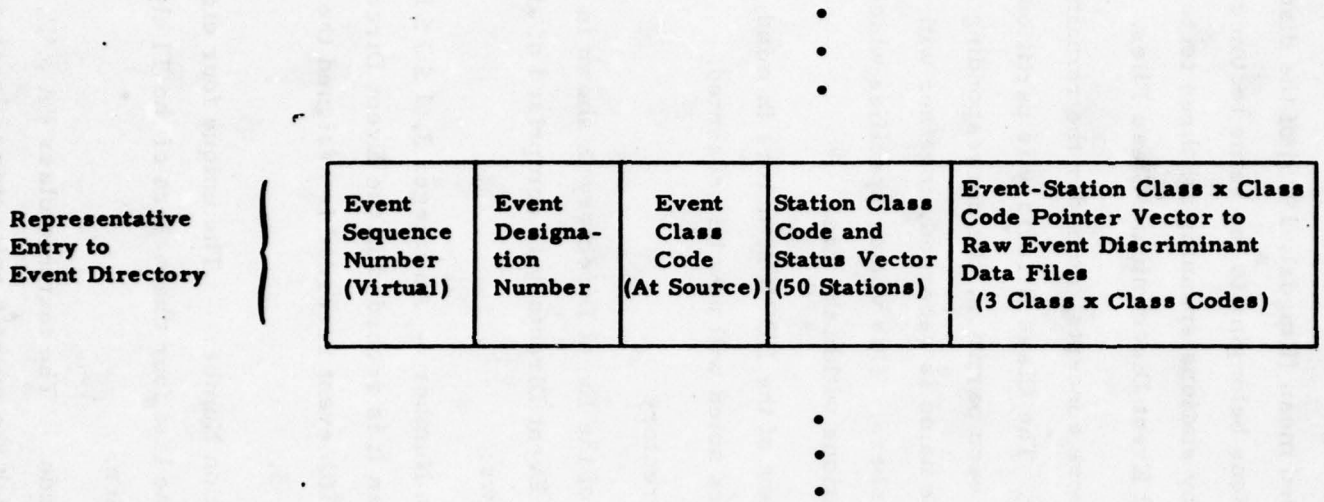

FIGURE IV-3

STRUCTURE OF THE EVENT DIRECTORY

- Station Class Code and Status Vector - A fifty character string where each character represents the tectonic class ('A', 'I', or 'R') of the associated reporting station. The character 0 indicates that the station did not report the event.

- Event Station Class by Class Code Pointer Vector - A vector whose elements point to Raw Event Discriminant Data File locations holding discriminant vectors that have the same event-station class by class code. Elements are partitioned by at the most three different codes.

In addition to the above information, the Event Directory also contains a header record specifying the total number of events in the directory, the number of Raw Event Discriminant Data Files utilized for discriminant vector entries, and the largest Event Sequence Number appearing in the Class Directory. These parameters are necessary for EDDB maintenance functions to be discussed in this subsection.

b. Raw Event Discriminant Data Files

All the Raw Event Discriminant Data Files have the same structure as shown in Figure IV-4. A representative Raw Event Discriminant Data File entry is comprised of attributes which may be defined as follows:

- Discriminant Vector - Array of discriminant measurements obtained by preprocessing waveform data from various recording stations. The array is partitioned in four categories depending on the type of data from which the discriminants are derived, namely, long-period signals/noise, short-period regional signal/noise, short-period teleseismic signals/noise, and short-period signals/noise.

- Discriminant Status Vector - Five element array of ones and zeros indicating that discriminants derived from various data

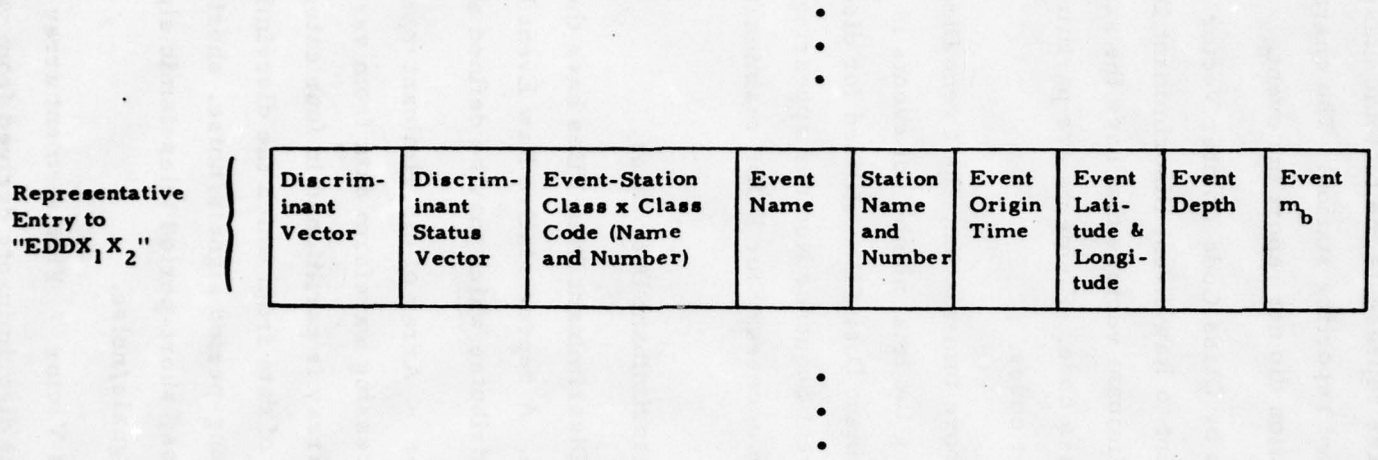

FIGURE IV-4

STRUCTURE OF A RAW EVENT DISCRIMINANT DATA FILE: "EDDX$_1$X$_2$"

types are present or absent in the discriminant vector. The data types are defined as follows; long-period signal, long-period noise, short-period signal, short-period noise, and regional teleseismic.

- Event-Station Class by Class Code - Tectonic class code derived by combining the event class code with the tectonic class of the reporting station, e.g., 'AI'.
- Event Name - The TI alphanumeric event designation.
- Station Name and Number - The TI alphanumeric station designation together with its assigned integer number K, $1 \leq K \leq 30$.
- Event Origin Time - Source time in 'YY DDD HH MM SS'.
- Event Latitude and Longitude - Source latitude and longitude in degrees, N(+), S(-), E(+), and W(-).
- Event Depth - Source depth in km.
- Event m_b - Event magnitude.

c. Averaged Event Discriminant Class Files

All the Averaged Event Discriminant Class Files have the same structure as shown in Figure IV-5. A representative Averaged Event Discriminant Class File entry is comprised of attributes which may be defined as follows:

- Average Discriminant Vector - The unbiased mean (Ringdal, 1975) of all discriminant vectors having the same event-station class by class code for the given event.
- Cumulative Discriminant Status Vector - The sum of all discriminant status vectors having the same event-station class by class code for the given event.

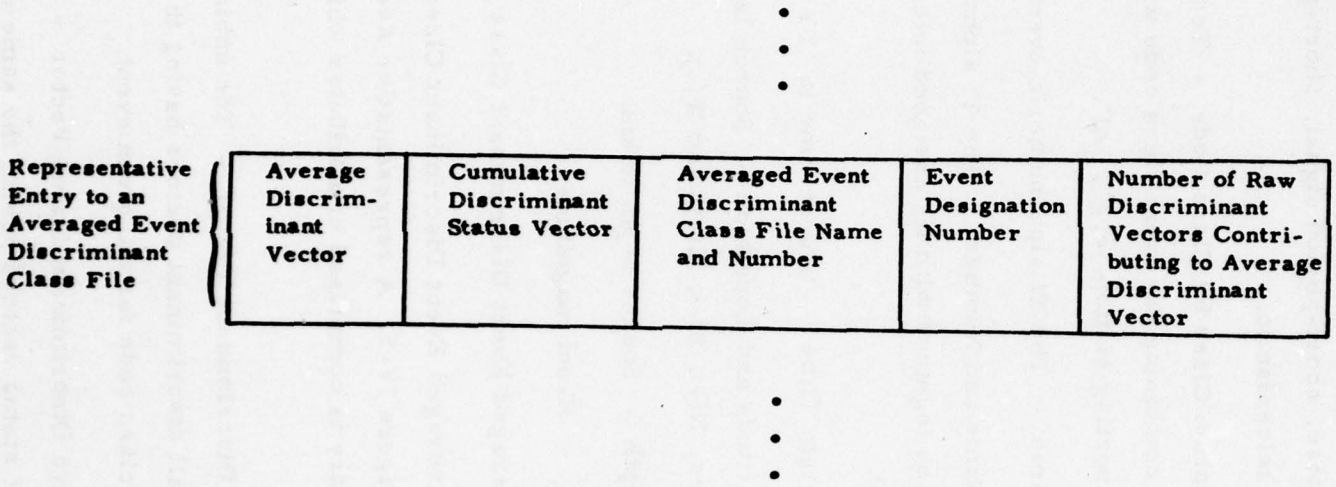

FIGURE IV-5

STRUCTURE OF AN AVERAGED EVENT DISCRIMINANT CLASS FILE

- Averaged Event Discriminant Class File Name and Number - The tectonic class code ≡ event-station class by class code associated with this file, e.g., 'AI'.
- Event Designation Number - The unique four digit number appearing as the last four characters of the TI alphanumeric event designation.
- Number of Raw Discriminant Vectors Contributing to Average Discriminant Vector - Self defining.

d. Class Directory

The structure of the Class Directory is shown in Figure IV-6. Note that all attributes comprising a representative entry to the Class Directory are either self-defining or have been previously defined in connection with other EDDB files.

2. Creation of the EDDB

The Event Discriminant Data Base (EDDB) is generated from seven track Discriminant Tapes produced by the seismic data preparation software on the IBM 360/44 computer (Schmidt, 1978). A detailed description of the individual discriminant measurements stored on these tapes and the algorithms from which the measurements are derived may be found in Section III of this report.

The off-line PDP-15/50 program DDBASE reads the seven track Discriminant Tapes and initializes the EDDB Event Directory and Raw Event Discriminant Data Files discussed in Subsection IV-B-1. The general flow of DDBASE is shown in Figure IV-7. Note that the DDBASE initializes the EDDB one event at a time, hence new events may be continually added to the data base as they are processed.

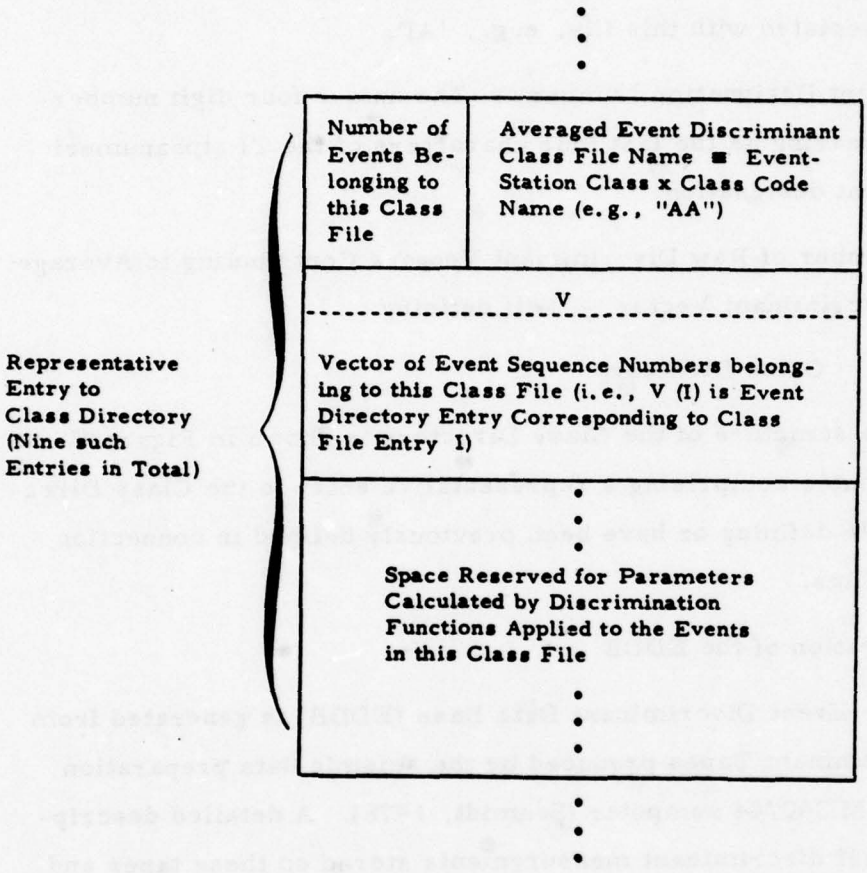

FIGURE IV-6

STRUCTURE OF THE CLASS DIRECTORY

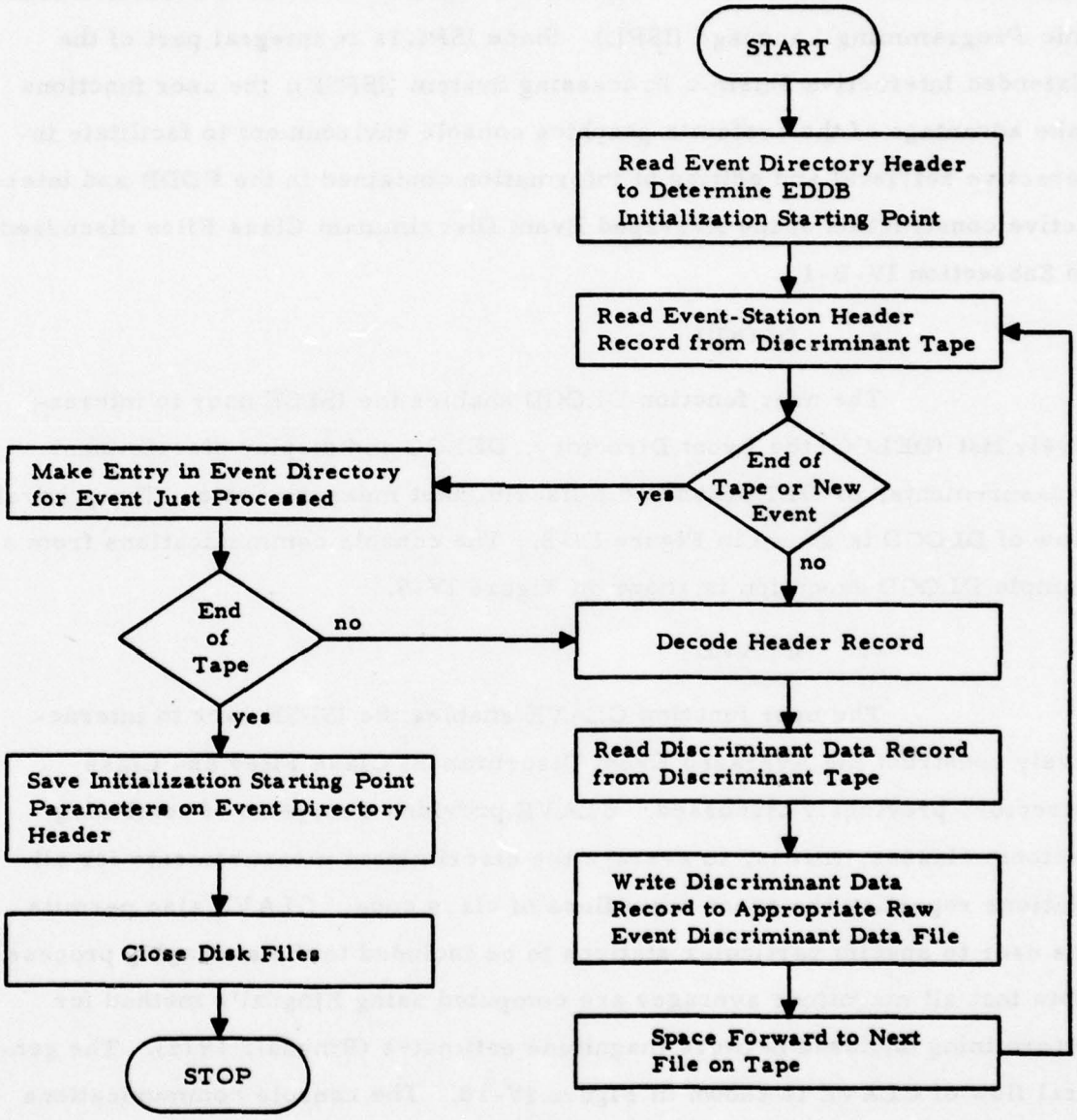

FIGURE IV-7

GENERAL FLOW OF DDBASE

3. Maintenance of the EDDB

Subsequent to EDDB initialization by means of DDBASE, the data base is maintained by user functions programmed in the Interactive Seismic Programming Language (ISPL). Since ISPL is an integral part of the Extended Interactive Seismic Processing System (ISPSE), the user functions take advantage of the system's graphics console environment to facilitate interactive retrieval and editing of information contained in the EDDB and interactive construction of the Averaged Event Discriminant Class Files discussed in Subsection IV-B-1.

a. DLOGD

The user function DLOGD enables the ISPSE user to interactively list (DELOG) the Event Directory, DELOG and display discriminant measurements, or DELOG and edit discriminant measurements. The general flow of DLOGD is shown in Figure IV-8. The console communications from a sample DLOGD execution is shown in Figure IV-9.

b. CLAVE

The user function CLAVE enables the ISPSE user to interactively construct the Averaged Event Discriminant Class Files and Class Directory previously discussed. CLAVE provides the option of combining tectonic classes, that is, to average the discriminant measurements for all stations reporting the event regardless of class code. CLAVE also permits the user to specify particular stations to be included in the averaging process. Note that all magnitude averages are computed using Ringdal's method for determining unbiased network magnitude estimates (Ringdal, 1975). The general flow of CLAVE is shown in Figure IV-10. The console communications from a sample CLAVE execution is shown in Figure IV-11.

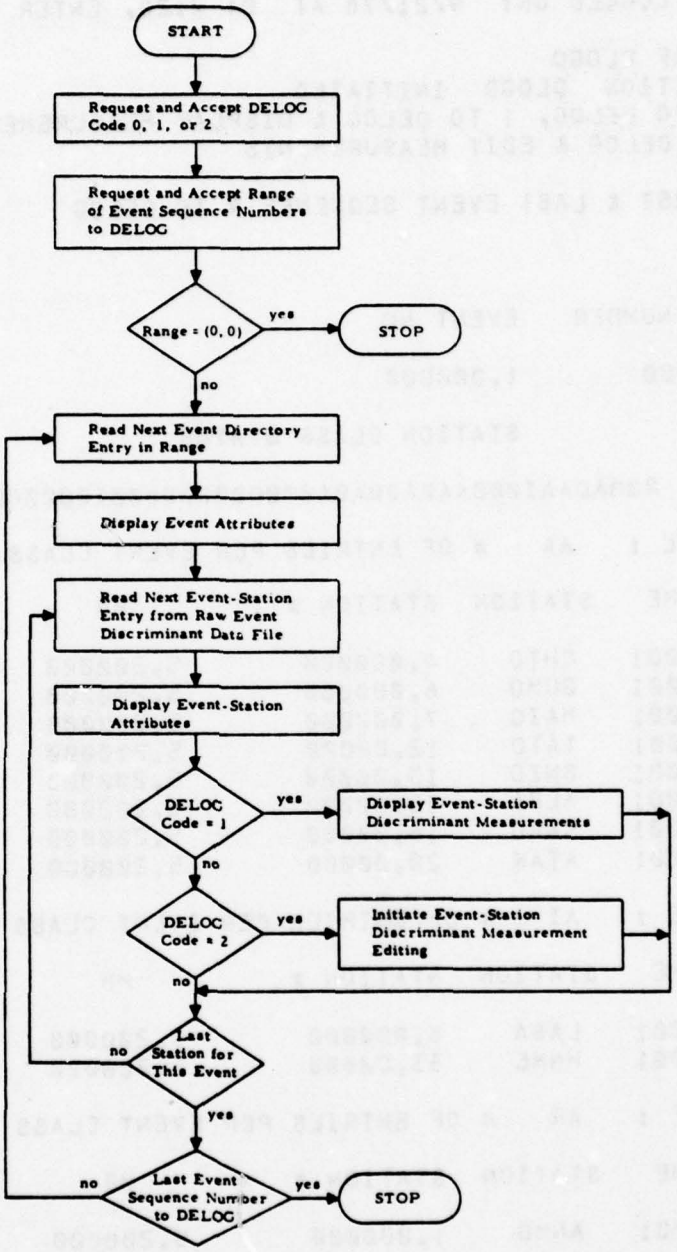

FIGURE IV-8

GENERAL FLOW OF DLOGD

```
TI-ISPSE LOGGED ON:  9/21/78 AT  0: 0:28, ENTER COMMAND OR ,HELP

.... ,PERF DLOGD
USER FUNCTION  DLOGD  INITIATED
ENTER 0 TO DELOG, 1 TO DELOG & DISPLAY MEASUREMENTS,
AND 2 TO DELOG & EDIT MEASUREMENTS
.... 0
ENTER FIRST & LAST EVENT SEQUENCE # TO DELOG
.... 1
.... 1

SEQUENCE NUMBER    EVENT NO

   1.000000        1,000000

CLASS              STATION CLASS STATUS

A          R00AOAAI000AA0A00A0A0000000000000I0000000000000000000

CLASS CODE :   AA   # OF ENTRIES PER EVENT CLASS :   8,000000

 EVENT NAME   STATION  STATION #          MB          DEPTH

33*726SP0001   CHTO    4,000000        5,200000       0,0000000
35*726LR0001   GUMO    6,000000        5,200000       0,0000000
36*726SP0001   MAIO    7,000000        5,200000       0,0000000
41*726LR0001   TATO    12,00000        5,200000       0,0000000
42*726LR0001   SNZO    13,00000        5,200000       0,0000000
44*726LR0001   ALPA    15,00000        5,200000       0,0000000
52*726SP0001   KAAO    18,00000        5,200000       0,0000000
54*726LR0001   ATAK    20,00000        5,200000       0,0000000

CLASS CODE :   AI   # OF ENTRIES PER EVENT CLASS :   2,000000

 EVENT NAME   STATION  STATION #          MB          DEPTH

37*726SP0001   LASA    8,000000        5,200000       0,0000000
12*726SP0001   HNME    33,00000        5,200000       0,0000000

CLASS CODE :   AR   # OF ENTRIES PER EVENT CLASS :   1,000000

 EVENT NAME   STATION  STATION #          MB          DEPTH

30*726SP0001   ANMO    1,000000        5,200000       0,0000000
```

FIGURE IV-9

SAMPLE DLOGD EXECUTION

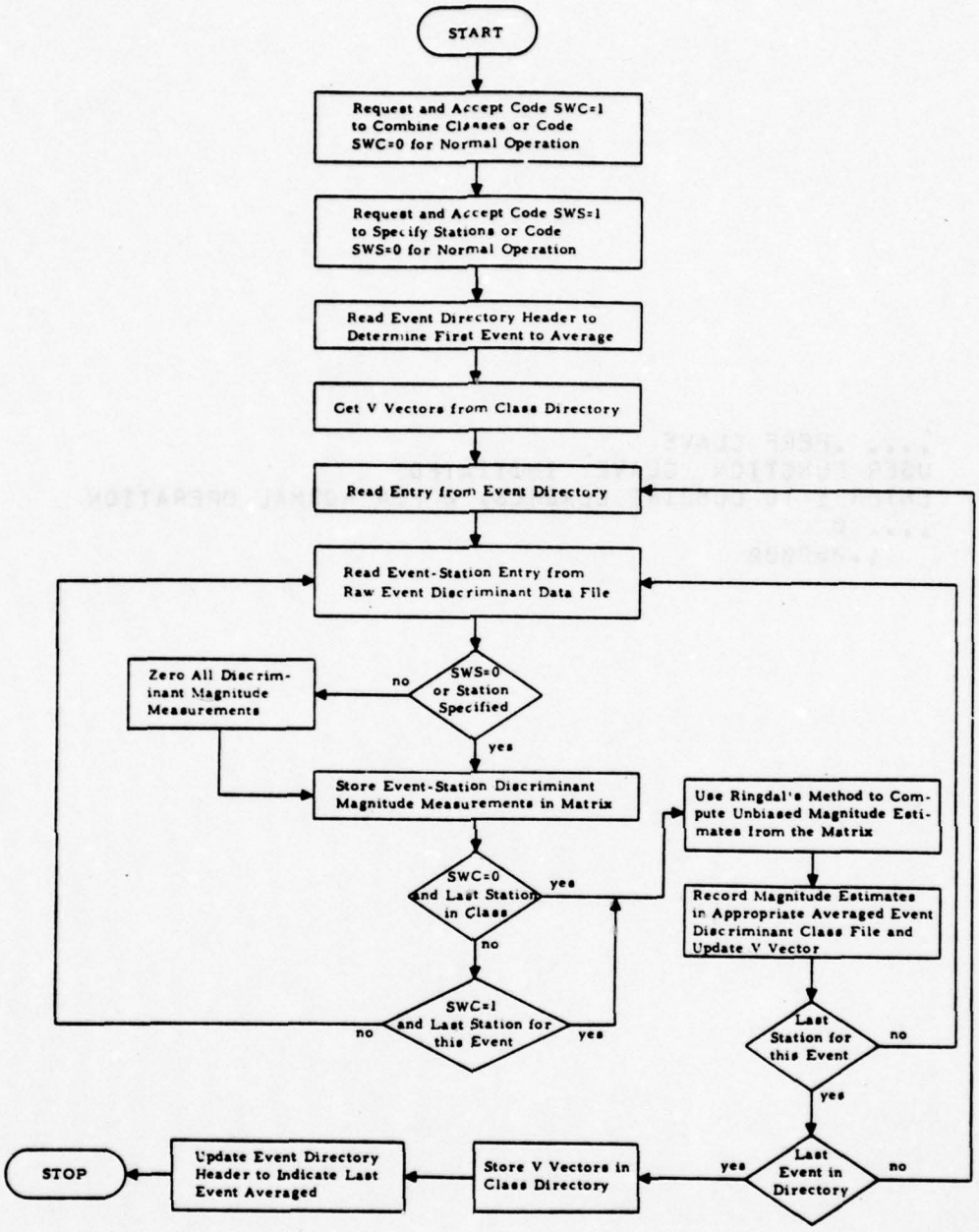

FIGURE IV-10

GENERAL FLOW OF CLAVE

```
.... .PERF CLAVE
USER FUNCTION  CLAVE  INITIATED
ENTER 1 TO COMBINE CLASSES, 0 FOR NORMAL OPERATION
.... 0
   1.000000
```

FIGURE IV-11

SAMPLE CLAVE EXECUTION

C. APPLICATION OF DISCRIMINATION OPERATORS TO THE EVENT DISCRIMINANT DATA BASE (EDDB)

The purpose of this section is to describe an event identification algorithm for classifying events either as earthquakes or as possible explosions, and to provide a description of the software designed for implementation of that algorithm. A multivariate approach is taken to the problem of event identification in this study. The basis for the event identification algorithm is the hypothesis that given a statistically representative set of normal earthquakes, it is possible to identify anomalous events by their deviation from the mean of the base set. To this end, z-statistics relative to the means and standard deviations of the discriminants over the earthquake set are calculated, and correlation terms are computed between events. Threshold tests are then used to classify the events on the basis of these correlation terms.

The Event Discriminant Data Base (EDDB) management system allows the analyst to look at the edited signal phases from which the discriminant measurements were derived for a particular event-station pair. This is done with the aid of the system functions DPSCAN, SELEV, and FILTER described by Ringdal et al. (1975). With these functions it is possible to select any phase desired and to study any frequency band of interest. It is also possible to develop user functions to make independent measurements of the various quantities used to calculate the discriminants. These capabilities, together with the (previously mentioned) EDDB maintenance functions discussed in Subsection IV-B provide the system with a large degree of flexibility. Specifically, an analyst may easily override machine decisions and/or measurements and substitute his own. Note that editing operations via DLOGD should be done before performing the user function CLAVE to calculate the average unbiased measurements for each event.

The multivariate analysis user functions for event identification operate on the average class files which have been generated by the user function CLAVE. The actual discriminant values are calculated from the average event measurements and employed in identifying the events. The discriminants and their positions in the class file records are listed in Table IV-1.

The general flow of the event identification algorithm is as follows. The first step is to select a base set of normal earthquakes. This base set is used to identify as many of the other events as possible as belonging to one of several other possible sets. These sets include uncorrelated events, possible explosions, and several types of presumed explosions. The characteristics of each set are determined by its initial members. In other words, the various sets represent the properties of the events forming the sets. Classification of the events is based on threshold inner products (correlation terms) of vectors for each event containing a z-statistic for each discriminant value computed against the mean and standard deviation for the discriminant over the earthquake set. A z-statistic, z, is defined as $z = (x-\mu)/\sigma$, where x is a given observation and μ and σ are a related mean and standard deviation, respectively. The projections for a particular event must then pass or fail a threshold test a specified number of times before the event is moved to other than the uncorrelated or possible explosion set. As the presumed explosion sets are filled attempts are made to subclassify each set. Events that correlate above a preset threshold are used to generate a mean z-vector for the set. These mean z-vectors are used in computing later correlation terms. Events that do not meet this criterion are moved into the next explosion set where further subclassification is attempted when enough events are present. In this manner, an event sifts down through the explosion sets until it is either classified as one of eight separate types or it passes into the set representing all other types of explosions. This general set does not have a mean z-vector and subclassification

TABLE IV-1

EVENT DISCRIMINANTS

Discriminant Number	Discriminant
	Long-Period
1	$M_o - M_L$
2	$M_{s13} - M_o$
3	$(M_{s13} - M_{s16})/0.1$
4	$m_b - M_o$
5	M_{s25} transverse $- M_{s25}$ vertical (LQ/LR)
	Short-Period
6	$m_{0.3} - m_b$
7	$(m_{0.8} - m_{0.3})/0.4$
8	$(m_{0.8} - m_{0.5})/0.2$
9	$(m_{1.3} - m_{0.8})/0.2$
10	$\bar{f} - \bar{\sigma}_\phi$
11	$(\bar{f} + \bar{\sigma}_\phi)/2.0$
12	Minimum broadband complexity (minimum of station complexities for an event)

where

M_{sT} is a long-period magnitude with a period of T seconds

$M_o = (M_{s32} + M_{s25} + M_{s20} + M_{s16})/4$

$M_L = (M_{s50} + M_{s40})/2$

m_b is the teleseismic event magnitude

m_f is a short-period magnitude at a frequency of f Hz

$\bar{f}$ is the mean frequency, and

$\bar{\sigma}_\phi$ is the mean phase standard deviation.

of it is not possible. This procedure is intended to serve only as a bootstrap for the event identification methods used by Sax (1976). However, if carried far enough, this procedure itself can be used for event identification. The methods used by Sax involve projection of vectors of earthquake-based z-statistics for each discriminant against a mean z-vector for a given type of explosion. The mean z-vectors used in this method would be obtained by the method described above. The event identification bootstrapping software is described below.

The user function DBOOT provides the analyst with a system of auxiliary user functions which operate on the EDDB with the goal of event identification. The general flow of DBOOT is as follows. First, the class file on which to operate is selected by inputing the appropriate class number in the range from 1 to 9. If the selected class file does not contain any events, DBOOT is terminated. Following this the various parameters, earthquake means, and standard deviations (SD), and the partition link list (defining the event sets) are restored from the class directory to their last state (i.e., as they were at the end of the previous identification session for the class file). Various user functions can then be performed at the analyst's discretion by making selections from a descriptive menu of functions.

These functions are described in detail later in this subsection. Briefly, they are as follows:

- PARM - enables the analyst to set the various parameters used throughout the other functions.
- SETEQ - allows a set of known earthquakes to be selected from the events in a class file to serve as a base for classification.
- SETU - adds new events to the uncorrelated (U) set.

- EQNRM - calculates the means and standard deviations of the discriminants over the events in the earthquake set. Calculates, ranks, and displays a modified norm for each event vector of z-statistics based on the means and standard deviations.
- PXGEN - generates the possible explosion (PX) set from the U set.
- EXPCL - attempts to subclassify the PX set and to generate a file of probable explosions (X1 set).
- SUBEX - attempts to subclassify a particular set of probable explosions and to generate a mean z-vector for the set.
- PARTY - displays the events in a given set.

Upon termination of DBOOT the parameters, earthquake mean and standard deviation vectors, and the partition link list are saved in the class directory. Figure IV-12 illustrates the structure and flow of DBOOT.

PARM enables the analyst to set the various parameters used throughout the bootstrapping procedure. These parameters are primarily comprised of various test thresholds and counter limits. A description of each parameter and its previous value is displayed each time this function is performed. Parameters can be set or reset at any time during classification; however, in general it is recommended that the parameters be kept constant during a given classification attempt. Otherwise, inconsistent classifications may result. Figure IV-13 illustrates PARM.

The function of SETEQ is to allow a set of earthquakes to be selected from the events in a given class file to act as a basis for further classification. The event sequence number of a 'known' earthquake is input and the event sequence numbers in the file are searched for this number.

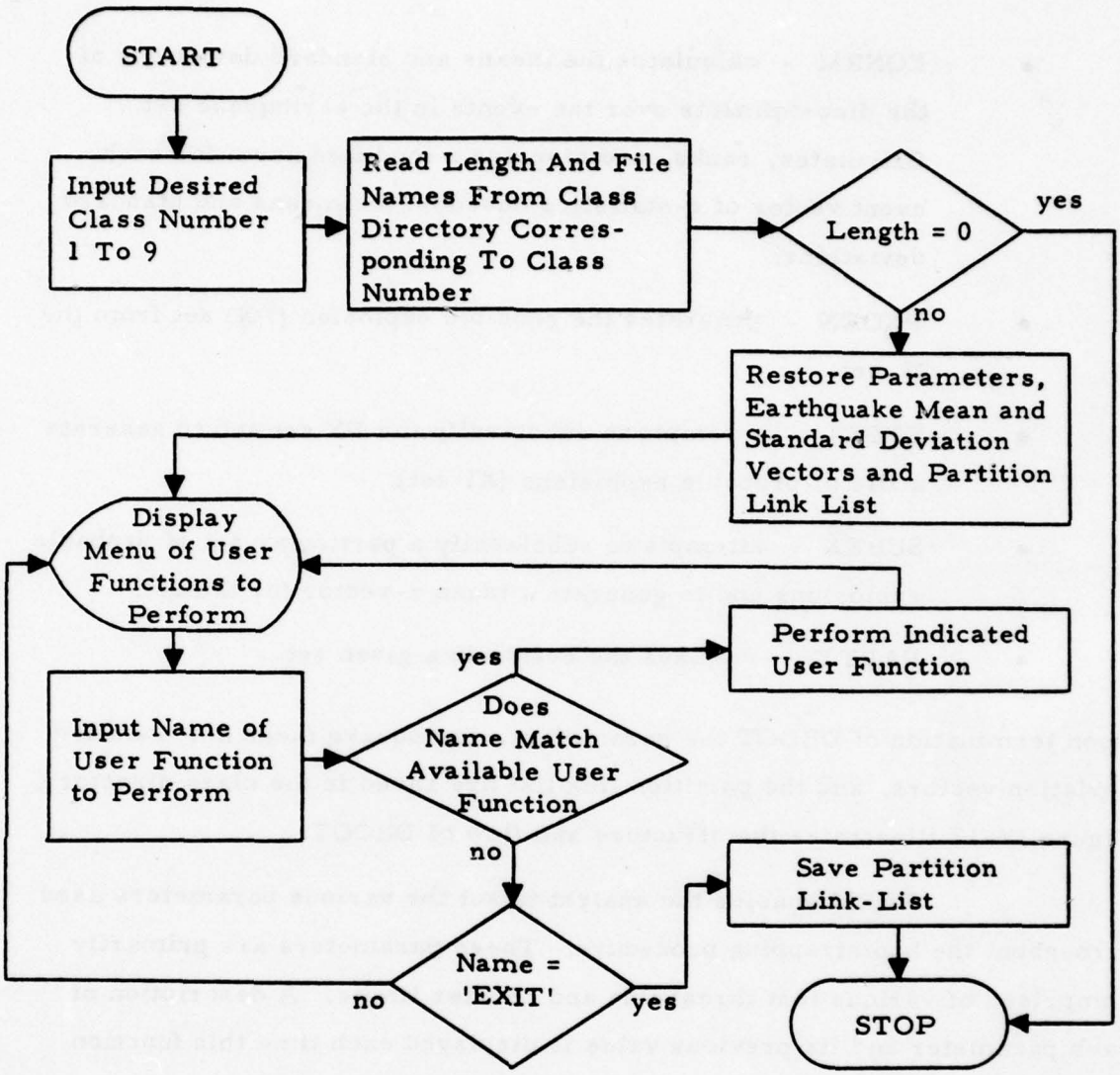

FIGURE IV-12

USER FUNCTION DBOOT

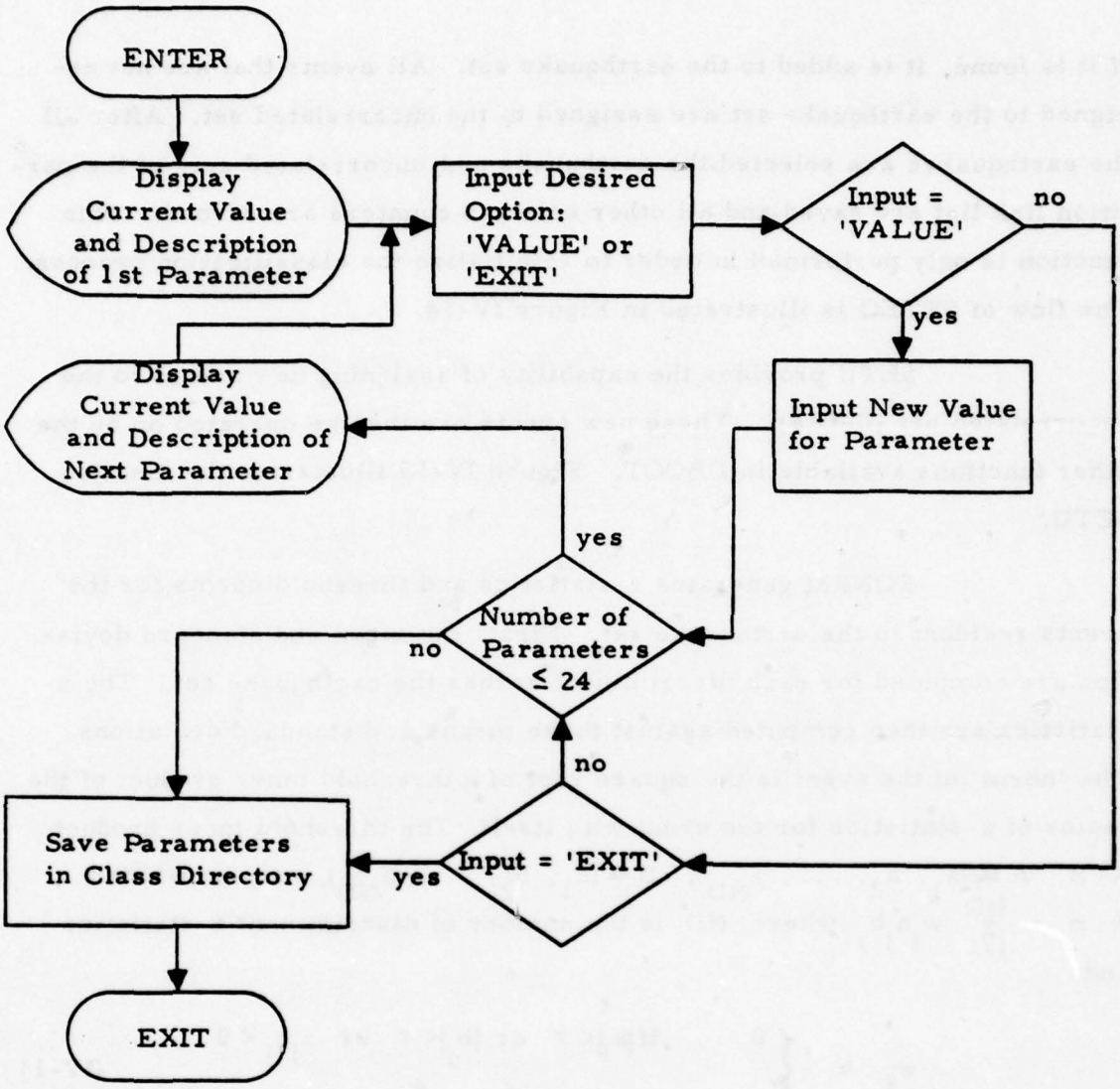

FIGURE IV-13

USER FUNCTION PARM

If it is found, it is added to the earthquake set. All events that are not assigned to the earthquake set are assigned to the uncorrelated set. After all the earthquakes are selected, the earthquake and uncorrelated sets of the partition link list are saved and all other sets and counters are zeroed. This function is only performed in order to reinitialize the classification process. The flow of SETEQ is illustrated in Figure IV-14.

SETU provides the capability of assigning new events to the uncorrelated set (U-file). These new events can then be operated on by the other functions available in DBOOT. Figure IV-15 illustrates the function SETU.

EQNRM generates z-statistics and threshold norms for the events resident in the earthquake set. First, the mean and standard deviation are computed for each discriminant across the earthquake set. The z-statistics are then computed against these means and standard deviations. The 'norm' of the event is the square root of a threshold inner product of the vector of z-statistics for the event with itself. The threshold inner product, $A \cdot B$, $A \equiv (a_1, a_2, \ldots, a_{ND})$, $B \equiv (b_1, b_2, \ldots, b_{ND})$, may be written $A \cdot B = \sum_{j=1}^{ND} w_j a_j b_j$ where ND is the number of discriminant z-statistics and

$$w_j = \begin{cases} 0 & \text{if } |a_j| < \tau \text{ or } |b_j| < \tau \text{ or } a_j b_j < 0 \\ 1 & \text{otherwise} \end{cases} \qquad \text{(IV-1)}$$

where τ is a selected threshold on the z-statistic. This type of correlation term is used in later functions as a measure of the similarity of two events. It emphasizes the major similarities between events and allows for a certain degree of 'noise' by making use of the threshold on the vector components. After the norms are computed for all of the events they are ranked from high to low and are displayed. These norms are used in determining the test threshold in PXGEN to be discussed next. Ideally, the threshold should be

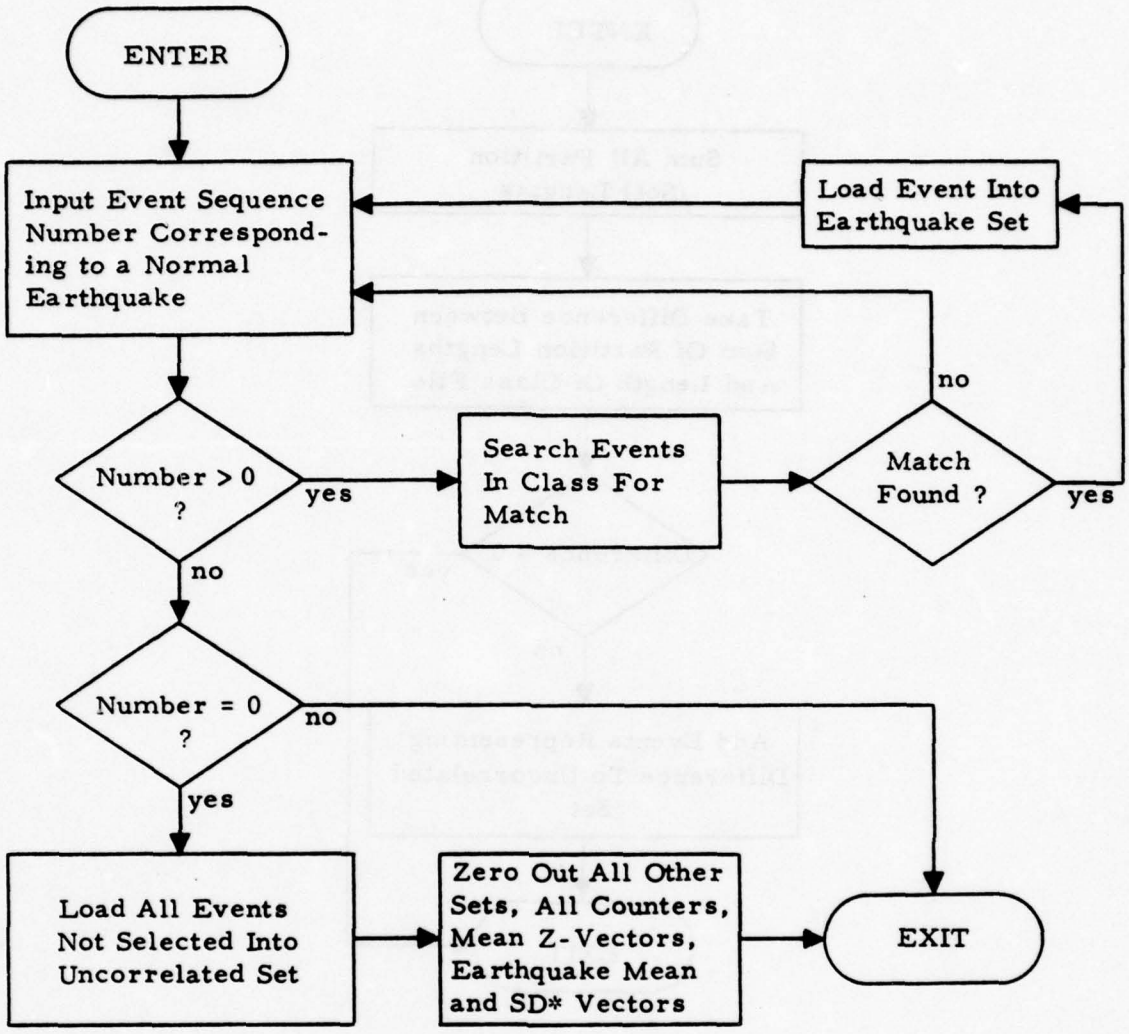

*SD = Standard Deviation

FIGURE IV-14

USER FUNCTION SETEQ

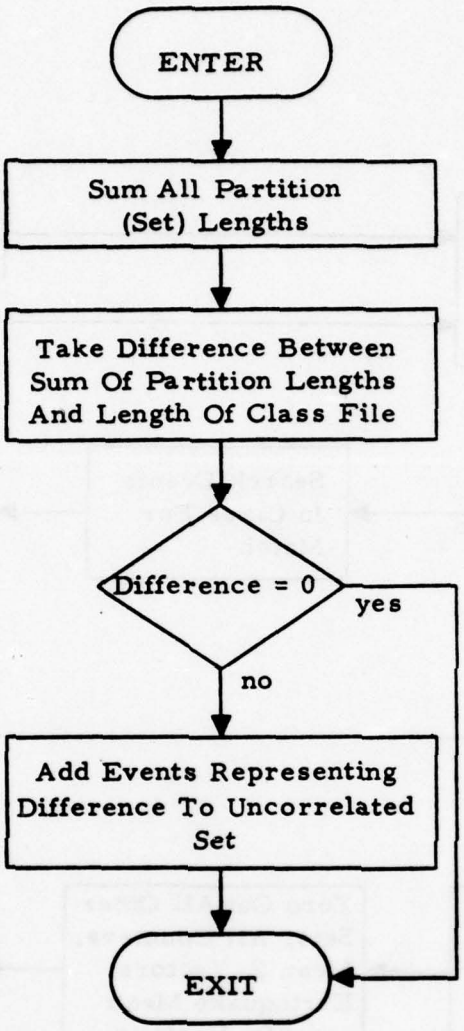

FIGURE IV-15

USER FUNCTION SETU

significantly inside the range displayed by the earthquakes in order to ensure that explosions are not erroneously classified as earthquakes. Finally, the mean and standard deviations are saved before returning to DBOOT to allow restoration of the system in future runs. Figure IV-16 diagrams the flow of EQNRM.

PXGEN generates a set of possible explosions (PX - file) from the U - file. An event is selected from a display of those in the U file. A z-statistic is computed against the earthquake mean and standard deviation for each discriminant associated with the event. A modified norm of this z-vector is then computed by taking the square root of the threshold auto-inner product. This norm is then tested against a predetermined threshold. On the basis of this threshold test, the event is classified as an earthquake ($\leq$ threshold) or a possible explosion ($>$ threshold), and it is moved to the appropriate set. The flow of PXGEN is diagrammed in Figure IV-17.

EXPCL attempts to subclassify the possible explosions into a 'known' explosion group providing the number in the file (PX - file) meets or exceeds a specified minimum set in PARM. An event is selected from a display of those resident in the PX - file. A threshold inner product, or correlation term, is then computed for the selected event's z-vector against those z-vectors representing all the other events. The maximum correlation term is then chosen and tested against a preset threshold. If the event pair associated with the maximum correlation term has never been chosen before or if the test result is different than before, the event pair is considered valid. Otherwise, it is discarded and the next highest correlation term is passed through the same tests. This procedure is repeated until either a valid pair is found or all event pairs available have been tested. Once a valid pair has been found the results are stored and counters are changed accordingly for both events in the pair. If the event pair has passed the threshold test, that is, if the correlation term is greater than the threshold, the success

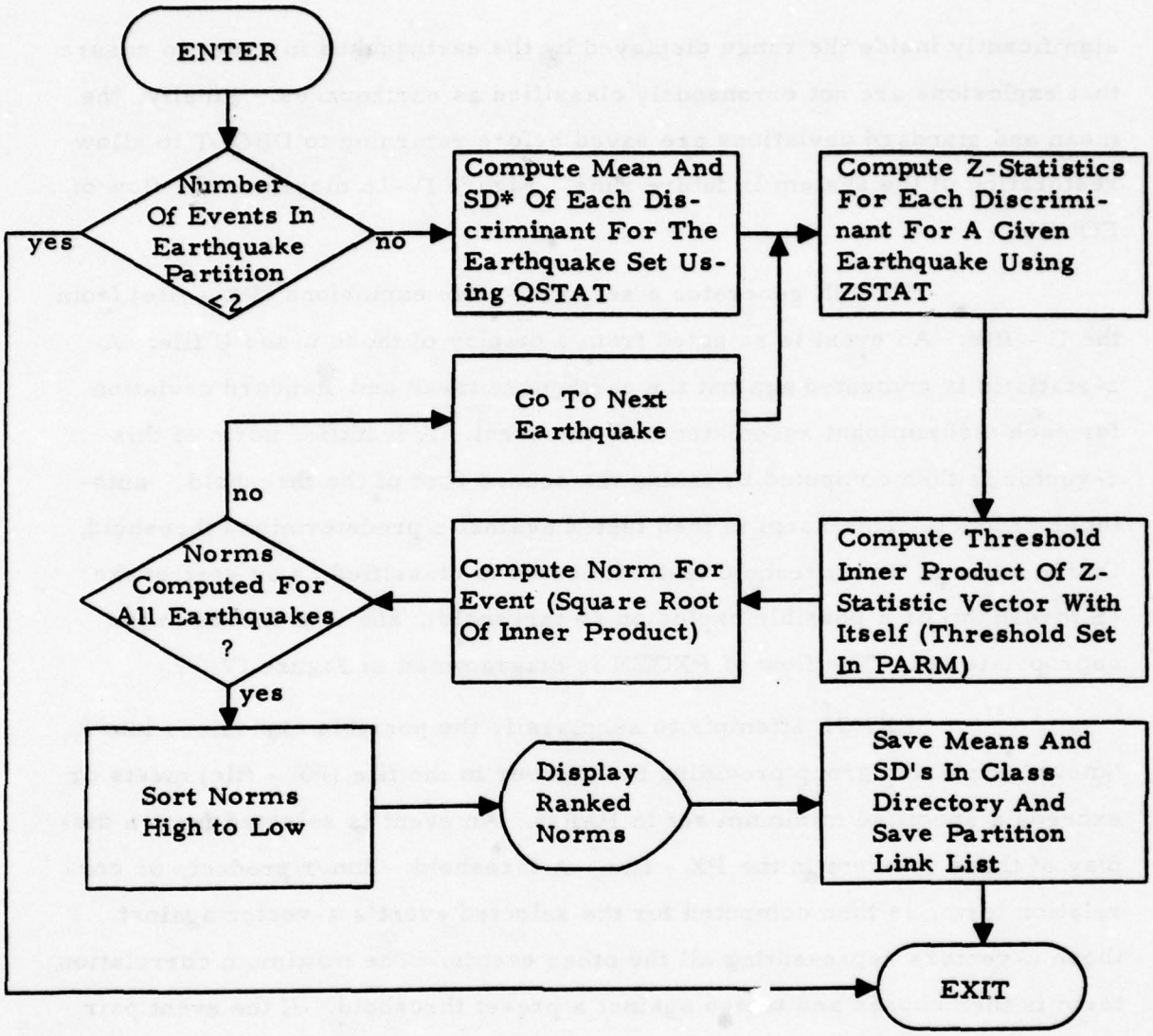

*SD = Standard Deviation

FIGURE IV-16

USER FUNCTION EQNRM

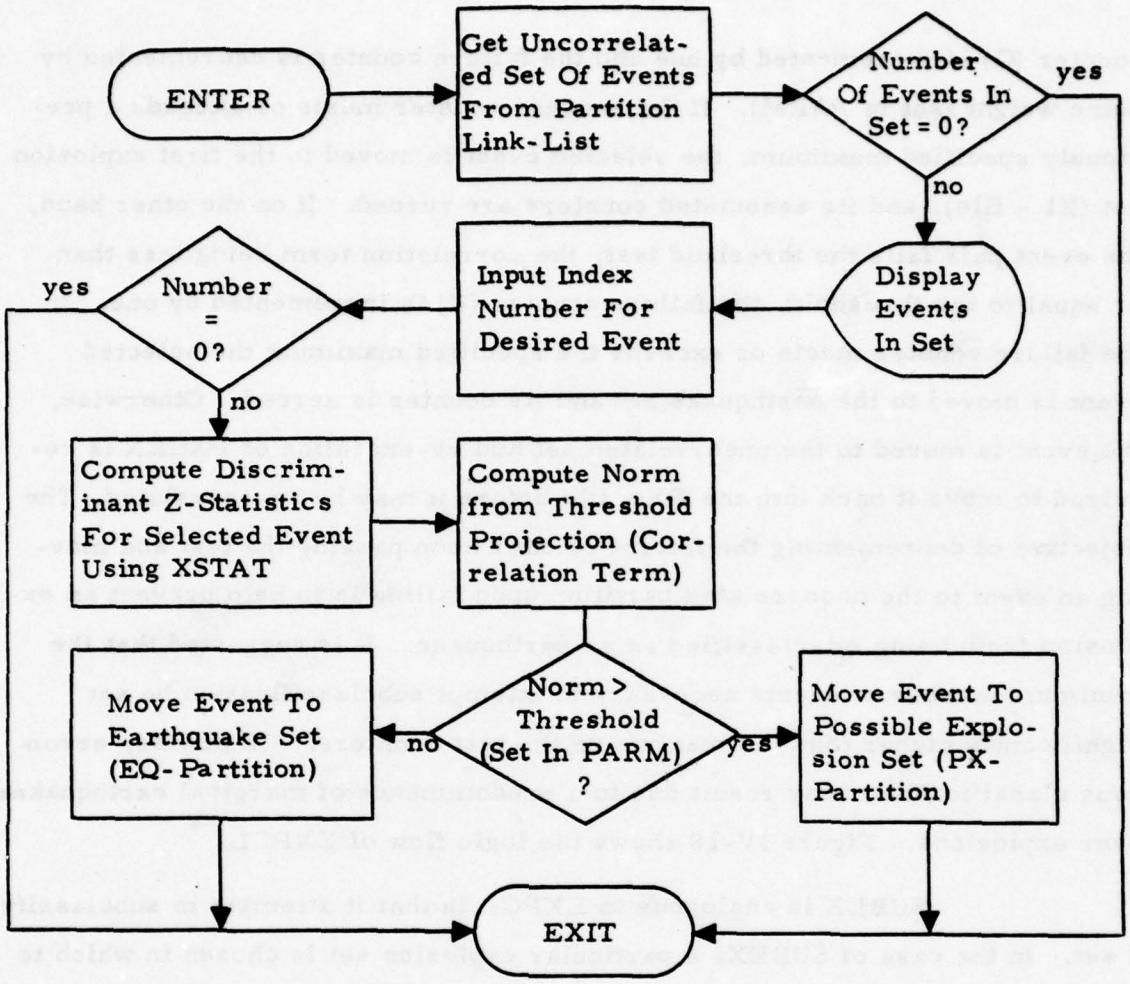

FIGURE IV-17

USER FUNCTION PXGEN

counter (C) is incremented by one and the failure counter is decremented by some weight (set in PARM). If the success counter meets or exceeds a previously specified maximum, the selected event is moved to the first explosion set (X1 - file), and its associated counters are zeroed. If on the other hand, the event pair fails the threshold test, the correlation term being less than or equal to the threshold, the failure counter (K) is incremented by one. If the failure counter meets or exceeds the specified maximum the selected event is moved to the earthquake set and its counter is zeroed. Otherwise, the event is moved to the uncorrelated set and re-execution of PXGEN is required to move it back into the PX - file before it may be re-correlated. The objective of decrementing the failure counter upon passing the test and moving an event to the uncorrelated partition upon failing is to help prevent an explosion from being misclassified as an earthquake. It is suggested that the minimum number of events necessary to attempt subclassification be set significantly higher than the maxima on the test counters. Otherwise, erroneous classifications may result due to a predominance of marginal earthquakes over explosions. Figure IV-18 shows the logic flow of EXPCL.

SUBEX is analogous to EXPCL in that it attempts to subclassify a set. In the case of SUBEX, a particular explosion set is chosen in which to attempt subclassification. As before, a specified number of events is necessary before subclassification can be initiated. After this condition has been met, it is possible to select an event from a display of those in the set. However, only events that have never passed the threshold test, that is, events that are not already included in the mean z-vector for the set, can be selected. The threshold inner product or correlation term is again computed between the selected event's z-vector and the z-vectors of all the other events. If an event has previously passed the threshold test either as a selected event or a matched event the mean z-vector for the set is used in computing the correlation term. The maximum correlation term is then subjected to a

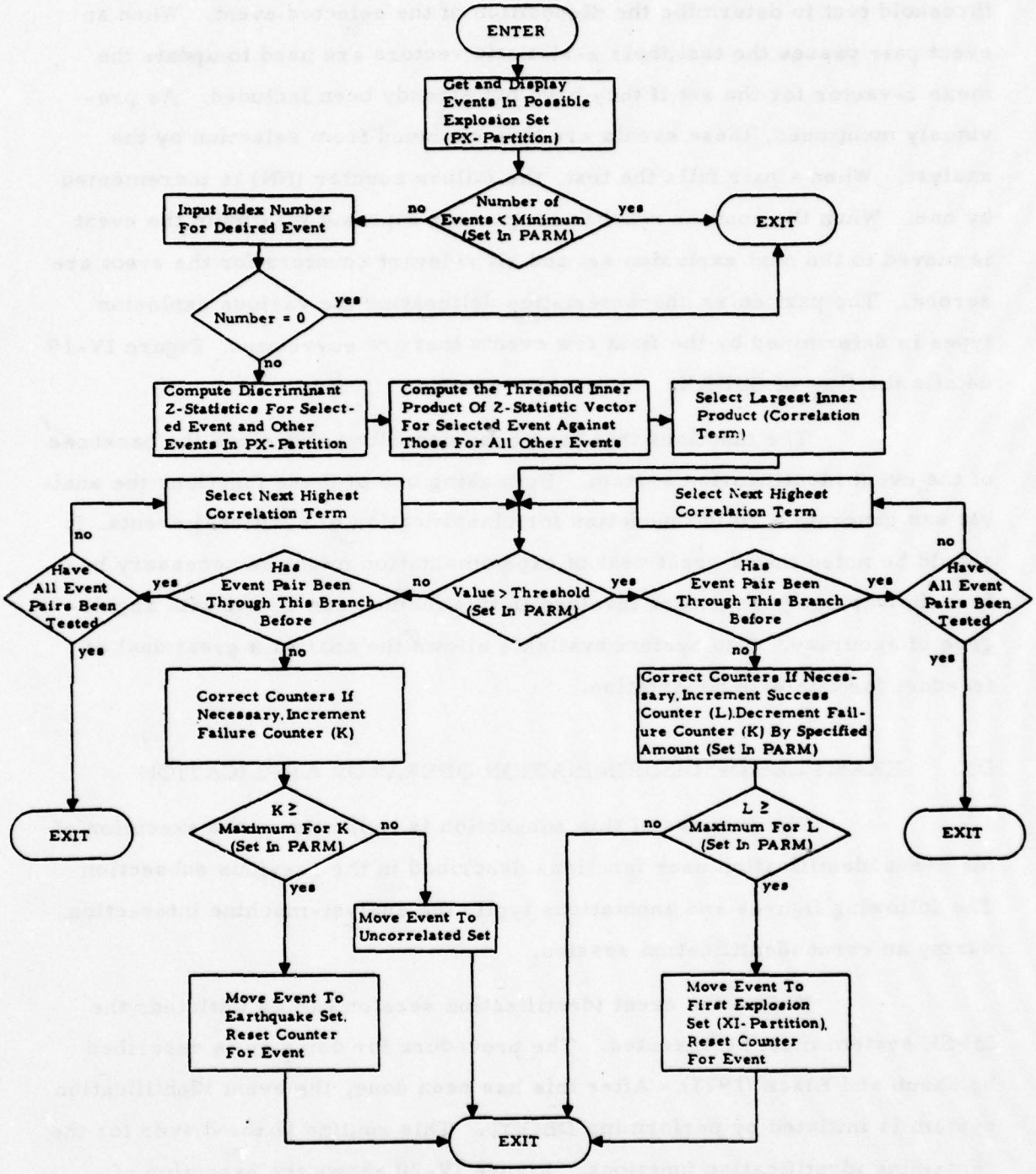

FIGURE IV-18

USER FUNCTION EXPCL

threshold test to determine the disposition of the selected event. When an event pair passes the test,their z-statistic vectors are used to update the mean z-vector for the set if they have not already been included. As previously mentioned, these events are then excluded from selection by the analyst. When a pair fails the test, the failure counter (NN) is incremented by one. When the counter reaches or exceeds a preset maximum the event is moved to the next explosion set and all relevant counters for the event are zeroed. The particular characteristics delineating the various explosion types is determined by the first few events that are correlated. Figure IV-19 details the flow of SUBEX.

The functions that have been described above are the backbone of the event identification system. By making use of these functions the analyst can generate a solid foundation for classification of additional events. It should be noted that a great deal of experimentation might be necessary before the various parameters involved in this method can be set with any degree of accuracy. The system available allows the analyst a great deal of freedom for this experimentation.

D. EXAMPLES OF DISCRIMINATION OPERATOR APPLICATION

The purpose of this subsection is to illustrate the execution of the event identification user functions described in the previous subsection. The following figures and annotations typify the analyst-machine interaction during an event identification session.

Before the event identification session can be initiated, the ISPSE system must be executed. The procedure for doing so is described by Shaub and Black (1977). After this has been done, the event identification system is initiated by performing DBOOT. This routine is the driver for the remaining identification functions. Figure IV-20 shows the execution of

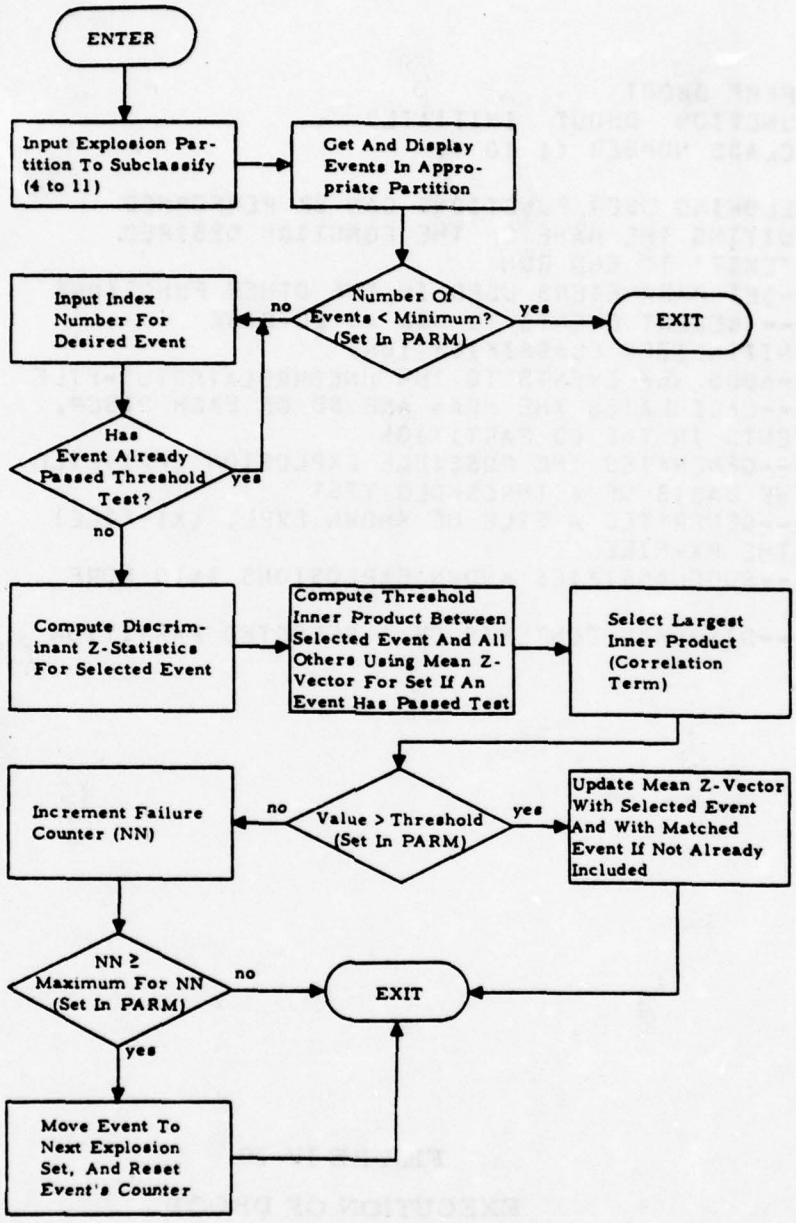

FIGURE IV-19

USER FUNCTION SUBEX

```
.... .PERF DBOOT
USER FUNCTION  DBOOT  INITIATED
INPUT CLASS NUMBER (1 TO 9)
.... 1
THE FOLLOWING USER FUNCTIONS CAN BE PERFORMED
BY INPUTTING THE NAME OF THE FUNCTION DESIRED
INPUT 'EXIT' TO END RUN
PARM---SET PARAMETERS USED IN THE OTHER FUNCTIONS
SETEQ--- SELECT EVENTS TO USE AS EQ-BASE
    (INITIALIZES CLASSIFICATION)
SETU---ADDS NEW EVENTS TO THE UNCORRELATED(U)-FILE
EQNRM---CALCULATES THE MEAN AND SD OF EACH DISCR.
FOR EVENTS IN THE EQ PARTITION
PXGEN---GENERATES THE POSSIBLE EXPLOSION (PX)-FILE
  ON THE BASIS OF A THRESHOLD TEST
EXPCL---GENERATES A FILE OF KNOWN EXPL. (X1-FILE)
 FROM THE PX-FILE
SUBEX---SUBCLASSIFIES KNOWN EXPLOSIONS INTO MORE
GROUPS
PARTY---DISPLAYS CONTENTS OF A SELECTED PARTITION
....
```

FIGURE IV-20

EXECUTION OF DBOOT

DBOOT. Note the menu describing the various user functions that can be performed from DBOOT. This menu is displayed after every execution of one of the subsidiary functions.

Figure IV-21 illustrates the selection of 'normal' earthquakes by using SETEQ. The number of earthquakes in the base population is displayed as each match is found. SETEQ can be aborted without affecting previous classifications and counters by inputting a negative number. After an earthquake set has been selected the function is exited by inputting zero as shown.

Figure IV-22 illustrates execution of PARTY. This function can be used to display any event classification partition by inputting the proper partition number as seen in the figure. The contents are listed with their index into the partition, their event sequence number, and their event designation number. The event sequence number is the numerical order of the events in the Event Discriminant Data Base (EDDB). The event designation number is the identifying number for the event and corresponds to the event number in the Area of Interest event listings. In this example, the earthquakes selected in SETEQ are displayed.

Figure IV-23 illustrates execution of SETU. The error messages shown on the figure result from trying to access empty partitions. This occurs when determining how many events are included in the various groups. As seen in this figure, all the events are accounted for in the partitions. There are no new events to add to the uncorrelated file.

Figure IV-24 shows how PARM is used to set the parameters used throughout the identification procedure. Note that the character string 'VALUE' must be input to change the value for a particular parameter and the string 'EXIT' must be input to terminate the function.

```
.... SETEQ
INPUT EVENT SEQUENCE # CORRESPONDING TO A 'NORMAL'
EARTHQUAKE----INPUT 0 TO EXIT SEARCH
INPUT A NEGATIVE NUMBER TO ABORT 'SETEQ'
.... 5
MATCH FOUND-----# OF EQ IS NOW
   1.000000
INPUT EVENT SEQUENCE # CORRESPONDING TO A 'NORMAL'
EARTHQUAKE----INPUT 0 TO EXIT SEARCH
INPUT A NEGATIVE NUMBER TO ABORT 'SETEQ'
.... 6
MATCH FOUND-----# OF EQ IS NOW
   2.000000
INPUT EVENT SEQUENCE # CORRESPONDING TO A 'NORMAL'
EARTHQUAKE----INPUT 0 TO EXIT SEARCH
INPUT A NEGATIVE NUMBER TO ABORT 'SETEQ'
.... 11
MATCH FOUND-----# OF EQ IS NOW
   3.000000
INPUT EVENT SEQUENCE # CORRESPONDING TO A 'NORMAL'
EARTHQUAKE----INPUT 0 TO EXIT SEARCH
INPUT A NEGATIVE NUMBER TO ABORT 'SETEQ'
.... 13
MATCH FOUND-----# OF EQ IS NOW
   4.000000
INPUT EVENT SEQUENCE # CORRESPONDING TO A 'NORMAL'
EARTHQUAKE----INPUT 0 TO EXIT SEARCH
INPUT A NEGATIVE NUMBER TO ABORT 'SETEQ'
.... 14
MATCH FOUND-----# OF EQ IS NOW
   5.000000
INPUT EVENT SEQUENCE # CORRESPONDING TO A 'NORMAL'
EARTHQUAKE----INPUT 0 TO EXIT SEARCH
INPUT A NEGATIVE NUMBER TO ABORT 'SETEQ'
.... 16
MATCH FOUND-----# OF EQ IS NOW
   6.000000
INPUT EVENT SEQUENCE # CORRESPONDING TO A 'NORMAL'
EARTHQUAKE----INPUT 0 TO EXIT SEARCH
INPUT A NEGATIVE NUMBER TO ABORT 'SETEQ'
.... 23
MATCH FOUND-----# OF EQ IS NOW
   7.000000
```

FIGURE IV-21

EXECUTION OF SETEQ
(PAGE 1 OF 2)

```
INPUT EVENT SEQUENCE # CORRESPONDING TO A 'NORMAL'
EARTHQUAKE----INPUT 0 TO EXIT SEARCH
INPUT A NEGATIVE NUMBER TO ABORT 'SETEQ'
.... 24
MATCH FOUND------# OF EQ IS NOW
   8.000000
INPUT EVENT SEQUENCE # CORRESPONDING TO A 'NORMAL'
EARTHQUAKE----INPUT 0 TO EXIT SEARCH
INPUT A NEGATIVE NUMBER TO ABORT 'SETEQ'
.... 25
MATCH FOUND------# OF EQ IS NOW
   9.000000
INPUT EVENT SEQUENCE # CORRESPONDING TO A 'NORMAL'
EARTHQUAKE----INPUT 0 TO EXIT SEARCH
INPUT A NEGATIVE NUMBER TO ABORT 'SETEQ'
.... 26
MATCH FOUND------# OF EQ IS NOW
   10.00000
INPUT EVENT SEQUENCE # CORRESPONDING TO A 'NORMAL'
EARTHQUAKE----INPUT 0 TO EXIT SEARCH
INPUT A NEGATIVE NUMBER TO ABORT 'SETEQ'
.... 32
MATCH FOUND------# OF EQ IS NOW
   11.00000
INPUT EVENT SEQUENCE # CORRESPONDING TO A 'NORMAL'
EARTHQUAKE----INPUT 0 TO EXIT SEARCH
INPUT A NEGATIVE NUMBER TO ABORT 'SETEQ'
.... 34
MATCH FOUND------# OF EQ IS NOW
   12.00000
INPUT EVENT SEQUENCE # CORRESPONDING TO A 'NORMAL'
EARTHQUAKE----INPUT 0 TO EXIT SEARCH
INPUT A NEGATIVE NUMBER TO ABORT 'SETEQ'
.... 0
```

FIGURE IV-21

EXECUTION OF SETEQ
(PAGE 2 OF 2)

```
.... PARTY
ENTER PARTITION # ; 1=EQ, 2=U, 3=PX, 4=X1, ETC....
.... 1

PARTITION INDEX    EVENT SEQ #   EVENT DSGN #

    1.000000         5.000000        68.00000
    2.000000         6.000000        73.00000
    3.000000        11.00000          3.000000
    4.000000        13.00000         34.00000
    5.000000        14.00000         35.00000
    6.000000        16.00000         39.00000
    7.000000        23.00000        143.0000
    8.000000        24.00000        149.0000
    9.000000        25.00000        151.0000
   10.00000         26.00000         77.00000
   11.00000         32.00000         30.00000
   12.00000         34.00000         47.00000
```

FIGURE IV-22

EXECUTION OF PARTY

```
.... SETU
ERROR..P1 VACUOUS OR N1 OUT OF RANGE FOR LLIST
ERROR..P1 VACUOUS OR N1 OUT OF RANGE FOR LLIST
ERROR..P1 VACUOUS OR N1 OUT OF RANGE FOR LLIST
ERROR..P1 VACUOUS OR N1 OUT OF RANGE FOR LLIST
ERROR..P1 VACUOUS OR N1 OUT OF RANGE FOR LLIST
ERROR..P1 VACUOUS OR N1 OUT OF RANGE FOR LLIST
ERROR..P1 VACUOUS OR N1 OUT OF RANGE FOR LLIST
ERROR..P1 VACUOUS OR N1 OUT OF RANGE FOR LLIST
ERROR..P1 VACUOUS OR N1 OUT OF RANGE FOR LLIST
ERROR..P1 VACUOUS OR N1 OUT OF RANGE FOR LLIST
THE # OF NEW EVENTS TO BE ADDED TO THE U-FILE IS
  0.0000000
```

FIGURE IV-23

EXECUTION OF SETU

```
.... PARM
PREVIOUS VALUE FOR  PROJECTION THRESHOLD =        1.000000
INPUT 'VALUE' TO CHANGE PREVIOUS VALUE
HIT [CR] TO CONTINUE
INPUT 'EXIT' TO RETURN TO MAIN
....
PREVIOUS VALUE FOR  THRESHOLD ON EQ NORMS =       5.000000
INPUT 'VALUE' TO CHANGE PREVIOUS VALUE
HIT [CR] TO CONTINUE
INPUT 'EXIT' TO RETURN TO MAIN
....
PREVIOUS VALUE FOR  MINIMUM # OF POSS. EXPL.=     3.000000
INPUT 'VALUE' TO CHANGE PREVIOUS VALUE
HIT [CR] TO CONTINUE
INPUT 'EXIT' TO RETURN TO MAIN
....
PREVIOUS VALUE FOR  LOW THRESH TO SUBCL EXPL=     15.00000
INPUT 'VALUE' TO CHANGE PREVIOUS VALUE
HIT [CR] TO CONTINUE
INPUT 'EXIT' TO RETURN TO MAIN
.... VALUE
.... 25
PREVIOUS VALUE FOR  K (FAIL CTR)) DECREMENT =  0.0000000
INPUT 'VALUE' TO CHANGE PREVIOUS VALUE
HIT [CR] TO CONTINUE
INPUT 'EXIT' TO RETURN TO MAIN
....
```

FIGURE IV-24

EXECUTION OF PARM
(PAGE 1 OF 2)

```
PREVIOUS VALUE FOR  LIMIT ON FAIL. COUNT (K)=    2.000000
INPUT 'VALUE' TO CHANGE PREVIOUS VALUE
HIT [CR] TO CONTINUE
INPUT 'EXIT' TO RETURN TO MAIN
....
PREVIOUS VALUE FOR  LIM. ON SUCCESS COUNT(L)=    2.000000
INPUT 'VALUE' TO CHANGE PREVIOUS VALUE
HIT [CR] TO CONTINUE
INPUT 'EXIT' TO RETURN TO MAIN
....
PREVIOUS VALUE FOR  MIN. # OF KNOWN EXPL. =      2.000000
INPUT 'VALUE' TO CHANGE PREVIOUS VALUE
HIT [CR] TO CONTINUE
INPUT 'EXIT' TO RETURN TO MAIN
....
PREVIOUS VALUE FOR  LOW THRESH. FOR X1 EXPL.=    15.00000
INPUT 'VALUE' TO CHANGE PREVIOUS VALUE
HIT [CR] TO CONTINUE
INPUT 'EXIT' TO RETURN TO MAIN
.... VALUE
.... 50
PREVIOUS VALUE FOR  LIM.--X1 FAIL. COUNT(NN)=    2.000000
INPUT 'VALUE' TO CHANGE PREVIOUS VALUE
HIT [CR] TO CONTINUE
INPUT 'EXIT' TO RETURN TO MAIN
.... EXIT
```

FIGURE IV-24

EXECUTION OF PARM
(PAGE 2 OF 2)

Figure IV-25 illustrates execution of EQNRM. This routine calculates threshold norms for vectors of discriminant z-statistics for each earthquake. The method is described in the previous subsection. The sorted norms seen in the figure can be used in selecting a threshold for the threshold test in PXGEN. The system errors also present in the figure for the operator XSTAT occur when the discriminant z-statistics are computed for an event. They indicate one or more unavailable discriminants in one or more events. The validity of the various computations is not affected. Empty discriminant components are due to the unavailability of signal windows or of detected signals. The calculator of the norms and also of correlation terms (projections) is designed to account for this situation. This error message is also seen in the figures relating to PXGEN, EXPCL, and SUBEX (Figures IV-26, IV-27, and IV-28).

Figure IV-26 illustrates execution of PXGEN. The event selected from the displayed list can be classified as either an anomalous event or an earthquake on the basis of its vector norm. This function can be performed until all entries in the uncorrelated (U)-file have been classified as either a possible explosion/anomalous event or an earthquake.

Figure IV-27 shows how EXPCL is used to subclassify possible explosions or other possibly anomalous events into other classes (earthquake or explosion/anomalous event). As explained in the previous subsection, this subclassification is done on the basis of threshold tests on the correlation terms (projections in the figure) and counters on the numbers of successes and failures. In this example, the event is moved into the first explosion/anomalous event partition. At present, it is possible to move all events except one into other partitions by reiterating this function.

Figure IV-28 illustrates execution of SUBEX in an attempt to subclassify partition number 4. As can be seen in the figure, only events that have not already been included in the mean z-vector can be selected.

```
.... EQNRM
 SYSTEM ERROR - XSTAT : NUMBER OF NON-ZERO DISCRIMINANTS IS ZERO
 SYSTEM ERROR - XSTAT : NUMBER OF NON-ZERO DISCRIMINANTS IS ZERO
EVENT SEQ #      THRESHOLDED NORM
   23.000000        10.17458
   26.000000        8.963270
   11.000000        8.901101
   34.000000        8.138978
   14.000000        7.629974
   24.000000        7.357829
   32.000000        7.216766
   25.000000        5.755521
   6.000000         1.508593
   16.000000        2.604983
   5.000000         2.546146
   13.000000        2.374783
```

FIGURE IV-25

EXECUTION OF EQNRM

```
.... PXGEN
UNCLASSIFIED EVENTS

PARTITION INDEX    EVENT SEQ #   EVENT DSGN #

    1.000000         4.000000        56.00000
    2.000000         7.000000        18.00000
    3.000000         8.000000        19.00000
    4.000000         9.000000        20.00000
    5.000000        10.00000          1.000000
    6.000000        12.00000          7.000000
    7.000000        15.00000         37.00000
    8.000000        17.00000         49.00000
    9.000000        18.00000         50.00000
   10.00000         19.00000         59.00000
   11.00000         20.00000         14.00000
   12.00000         21.00000         61.00000
   13.00000         22.00000         62.00000
   14.00000         27.00000         21.00000
   15.00000         28.00000         22.00000
   16.00000         29.00000         17.00000
   17.00000         30.00000         16.00000
   18.00000         31.00000         81.00000
   19.00000         33.00000         36.00000
   20.00000         35.00000         53.00000

INPUT INDEX # OF DESIRED EVENT (INPUT 0 TO RETURN)
.... 1
 SYSTEM ERROR - XSTAT : NUMBER OF NON-ZERO DISCRIMINANTS IS ZERO
NORM OF EVENT=    2.717050
EVENT CLASSIFIED AS EARTHQUAKE
```

FIGURE IV-26

EXECUTION OF PXGEN

```
.... EXPCL

PARTITION INDEX   EVENT SEQ #  EVENT DSGN #

    1.000000        9.000000        20.00000
    2.000000       10.00000          1.000000
    3.000000       12.00000          7.000000
    4.000000       17.00000         49.00000
    5.000000       18.00000         50.00000
    6.000000       19.00000         59.00000
    7.000000       20.00000         14.00000
    8.000000       22.00000         62.00000
    9.000000       27.00000         21.00000
   10.00000        28.00000         22.00000
   11.00000        29.00000         17.00000
   12.00000        30.00000         16.00000
   13.00000        31.00000         81.00000
   14.00000        35.00000         53.00000

INPUT INDEX OF DESIRED EVENT  (INPUT 0 TO RETURN)
.... 7
 SYSTEM ERROR - XSTAT : NUMBER OF NON-ZERO DISCRIMINANTS IS ZERO
 SYSTEM ERROR - XSTAT : NUMBER OF NON-ZERO DISCRIMINANTS IS ZERO
ENTER 1 TO DISPLAY PROJECTIONS, 0 OTHERWISE
.... 1
  EVENT SEQ # VS. EVENT SEQ # = PROJECTION
    20.00000        29.00000        295.8361
    20.00000        30.00000        241.9291
    20.00000        35.00000        216.6561
    20.00000        28.00000        167.8350
    20.00000        27.00000        162.5761
    20.00000        31.00000        159.3719
    20.00000        12.00000        152.2128
    20.00000        22.00000        120.2072
    20.00000        19.00000        119.5359
    20.00000         9.000000       111.9355
    20.00000        10.00000         26.86032
    20.00000        18.00000          8.438536
    20.00000        17.00000          3.344371
EVENT CLASSIFIED AS EXPLOSION----MOVED TO X1-PART.
```

FIGURE IV-27

EXECUTION OF EXPCL

```
.... SUBEX
INPUT EXPLOSION PARTITION # TO SUBCLASSIFY
PARTITIONS 4 TO 11 CORRESPOND TO EXPLOSION TYPES
   1 TO 8-----PART. 12 CORRESPONDS TO ALL OTHERS
.... 4

PARTITION INDEX    EVENT SEQ #   EVENT DSGN #

   1.000000         7.000000        18.00000
   2.000000         8.000000        19.00000
   3.000000        20.00000         14.00000
   4.000000        29.00000         17.00000
   5.000000         9.000000        20.00000
   6.000000        10.00000          1.000000
   7.000000        12.00000          7.000000
   8.000000        18.00000         50.00000
   9.000000        19.00000         59.00000
  10.000000        22.00000         62.00000
  11.00000         27.00000         21.00000
  12.00000         28.00000         22.00000
  13.00000         30.00000         16.00000

INPUT INDEX OF EVENT SEQ # DESIRED
     INPUT 0 TO RETURN
.... 1
EVENT HAS ALREADY BEEN INCLUDED IN MEAN Z
INPUT INDEX OF EVENT SEQ # DESIRED
     INPUT 0 TO RETURN
.... 2
 SYSTEM ERROR - XSTAT : NUMBER OF NON-ZERO DISCRIMINANTS IS ZERO
 SYSTEM ERROR - XSTAT : NUMBER OF NON-ZERO DISCRIMINANTS IS ZERO
ENTER 1 TO DISPLAY PROJECTIONS, 0 OTHERWISE
.... 1
  EVENT SEQ # VS. EVENT SEQ # = PROJECTION
    8.000000        20.00000        223.0576
    8.000000        29.00000        213.9701
    8.000000         7.000000       213.9701
    8.000000        30.00000        166.9546
    8.000000        27.00000        129.7897
    8.000000        28.00000        123.4988
    8.000000         9.000000       100.8050
    8.000000        12.00000         96.85367
    8.000000        19.00000         89.93691
    8.000000        22.00000         75.71339
    8.000000        10.00000         56.83710
    8.000000        18.00000         26.24136
UPDATING MEAN Z-VECTOR
MATCHING EVENT IS BEING USED TO UPDATE Z-VECTOR
```

FIGURE IV-28

EXECUTION OF SUBEX

The selected event is then either included in the mean z-vector, as in this example, or moved to the next explosion/anomalous event partition. As explained in the previous subsection, this decision is also based on the basis of threshold tests on the projections and counters. The matching event (i. e., the one with the largest projection against the selected event) is also used to update the mean z-vector if it has not been included. This is also illustrated in Figure IV-28.

A possible procedure for using the functions illustrated above to identify events is as follows:

- A base set of earthquakes is selected by using SETEQ.
- Any new events that are not resident in the partition linklist are added to the uncorrelated file by using SETU.
- The threshold on the calculation of the norms and projections is set using PARM.
- EQNRM is used to generate the mean and standard deviation vectors for the earthquake set and to compute and display the norms of the z-statistic vectors for the earthquakes.
- The threshold on the norms (used in PXGEN) is set using PARM. It is also possible to set the thresholds and counter limits for EXPCL and SUBEX at this time if previous experience is available. Otherwise, it might be necessary to test run several of the classification functions and reinitialize classification with SETEQ in order to gain the experience necessary to set the parameters.
- PXGEN is used to classify all the events in the uncorrelated file as other earthquakes or possible explosions/anomalous events.

- The possible explosions or anomalous events are further classified using EXPCL.
- The explosion/anomalous event partitions are then evaluated using SUBEX to determine if the events in a particular partition are similar.

The above scenario is only a rough outline of the various possible procedures for using the event identification functions. It should also be noted that the system described and illustrated here and in the previous subsections are prototypes and are subject to modifications.

SECTION V
RESULTS

An event identification package was applied to a data base of thirty-five events. The purpose was to quality check all components of the system, to obtain experience in setting thresholds for automatic detection and timing of edited signals, and for identification of normal shallow explosions and other event types. As expected as a result of this test, we identified intermittant program malfunctions and uncovered problems in designing signal filters, in properly timing edits, in defining independent discriminants, in properly operating the classification processor, and in optimally defining and applying multivariate discriminants. Our results indicated the feasibility of our goal of designing and operating a seismic event identification system which automatically edits data, computes discriminants, and which adaptively identifies and delimits groupings of unusual events without prior knowledge of such events. The detailed evaluation of these results are given in the remainder of this section.

Table V-1 shows the discriminant calculations used in this preliminary analysis. For brevity in future references, each discriminant will be referred to by the discriminant number shown in Table V-1.

The first five discriminant numbers are long-period discriminants. The first discriminant indicates the average center band magnitude of Rayleigh waves between 16 seconds and 32 seconds compared to the longer period magnitude between 40 seconds and 50 seconds. The second discriminant measures the shorter period Rayleigh wave magnitude at 13 seconds compared to the Rayleigh wave center band magnitude. The third discriminant measures the log-log slope of the Rayleigh waves between 13 seconds and 16

TABLE V-1

EVENT DISCRIMINANTS
(PAGE 1 OF 2)

Discriminant Number	Discriminant
	Long-Period
1	$M_o - M_L$
2	$M_{s13} - M_o$
3	$(M_{s13} - M_{s16})/0.1$
4	$m_b - M_o$
5	M_{s25} transverse $- M_{s25}$ vertical (LQ/LR)
	Short-Period
6	$m_{0.3} - m_b$
7	$(m_{0.8} - m_{0.3})/0.4$
8	$(m_{0.8} - m_{0.5})/0.2$
9	$(m_{1.3} - m_{0.8})/0.2$
10	$\bar{f} - \bar{\sigma}_\phi$
11	$(\bar{f} + \bar{\sigma}_\phi)/2.0$
12	Minimum broadband complexity (minimum of station complexities for an event)

where

M_{sT} is a long-period magnitude with a period of T seconds

$M_o = (M_{s32} + M_{s25} + M_{s20} + M_{s16})/4$

$M_L = (M_{s50} + M_{s40})/2$

m_b is the teleseismic event magnitude

m_f is a short-period magnitude at a frequency of f Hz

$\bar{f}$ is the mean frequency, and

$\bar{\sigma}_\phi$ is the mean phase standard deviation.

TABLE V-1

EVENT DISCRIMINANTS
(PAGE 2 OF 2)

	Event Sequence Number	Event Designation Number	Discriminant Number											
			1	2	3	4	5	6	7	8	9	10	11	12
Normal Earthquake Set	5	68	0.512	-0.400	-3.898	-1.072	-0.163	0.670	-2.531	-2.989	-3.723	-----	-----	-----
	6	73	0.682	-0.235	-3.313	-0.985	-0.024	0.581	-1.739	-4.011	-3.113	0.050	2.072	1.733
	11	3	0.853	0.076	-0.360	-0.520	-0.046	0.194	-1.843	-0.425	-4.851	0.054	1.892	1.741
	13	34	0.506	-0.360	-4.391	-1.083	0.006	1.020	-2.364	-2.538	-4.121	0.013	1.920	-----
	14	35	0.164	-0.409	-3.759	-1.710	0.083	1.199	-2.608	-2.207	-4.893	-0.113	1.755	2.381
	16	39	0.293	-0.464	-4.737	-1.411	0.012	0.997	-2.797	-3.008	-2.393	0.047	1.345	1.768
	23	143	0.203	-1.217	-8.787	-0.910	-0.097	0.526	-2.027	-2.380	-2.858	0.005	1.413	1.323
	24	149	0.245	-0.361	-4.034	-0.173	0.339	-0.130	0.197	-0.637	-2.182	0.060	1.280	1.425
	25	151	0.430	-0.333	-4.729	-0.810	0.141	0.955	-2.185	-2.470	-2.835	-0.232	1.859	1.306
	26	77	0.570	-0.671	-8.654	-0.467	0.185	0.824	-2.481	-2.087	-1.887	-0.167	1.532	1.459
	32	30	0.067	-0.668	-3.421	-2.422	0.162	0.217	-0.704	-2.189	-2.900	-0.158	1.280	1.045
	34	47	0.150	-0.258	-0.847	-1.997	0.166	0.085	-0.795	-2.355	-5.611	-0.054	1.145	1.316
Unclassified Events	1	38	1.281	-0.026	-1.886	-0.805	0.035	0.777	-3.354	-3.248	-3.431	-----	-----	-----
	2	48	0.600	0.100	-2.699	-0.241	-0.306	0.784	-3.365	-3.487	-3.513	-----	-----	-----
	3	55	0.361	-0.112	-1.895	-1.135	-0.012	0.888	-3.363	-4.243	-2.916	-----	-----	-----
	4	56	0.452	-0.146	-2.889	-1.324	-0.031	0.921	-2.967	-3.102	-3.034	-----	-----	-----
	7	18	0.105	0.614	-2.378	0.746	-0.094	-0.253	-0.106	2.082	-1.502	0.589	1.679	1.314
	8	19	0.582	-0.210	-4.373	0.542	-0.172	0.088	-0.789	-1.459	-1.405	0.528	1.503	1.397
	9	20	0.560	-0.235	-4.542	0.046	0.187	-0.384	0.943	-1.646	-3.513	0.255	1.583	1.279
	10	1	0.514	-0.043	-4.836	0.395	0.515	-0.415	0.711	3.337	-1.565	-0.114	1.989	1.346
	12	7	0.219	-0.301	-4.633	-----	0.340	-----	-3.770	-2.639	-2.679	0.380	1.476	1.833
	15	37	0.425	-0.272	-4.382	-1.549	-0.036	1.164	-3.645	-4.222	-3.165	-----	-----	-----
	17	49	0.192	-0.635	-3.465	-1.074	-0.216	0.374	-1.116	-1.815	-3.083	-0.218	1.215	1.222
	18	50	0.267	-0.642	-6.129	-1.113	0.232	-0.318	0.646	-1.532	-2.724	0.049	1.325	1.551
	19	59	0.896	0.142	-1.357	-0.802	0.455	0.550	-0.899	-1.197	-2.139	0.250	1.553	1.590
	20	14	0.892	-0.145	-4.400	-0.665	-0.015	0.784	-2.340	-1.416	-3.297	0.826	2.105	1.555
	21	61	0.602	-0.082	-2.888	-0.808	-0.062	0.750	-2.947	-3.458	-2.960	-----	-----	-----
	22	62	0.517	-0.115	-2.095	-1.647	0.134	0.983	-2.705	-2.524	-4.730	0.288	1.915	-----
	27	21	0.718	0.152	-2.433	-0.095	0.012	-0.244	0.409	-0.099	-3.505	0.349	1.652	1.306
	28	22	0.112	-0.504	-3.965	-1.055	-0.137	0.327	-0.198	-1.417	-3.568	0.393	2.293	1.392
	29	17	0.703	0.229	0.900	-0.084	-0.120	-0.183	0.186	-1.500	-2.797	0.684	1.638	1.389
	30	16	0.578	-0.070	-2.341	-0.456	0.208	0.385	-2.095	-4.306	-1.781	0.580	1.456	1.146
	31	81	0.259	-0.134	-2.507	0.895	-0.058	-0.120	-0.051	-0.342	-1.355	0.365	1.251	1.294
	33	36	0.534	-0.024	-3.061	-1.345	-0.081	1.194	-3.473	-3.788	-3.551	-----	-----	-----
	35	53	0.624	-0.063	-1.397	0.505	-0.065	-1.034	2.034	-0.738	-1.652	0.489	1.472	1.358

seconds. The fourth discriminant measures short-period compressional wave magnitude m_b relative to the average Rayleigh wave center band magnitude representing M_s versus m_b reduced to a scalar discriminant. The fifth discriminant measures the Love wave magnitude relative to the Rayleigh wave magnitude at a period of 25 seconds.

The discriminant numbers six through twelve are short-period discriminants. The sixth discriminant measures the magnitude at 0.3 Hz relative to m_b. The seventh discriminant measures the average log-log slope of the P wave between 0.3 Hz and 0.8 Hz; the eighth, between 0.5 Hz and 0.8 Hz; and the ninth, between 0.8 Hz and 1.3 Hz. The absence of frequencies higher than 1.3 Hz was caused by malfunction of filters due to leakage, which needs to be corrected before valid results can be shown. The tenth and eleventh discriminants are scalar quantities representing the relationship between the frequency and phase standard deviation of P waves. The twelfth discriminant is a measure of complexity of P waves. The absence of discriminants based on measurements of regional phases was due to the sparsity of measurements available in the data base.

Table V-1, part 2, is a listing of event discriminant measurements by discriminant number and event numbers. The event designation number refers to the event numbers in Table I-2 which is an event location list. The event sequence number indicates the order in which events were entered into the event identification disk file. The event list in Table V-1 is grouped to show the initial normal shallow earthquake set and to show the initial set of unknown events entered into the identification system.

Figure V-1 shows a schematic representation of a discriminant. The population on the left represents normal shallow earthquakes. The population on the right represents the unusual group of events we wish to correlate. In order to obtain robust statistical measures of these populations we characterize the populations by percentiles. This is conveniently done by sorting

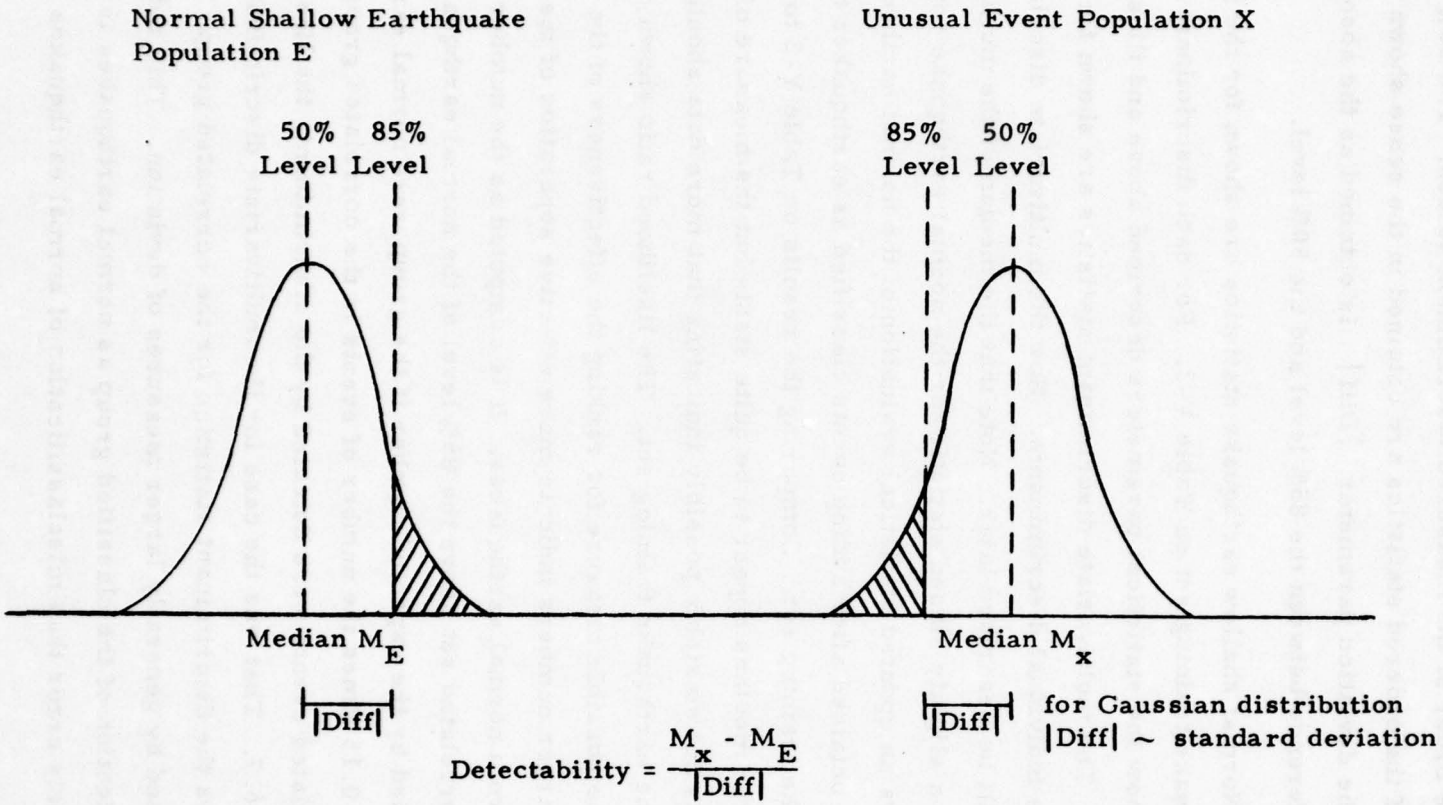

FIGURE V-1

SCHEMATIC OF EVENT DISCRIMINANT POPULATIONS

the events in the order of the measured discriminant values. The 50% level and 85% level of the ordered statistics are obtained in the sense shown on Figure V-1. The deviation parameter |Diff| is obtained as the absolute value of the difference between the 85% level and the 50% level.

Normal shallow earthquake statistics are shown for the initially selected earthquake training set on Table V-2. For each discriminant number, these results show the statistical parameters described above and illustrated on Figure V-1. The multivariate discriminant statistics are shown for comparison with the individual discriminants. How the multivariate discriminant is calculated will be described later. Note that the median of the multivariate discriminant is a slightly biased statistic for the normal earthquake population. Table V-3 shows an updated statistical evaluation of the normal earthquakes. The update was obtained after adding events classified as earthquakes to the initial earthquake training set. Comparing the results on Table V-3 to those on Table V-2, the medians appear to be quite stable but the measure of deviation |Diff| is not so stable possibly indicating that more data should have been used for the earthquake training set. The likelihood ratio shown on Table V-3 is one possible measure for ranking the effectiveness of the discriminants. Larger numbers indicate more effective separation of the non-normal group from normal earthquakes. It is computed as the number of events in the correlated set above the 85% level of the normal earthquake population divided by the expected number if the group were normal earthquakes, that is 0.15 times the number of events in the correlated group. If all of the correlated events were detected by the discriminant, the likelihood value would be 6.7. That was the case for the multivariate discriminant. Table V-4 shows the discriminant statistics for the correlated group. These are characterized by generally larger measures of deviation. This indicates that misclassification of the classified group as normal earthquakes is probably a more likely error than misclassification of normal earthquakes as

TABLE V-2

NORMAL EARTHQUAKE STATISTICS

Discriminant Number	Median	85% Level	|Difference|
1	0.36	0.57	0.21
2	-0.38	-0.26	0.12
3	-3.97	-3.31	0.66
4	-1.03	-0.52	0.51
5	0.05	-0.05	0.10
6	0.63	0.19	0.44
7	-2.11	-0.79	1.32
8	-2.37	-2.09	0.28
9	-3.01	-2.39	0.62
10	0.01	0.05	0.04
11	1.53	1.91	0.38
12	1.44	1.32	0.12
MVD*	0.95	9.23	8.28

*MVD: Multivariate Discriminant

TABLE V-3

UPDATED NORMAL EARTHQUAKE STATISTICS WITH THRESHOLD SET AT 85% LEVEL OF EARTHQUAKE POPULATION

Discriminant Number	Median	85% Level	|Difference|	Likelihood Ratio***
1	0.42	0.59	0.17	2.6
2	-0.33	-0.10	0.23	3.6
3	-3.46	-2.39	1.07	3.1
4	-1.08	-0.66	0.42	4.6
5	-0.01	-0.07	0.06	2.1
6	-0.82	0.21	0.61	4.1
7	-2.36	-0.96	1.40	5.1
8	-2.47	-1.95	0.52	5.6
9	-3.03	-2.61	0.42	3.6
10	-0.02	0.05	0.07	6.2
11	1.47	1.89	0.42	2.1
12	1.43	1.26	0.17	0.6
MVD*	1.22	6.45	5.23	6.7**

* MVD: Multivariate Discriminant.

** Maximum attainable value for this likelihood test representing no error.

*** Likelihood of correct identification of the correlated group.

TABLE V-4

CORRELATED GROUP STATISTICS WITH THRESHOLD SET AT 85% LEVEL OF EXPLOSION POPULATION

Discriminant Number	Median	85% Level	|Difference|	Likelihood Ratio***
1	0.58	0.26	0.32	2.4
2	-0.07	-0.21	0.14	4.7
3	-2.43	-4.40	1.97	1.6
4	-0.08	-0.80	0.72	5.5
5	-0.02	0.21	0.22	0.4
6	-0.12	0.55	0.67	4.3
7	-0.11	-2.09	1.98	3.9
8	-1.42	-1.65	0.23	5.9
9	-2.14	-3.51	1.37	2.0
10	0.39	0.25	0.14	6.7**
11	1.64	1.47	0.17	3.4
12	1.36	1.40	0.04	3.6
MVD*	56.76	37.44	19.32	6.7**

* MVD: Multivariate Discriminant.

** Maximum attainable value for this likelihood test representing no error.

*** Likelihood of correct identification of earthquakes.

members of the correlated group. The exception is discriminant number ten which provided complete separation of the normal earthquake below the 85% level of the correlated group. The likelihood ratio for correct identification of earthquakes was calculated as the number of normal earthquakes beyond the 85% level of the correlated group compared to the expected number of correlated events beyond their 85% level, i.e., 0.15 times the number of events in the correlated group. Note that the multivariate discriminant indicated complete separation of normal earthquakes below the 85% level of the correlated group.

Table V-5 shows event discriminants sorted by the measured discriminant values. This is a convenient form for representing populations to determine the medians and 85% levels. Also, the event designation numbers are given for the ranking of events with respect to each discriminant.

Based on the results of the event classification analysis, six initially unknown events are correlated with normal earthquakes. These were added to the initial earthquake training set to obtain an updated earthquake training set. Event designation number 68 was dropped from the training set due to an edit timing error caused by a programming error. The event identification process identified fourteen events as similar members of a group designated as correlated group number one. In that group, event designation number seven was dropped due to a programming error in the timing of edits. Three events were categorized as not normal earthquakes and as not members of the correlated group number one. Table V-6 summarizes these results. Refer back to Table V-5 for the relative ranking of events in these groupings with respect to particular discriminants. Refer back to Table V-2 through V-4 for statistical summaries.

Table V-7 shows the detectability of the correlated event group number one and three uncorrelated events, which are at this point considered as unknown and which are not normal shallow depth earthquakes. The

TABLE V-5

EVENTS SORTED BY MEASURED DISCRIMINANT VALUE
(PAGE 1 OF 13)

SORTED EVENT DISCRIMINANTS

DISCRIMINANT #= 1.000000

EVENT SEQ #	EVENT DESGN #	DISCR. VALUE
1.000000	38.00000	1.281485
19.00000	59.00000	0.8961941
20.00000	14.00000	0.8923602
11.00000	3.000000	0.8534517
27.00000	21.00000	0.7178801
29.00000	17.00000	0.7027812
6.000000	73.00000	0.6821035
35.00000	53.00000	0.6238362
21.00000	61.00000	0.6015817
2.000000	48.00000	0.6004386
8.000000	19.00000	0.5818741
30.00000	16.00000	0.5780638
26.00000	77.00000	0.5698195
9.000000	20.00000	0.5604782
33.00000	36.00000	0.5336183
22.00000	62.00000	0.5171143
10.00000	1.000000	0.5139959
5.000000	68.00000	0.5119907
13.00000	34.00000	0.5063442
4.000000	56.00000	0.4516214
25.00000	151.0000	0.4301729
15.00000	37.00000	0.4246477
3.000000	55.00000	0.3606163
16.00000	39.00000	0.2931902
18.00000	50.00000	0.2669533
31.00000	81.00000	0.2585233
24.00000	149.0000	0.2450056
12.00000	7.000000	0.2186967
23.00000	145.0000	0.2034087
17.00000	49.00000	0.1919603
14.00000	35.00000	0.1635789
34.00000	47.00000	0.1496212
28.00000	22.00000	0.1121235
7.000000	18.00000	0.1051522
32.00000	30.00000	0.6657410E-01

TABLE V-5

EVENTS SORTED BY MEASURED DISCRIMINANT VALUE
(PAGE 2 OF 13)

SORTED EVENT DISCRIMINANTS

DISCRIMINANT #= 2.000000

EVENT SEQ #	EVENT DESGN #	DISCR. VALUE
7.000000	18.00000	0.6141447
29.00000	17.00000	0.2291999
27.00000	21.00000	0.1520773
19.00000	39.00000	0.1419783
2.000000	48.00000	0.1000224
11.00000	5.000000	0.7590890E-01
33.00000	36.00000	-0.2436399E-01
1.000000	38.00000	-0.2597964E-01
10.00000	1.000000	-0.4314971E-01
35.00000	53.00000	-0.6327271E-01
30.00000	16.00000	-0.7024443E-01
21.00000	61.00000	-0.8165729E-01
3.000000	55.00000	-0.1118910
22.00000	62.00000	-0.1154736
31.00000	31.00000	-0.1335688
20.00000	14.00000	-0.1445462
4.000000	56.00000	-0.1457167
8.000000	19.00000	-0.2102412
9.000000	20.00000	-0.2345200
6.000000	73.00000	-0.2348187
34.00000	47.00000	-0.2578360
15.00000	37.00000	-0.2720613
12.00000	7.000000	-0.3009868
25.00000	151.0000	-0.3326520
13.00000	34.00000	-0.3596938
24.00000	149.0000	-0.3614200
5.000000	68.00000	-0.3996466
14.00000	35.00000	-0.4087738
16.00000	39.00000	-0.4637179
28.00000	22.00000	-0.5044906
17.00000	49.00000	-0.6350853
18.00000	50.00000	-0.6417273
32.00000	30.00000	-0.6679270
26.00000	77.00000	-0.6705384
23.00000	143.0000	-1.216998

TABLE V-5

EVENTS SORTED BY MEASURED DISCRIMINANT VALUE
(PAGE 3 OF 13)

SORTED EVENT DISCRIMINANTS

DISCRIMINANT #= 3.000000

EVENT SEQ #	EVENT DESGN #	DISCR. VALUE
29.00000	17.00000	0.8997595
11.00000	3.000000	-0.3603995
34.00000	47.00000	-0.8469236
19.00000	59.00000	-1.357415
35.00000	53.00000	-1.397402
1.000000	38.00000	-1.885780
3.000000	55.00000	-1.895353
22.00000	62.00000	-2.094998
30.00000	16.00000	-2.341238
7.000000	18.00000	-2.377530
27.00000	21.00000	-2.432505
31.00000	81.00000	-2.507324
2.000000	48.00000	-2.698681
21.00000	61.00000	-2.888116
4.000000	56.00000	-2.889404
33.00000	36.00000	-3.060575
6.000000	73.00000	-3.313477
32.00000	30.00000	-3.420978
17.00000	49.00000	-3.464977
14.00000	35.00000	-3.758911
5.000000	68.00000	-3.898113
28.00000	22.00000	-3.965236
24.00000	149.0000	-4.034424
8.000000	19.00000	-4.373697
15.00000	57.00000	-4.382095
13.00000	34.00000	-4.390918
20.00000	14.00000	-4.400008
9.000000	20.00000	-4.541711
12.00000	7.000000	-4.632813
25.00000	151.0000	-4.729350
16.00000	39.00000	-4.737253
10.00000	1.000000	-4.835808
18.00000	50.00000	-6.129150
26.00000	77.00000	-8.653698
23.00000	143.0000	-8.787143

TABLE V-5

EVENTS SORTED BY MEASURED DISCRIMINANT VALUE
(PAGE 4 OF 13)

SORTED EVENT DISCRIMINANTS

DISCRIMINANT #= 4.000003

EVENT SEQ #	EVENT DESGN #	DISCR. VALUE
31.00000	31.00000	0.8952192
7.000000	18.00000	0.7463280
8.000000	19.00000	0.5422524
35.00000	53.00000	0.5049603
10.00000	1.000000	0.3952518
9.000003	20.00000	0.4643571E-01
12.00000	7.000000	0.0000000
29.00000	17.00000	-0.8439064E-01
27.00000	21.00000	-0.9485781E-01
24.00000	149.0000	-0.1727462
2.000000	48.00000	-0.2409449
30.00000	16.00000	-0.4555215
26.00000	77.00000	-0.4670366
11.00000	3.000000	-0.5195667
20.00000	14.00000	-0.6651423
19.00000	59.00000	-0.8017970
1.000000	38.00000	-0.8054416
21.00000	61.00000	-0.8079039
25.00000	151.0000	-0.8099695
23.00000	143.0000	-0.9101455
6.000000	73.00000	-0.9852136
28.00000	22.00000	-1.055499
5.000000	68.00000	-1.072161
17.00000	49.00000	-1.073619
13.00000	34.00000	-1.082644
18.00000	50.00000	-1.113121
3.000000	55.00000	-1.134726
4.000000	56.00000	-1.324359
33.00000	36.00000	-1.345183
16.00000	39.00000	-1.410806
15.00000	37.00000	-1.549138
22.00000	62.00000	-1.646932
14.00000	35.00000	-1.710390
34.00000	47.00000	-1.996634
32.00000	30.00000	-2.421961

TABLE V-5

EVENTS SORTED BY MEASURED DISCRIMINANT VALUE
(PAGE 5 OF 13)

SORTED EVENT DISCRIMINANTS

DISCRIMINANT #= 5.000000

EVENT SEQ #	EVENT DESGN #	DISCR. VALUE
10.00000	1.000000	0.5145466
19.00000	59.00000	0.4549572
12.00000	7.000000	0.3399252
24.00000	149.0000	0.3394221
18.00000	50.00000	0.2319742
30.00000	16.00000	0.2078829
9.000000	20.00000	0.1871995
26.00000	77.00000	0.1848801
34.00000	47.00000	0.1664774
32.00000	39.00000	0.1616617
25.00000	151.0000	0.1409117
22.00000	62.00000	0.1335987
14.00000	35.00000	0.8250213E-01
1.000000	38.00000	0.3482962E-01
27.00000	21.00000	0.1236534E-01
16.00000	39.00000	0.1154971E-01
13.00000	34.00000	0.6297946E-02
3.000000	55.00000	-0.1206172E-01
20.00000	14.00000	-0.1532853E-01
6.000000	73.00000	-0.2377582E-01
4.000000	56.00000	-0.3080845E-01
15.00000	37.00000	-0.3610981E-01
11.00000	3.000000	-0.4606116E-01
31.00000	81.00000	-0.5767143E-01
21.00000	61.00000	-0.6189013E-01
35.00000	53.00000	-0.6466675E-01
33.00000	36.00000	-0.8050597E-01
7.000000	18.00000	-0.9410161E-01
23.00000	143.0000	-0.9704590E-01
29.00000	17.00000	-0.1195118
28.00000	22.00000	-0.1367149
5.000000	68.00000	-0.1625949
8.000000	19.00000	-0.1724290
17.00000	49.00000	-0.2161083
2.000000	48.00000	-0.3064649

TABLE V-5

EVENTS SORTED BY MEASURED DISCRIMINANT VALUE
(PAGE 6 OF 13)

SORTED EVENT DISCRIMINANTS

DISCRIMINANT #= 6.000000

EVENT SEQ #	EVENT DESGN #	DISCR. VALUE
14.00000	35.00000	1.199142
33.00000	36.00000	1.194187
15.00000	37.00000	1.163749
13.00000	34.00000	1.019934
16.00000	39.00000	0.9970392
22.00000	62.00000	0.9834920
25.00000	151.0000	0.9554600
4.000000	56.00000	0.9208046
3.000000	55.00000	0.8880939
26.00000	77.00000	0.8239590
20.00000	14.00000	0.7839437
2.000000	48.00000	0.7839420
1.000000	38.00000	0.7774760
21.00000	61.00000	0.7498420
5.000000	68.00000	0.6697786
6.000000	73.00000	0.5812969
19.00000	59.00000	0.5497030
23.00000	143.0000	0.5256926
30.00000	16.00000	0.3850524
17.00000	49.00000	0.3744305
28.00000	22.00000	0.3267765
32.00000	32.00000	0.2169040
11.00000	3.000000	0.1942062
8.000000	19.00000	0.8777606E-01
34.00000	47.00000	0.8527875E-01
12.00000	7.000000	0.0000000
31.00000	81.00000	-0.1198176
24.00000	149.0000	-0.1295769
29.00000	17.00000	-0.1831255
27.00000	21.00000	-0.2439444
7.000000	18.00000	-0.2526371
18.00000	50.00000	-0.3180960
9.000000	20.00000	-0.3837500
10.00000	1.000000	-0.4147766
35.00000	53.00000	-1.033591

TABLE V-5

EVENTS SORTED BY MEASURED DISCRIMINANT VALUE
(PAGE 7 OF 13)

SORTED EVENT DISCRIMINANTS

DISCRIMINANT #= 7.000000

EVENT SEQ #	EVENT DESGN #	DISCR. VALUE
35.00000	53.00000	2.033546
9.000000	20.00000	0.9426957
10.00000	1.000000	0.7113269
18.00000	50.00000	0.6456962
27.00000	21.00000	0.4087380
24.00000	149.0000	0.1970640
29.00000	17.00000	0.1864126
31.00000	81.00000	-0.5148679E-01
7.000000	18.00000	-0.1062366
28.00000	22.00000	-0.1978615
32.00000	30.00000	-0.7040051
8.000000	19.00000	-0.7890734
34.00000	47.00000	-0.7946444
19.00000	59.00000	-0.8991653
17.00000	49.00000	-1.115621
6.000000	73.00000	-1.739066
11.00000	3.000000	-1.843077
23.00000	143.0000	-2.026750
30.00000	16.00000	-2.094837
25.00000	151.0000	-2.184510
20.00000	14.00000	-2.339602
13.00000	34.00000	-2.364003
26.00000	77.00000	-2.481439
5.000000	68.00000	-2.530518
14.00000	35.00000	-2.607703
22.00000	62.00000	-2.705066
16.00000	39.00000	-2.796709
21.00000	61.00000	-2.946625
4.000000	56.00000	-2.967224
1.000000	38.00000	-3.353940
3.000000	55.00000	-3.362595
2.000000	48.00000	-3.364868
33.00000	56.00000	-3.473087
15.00000	37.00000	-3.644625
12.00000	7.000000	-3.770361

TABLE V-5

EVENTS SORTED BY MEASURED DISCRIMINANT VALUE
(PAGE 8 OF 13)

SORTED EVENT DISCRIMINANTS

DISCRIMINANT #= 8.000000

EVENT SEQ #	EVENT DESGN #	DISCR. VALUE
10.00000	1.000000	3.337009
7.000000	18.00000	2.082326
27.00000	21.00000	-0.9870589E-01
31.00000	81.00000	-0.3415936
11.00000	3.000000	-0.4250169
24.00000	149.0000	-0.6374735
35.00000	53.00000	-0.7380533
19.00000	59.00000	-1.197331
20.00000	14.00000	-1.416382
28.00000	22.00000	-1.417003
8.000000	19.00000	-1.459015
29.00000	17.00000	-1.499571
18.00000	50.00000	-1.532145
9.000000	20.00000	-1.646327
17.00000	49.00000	-1.814919
26.00000	77.00000	-2.087240
32.00000	30.00000	-2.188503
14.00000	35.00000	-2.206860
34.00000	47.00000	-2.354964
23.00000	143.0000	-2.379538
25.00000	151.0000	-2.470126
22.00000	62.00000	-2.523605
13.00000	34.00000	-2.537966
12.00000	7.000000	-2.638682
5.000000	68.00000	-2.989014
16.00000	39.00000	-3.007554
4.000000	56.00000	-3.102294
1.000000	38.00000	-3.247847
21.00000	61.00000	-3.457743
2.000000	48.00000	-3.486869
33.00000	36.00000	-3.787739
6.000000	73.00000	-4.011271
15.00000	37.00000	-4.221710
3.000000	55.00000	-4.243390
30.00000	16.00000	-4.306190

TABLE V-5

EVENTS SORTED BY MEASURED DISCRIMINANT VALUE
(PAGE 9 OF 13)

SORTED EVENT DISCRIMINANTS

DISCRIMINANT #= 9.000000

EVENT SEQ #	EVENT DESGN #	DISCR. VALUE
31.00000	81.00000	-1.355317
8.000000	19.00000	-1.404693
7.000000	18.00000	-1.502222
10.00000	1.000000	-1.565283
35.00000	53.00000	-1.652115
30.00000	16.00000	-1.781093
26.00000	77.00000	-1.886929
19.00000	59.00000	-2.139274
24.00000	149.0000	-2.181747
16.00000	39.00000	-2.393634
12.00000	7.000000	-2.679137
18.00000	50.00000	-2.723585
29.00000	17.00000	-2.796755
25.00000	151.0000	-2.834904
23.00000	143.0000	-2.857876
32.00000	30.00000	-2.900297
3.000000	55.00000	-2.915809
21.00000	61.00000	-2.960134
4.000000	56.00000	-3.033518
17.00000	49.00000	-3.083425
6.000000	73.00000	-3.113488
15.00000	37.00000	-3.165459
20.00000	14.00000	-3.297346
1.000000	38.00000	-3.430501
27.00000	21.00000	-3.505096
9.000000	20.00000	-3.513054
2.000000	48.00000	-3.513417
33.00000	36.00000	-3.550718
28.00000	22.00000	-3.568392
5.000000	68.00000	-3.722703
13.00000	34.00000	-4.121396
22.00000	62.00000	-4.730242
11.00000	3.000000	-4.851397
14.00000	35.00000	-4.893420
34.00000	47.00000	-5.610709

TABLE V-5

EVENTS SORTED BY MEASURED DISCRIMINANT VALUE
(PAGE 10 OF 13)

SORTED EVENT DISCRIMINANTS

DISCRIMINANT #= 10.00000

EVENT SEQ #	EVENT DESGN #	DISCR. VALUE
20.00000	14.00000	0.8262868
29.00000	17.00000	0.6843088
7.000000	18.00000	0.5886557
30.00000	16.00000	0.5804186
8.000000	19.00000	0.5275884
35.00000	53.00000	0.4889289
28.00000	22.00000	0.3926786
12.00000	7.000000	0.3803024
31.00000	81.00000	0.3647542
27.00000	21.00000	0.3487525
22.00000	62.00000	0.2880888
9.000000	20.00000	0.2545587
19.00000	59.00000	0.2498338
24.00000	149.0000	0.6007352E-01
11.00000	3.000000	0.5403280E-01
6.000000	73.00000	0.4966974E-01
18.00000	50.00000	0.4880795E-01
16.00000	39.00000	0.4675579E-01
13.00000	34.00000	0.1254082E-01
23.00000	143.0000	0.5267709E-02
33.00000	36.00000	0.0000000
1.000000	38.00000	0.0000000
4.000000	56.00000	0.0000000
5.000000	68.00000	0.0000000
2.000000	48.00000	0.0000000
3.000000	55.00000	0.0000000
21.00000	61.00000	0.0000000
15.00000	37.00000	0.0000000
34.00000	47.00000	-0.5356172E-01
14.00000	35.00000	-0.1132622
10.00000	1.000000	-0.1137602
32.00000	30.00000	-0.1579071
26.00000	77.00000	-0.1667642
17.00000	49.00000	-0.2182080
25.00000	151.0000	-0.2321825

TABLE V-5

EVENTS SORTED BY MEASURED DISCRIMINANT VALUE
(PAGE 11 OF 13)

SORTED EVENT DISCRIMINANTS

DISCRIMINANT #= 11.00000

EVENT SEQ #	EVENT DESGN #	DISCR. VALUE
28.00000	22.00000	2.293043
23.00000	14.00000	2.105371
6.000000	73.00000	2.072472
10.00000	1.000000	1.988594
13.00000	34.00000	1.919897
22.00000	62.00000	1.914817
11.00000	3.000000	1.891651
25.00000	151.0000	1.859027
14.00000	35.00000	1.755218
7.000000	18.00000	1.679335
27.00000	21.00000	1.652401
29.00000	17.00000	1.637867
9.000000	23.00000	1.583375
19.00000	59.00000	1.553226
26.00000	77.00000	1.532199
8.000000	19.00000	1.502919
12.00000	7.000000	1.476109
35.00000	53.00000	1.472136
30.00000	16.00000	1.456241
23.00000	143.0000	1.413250
16.00000	39.00000	1.345308
18.00000	50.00000	1.325080
32.00000	30.00000	1.280355
24.00000	149.0000	1.279927
31.00000	81.00000	1.251183
17.00000	49.00000	1.214591
34.00000	47.00000	1.145368
33.00000	36.00000	0.0000000
1.000000	38.00000	0.0000000
4.000000	56.00000	0.0000000
2.000000	48.00000	0.0000000
3.000000	55.00000	0.0000000
21.00000	61.00000	0.0000000
15.00000	37.00000	0.0000000
5.000000	68.00000	0.0000000

TABLE V-5

EVENTS SORTED BY MEASURED DISCRIMINANT VALUE
(PAGE 12 OF 13)

SORTED EVENT DISCRIMINANTS

DISCRIMINANT #= 12.00000

EVENT SEQ #	EVENT DESGN #	DISCR. VALUE
14.00000	35.00000	2.380650
12.00000	7.000000	1.833109
16.00000	39.00000	1.768005
11.00000	3.000000	1.740994
6.000000	73.00000	1.733068
19.00000	59.00000	1.590322
20.00000	14.00000	1.554940
18.00000	50.00000	1.551296
26.00000	77.00000	1.459213
24.00000	149.0000	1.425343
8.000000	19.00000	1.396592
28.00000	22.00000	1.391832
29.00000	17.00000	1.389096
35.00000	53.00000	1.358329
10.00000	1.000000	1.346107
23.00000	143.0000	1.322733
34.00000	47.00000	1.316248
7.000000	18.00000	1.313726
25.00000	151.0000	1.305879
27.00000	21.00000	1.305663
31.00000	81.00000	1.294377
9.000000	20.00000	1.279096
17.00000	49.00000	1.221704
30.00000	16.00000	1.146245
32.00000	30.00000	1.044979
33.00000	36.00000	0.0000000
1.000000	38.00000	0.0000000
4.000000	56.00000	0.0000000
5.000000	68.00000	0.0000000
2.000000	48.00000	0.0000000
3.000000	55.00000	0.0000000
22.00000	62.00000	0.0000000
21.00000	61.00000	0.0000000
13.00000	34.00000	0.0000000
15.00000	37.00000	0.0000000

TABLE V-5

EVENTS SORTED BY MEASURED DISCRIMINANT VALUE
(PAGE 13 OF 13)

SORTED EVENT DISCRIMINANTS

DISCRIMINANT #=	MULTIVARIATE DISCRIMINANT
EVENT DESGN #	DISCR. VALUE
18.00000	91.92015
53.00000	72.41619
17.00000	71.10209
14.00000	68.32403
19.00000	66.60777
81.00000	62.26123
16.00000	56.76215
21.00000	51.16705
1.000000	46.33460
22.00000	38.05307
20.00000	37.43552
59.00000	34.12424
7.000000	30.54122
149.0000	28.20870
62.00000	23.57536
3.000000	20.57518
50.00000	9.972984
77.00000	9.228650
48.00000	6.847387
47.00000	3.655029
39.00000	3.212134
49.00000	2.544737
30.00000	1.904394
36.00000	1.501603
38.00000	1.493665
61.00000	1.220119
73.00000	0.0000000
60.00000	0.0000000
55.00000	0.0000000
56.00000	0.0000000
151.0000	0.0000000
37.00000	0.0000000
143.0000	0.0000000
34.00000	0.0000000
35.00000	0.0000000

TABLE V-6

EVENT IDENTIFICATION RESULTS
(PAGE 1 OF 2)

INITIAL NORMAL EARTHQUAKE TRAINING SET		
Event Sequence Number	Event Designation Number	Comments
5	68	Dropped due to program error.
6	73	
11	3	
13	34	
14	35	
16	39	
23	143	
24	149	
25	151	
26	77	
32	30	
34	47	
UNKNOWN EVENTS CLASSIFIED AS EARTHQUAKES		
Event Sequence Number	Event Designation Number	Comments
3	55	
4	56	
15	37	
21	61	
33	36	
17	49	

TABLE V-6

EVENT IDENTIFICATION RESULTS

(PAGE 2 OF 2)

CORRELATED EVENT GROUP NUMBER ONE		
Event Sequence Number	Event Designation Number	Comments
7	18	
8	19	
20	14	
29	17	
9	20	
10	1	
12	7	Dropped due to program error.
19	59	
22	62	
27	21	
28	22	
30	16	
31	81	
35	53	
UNKNOWN EVENTS NEITHER CLASSIFIED AS GROUP NUMBER ONE OR AS NORMAL SHALLOW FOCUS EARTHQUAKES		
Event Sequence Number	Event Designation Number	Comments
1	38	
2	48	
18	50	

TABLE V-7

DETECTABILITY OF CORRELATED EVENT GROUP NUMBER ONE AND UNCORRELATED UNKNOWNS

Discriminant Number	Detectability			
	Group No. One	Event 38	Event 48	Event 50
1	0.94	5.05	1.05	-0.90
2	1.13	1.32	1.86	-1.34
3	0.96	1.46	0.71	-2.50
4	2.37	0.65	1.99	-0.07
5	-0.05	0.75	-4.93	4.00
6	-1.54	2.62	2.62	0.82
7	1.61	-0.71	-0.71	2.15
8	2.02	-1.50	-1.96	1.81
9	2.12	-0.95	-1.14	0.74
10	5.59	N.A.*	N.A.	1.00
11	0.40	N.A.	N.A.	-0.35
12	-0.41	N.A.	N.A.	0.71
MVD	9.62	-0.95	1.07	1.67

N.A.: Not available due to lack of detections.

identification process will retain these events as unknown unusual events until sufficient event data are entered into the system to group them into another correlated grouping of similar events.

For robustness, the detectabilities were estimated by computing the difference between the abnormal group or abnormal event median and the median of the updated earthquake population. Abnormal event medians are taken as the observed discriminant value. This difference of medians was divided by the normal earthquake population deviation; computed as the difference between the 85% level of normal earthquakes and the median of normal earthquakes as shown on Figure V-1.

The detectability of correlated group number one for discriminants number one through twelve were used as weights for combining discriminant observations into a single multivariate discriminant. The operator for applying these group projection weights to an observed set of discriminants is shown by equation (IV-1). The results of the multivariate discriminant calculations sorted by discriminant value are shown on part 13 of Table V-5. Medians and deviations are shown on Tables V-2 through V-4. Remember that each observation of an unknown event discriminant vector is transformed into a detectability vector by subtracting the normal earthquake median and dividing by the normal earthquake deviation. This converts each discriminant observation vector into a homogeneous set of dimensionless components of a z-vector. To this, the projection operator is applied with respect to the correlated group z-vector. A projection above a prescribed threshold is accepted as a new similar member of the group.

SECTION VI
CONCLUSIONS

Our goal was to develop a package to objectively evaluate the performance of a set of selected discriminants as potential components of a seismic event identification system. As a ground rule, the following operations were performed automatically to achieve an objective evaluation of performance.

- Determine ground motion by correcting for system response.
- Edit phases.
- Extract waveforms and determine detection status.
- Filter waveforms.
- Generate a signal measurement file.
- Generate an event source measurement file by operating on the signal measurement file.
- Generate an event discriminant file by operating on the source measurement file.
- Generate inductive grouping of event types by operating on the discriminant file.

The final results of this mode of discriminant processing are reproducibly determined subject to specification of a set of algorithms for determining the detection status of edits, algorithms for measuring signals or noise in edit windows, algorithms for converting signal measurements to unbiased estimates of source parameters, algorithms for converting deriving discriminants

from source parameter measurements, and decision functions for grouping events of similar discriminant characteristics. In addition, to start the process it was necessary to introduce a training set of normal shallow earthquakes, determine the statistical characteristics of their discriminants and use those characteristics to normalize the observed discriminants of subsequent unknown events.

Our initial test run was performed on thirty five events, twelve of which were selected as the initial normal shallow earthquake training set. Of the unknown set, six were correlated with normal shallow earthquakes and fourteen were correlated with a similar group of events which are not normal shallow earthquakes, and three remained as unknown unusual events which were neither classified as normal shallow earthquakes nor as the correlated group of unusual events. This test was performed with arbitrarily selected decision thresholds for grouping events. Based on statistics determined from the test and the observed grouping of events a threshold can be set to operate with any desired operating characteristics. For example, two normal earthquakes appeared to be included in the correlated group. By raising the threshold, the two apparent normal earthquakes could have been classified correctly without removing any other events from the correlated group. Two of the unknown unusual events were deep events from the Afghan-USSR border which appear to be similar to each other. The third unusual event was an intermediate depth event from the Kurile Islands.

Relative ranking performance of particular discriminants are apparent by examination of tables of likelihood tests and detectabilities shown in the preceding section. It should be kept in mind, however, that such rankings of discriminant effectiveness are only relevant to the single correlated group thus far obtained. Other apparently less effective discriminants may be important in detecting members of other unusual event groupings not yet observed. Once the decision rules are set, the package provides a multi-user

environment. The classification files can be used as permanent, maintainable and transportable files. As more events are added into such a system, the performance will improve as a result of building up the grouped populations of abnormal events and normal earthquake populations. This will result in better statistical estimates of population characteristics. In another sense, better performance can be anticipated by expanding the list of discriminants and the number of stations in the network.

SECTION VII
REFERENCES

Anglin, F. M., 1971; Discrimination of Earthquakes and Explosions using Short Period Seismic Array Data, Nature, Vol. 233, p. 51-52.

Aki, K., 1967; Scaling Law of Seismic Spectrum, J. Geophys. Res., 72, p. 1217-1231.

Aki, K., 1968; Seismic Displacements Near a Fault, J. Geophys. Res., 73, p. 5359-5376.

Alexander, S. S., and L. S. Turnbull, 1973; Long-Period Seismic Methods for Identifying Small Underground Nuclear Explosions, Final Report, Grant No. AFOSR-69-1796, The Pennsylvania State University, University Par, PA.

Archambeau, C. B., 1968; General Theory of Elastodynamic Source Fields, Rev. Geophys., 6, p. 241-288.

Archambeau, C. B., 1972; The Theory of Stress Wave Radiation from Explosions in Prestressed Media, Geophys. J. R. Astr. Soc., 29, p. 329.

Archambeau, C. B., and C. Sammis, 1970; Seismic Radiation from Explosions in Prestressed Media and the Measurement of Tectonic Stress in the Earth, Rev. Geophys., 8, p. 473.

Archambeau, C. B., D. G. Harkrider, and D. V. Helmberger, 1974; Studies of Multiple Seismic Events, California Institute of Technology, Final Contract Report (Draft) prepared for U.S. Arms Control and Disarmament Agency.

Bache, T. C., J. T. Cherry, and J. M. Savino, 1974; Application of Advanced Methods for Identification and Detection of Nuclear Explosions from the Asian Continent, Systems, Science and Software Semi-Annual Report No. SSS-R-75-2483, Contract Number F44620-74-C-0063, La Jolla, CA.

Bache, T. C., J. T. Cherry, K. G. Hamilton, J. F. Masso, and J. M. Savino, 1975; Application of Advanced Methods for Identification and Detection of Nuclear Explosions from the Asian Continent, Systems, Science and Software Report No. SSS-R-75-2646, Contract Number F44620-74-C-0063, La Jolla, CA.

Basham, P. W., 1969; Canadian Magnitudes of Earthquakes and Nuclear Explosions in South-Western North America, Geophys. J. R. Astr. Soc., 17, p. 1.

Basham, P. W., and F. M. Anglin, 1973; Multiple Discriminant Screening Procedure for Test Ban Verification, Nature, Vol. 246, p. 474-476.

Bell, A. G. R., 1978; Application of Two Multivariate Classification Techniques to the Problem of Seismic Discrimination, M. S. Thesis, The Pennsylvania State University, University Park, PA.

Ben-Menahem, A., and D. G. Harkrider, 1964; Radiation Patterns of Seismic Surface Waves from Buried Dipolar Point Source in a Flat Stratified Earth, J. Geophys. Res., 69, p. 2605-2620.

Berckhemer, H., and K. H. Jacob, 1968; Investigation of the Dynamical Process in Earthquake Foci by Analyzing the Pulse Shape of Body Waves, Final Sci. Rep. AF61(052)-801, Air Force Cambridge Research Laboratories, Cambridge, MA.

Bishop, R. H., 1963; Spherical Shock Waves from Underground Explosions, Close-In Phenomena of Buried Explosions, Final Rep. SC-4907(RR), 115, Sandia Corporation, Albuquerque, NM.

Booker, A., and W. Mitronovas, 1964; Application of Statistical Discrimination to Classify Seismic Events, Bull. Seismol. Soc. Am., 54, p. 961-971.

Booth, D. C., P. D. Marshall, and J. B. Young, 1974; Long and Short Period P-Wave Amplitudes from Earthquakes in the Range 0°-114°, Geophys. J. R. Astr. Soc., 39, p. 523-537.

Brune, J. N., 1970; Tectonic Stress and the Spectra of Seismic Shear Waves from Earthquakes, J. Geophys. Res., 75, p. 4997-5009.

Burridge, R., and L. Knopoff, 1964; Body Force Equivalents for Seismic Dislocations, Bull. Seismol. Soc. Am., 54, p. 1874-1888.

Capon, J., R. J. Greenfield, and R. T. Lacoss, 1969; Long Period Signal Processing Results for the Large Aperture Seismic Array, Geophysics, 34, p. 17.

Carpenter, E. W., 1967; Teleseismic Signals Calculated for Underground Underwater, and Atmospheric Explosions, Geophysics, 32, p. 17-32.

Chinnery, M. A., 1960; Some Physical Aspects of Earthquake Source Mechanism, J. Geophys. Res., 65, p. 3852.

Chinnery, M. A., 1961; The Deformation of the Ground Around Surface Faults, Bull. Seismol. Soc. Am., 51, p. 355.

Der, Z. A., 1977; On the Existence, Magnitude and Causes of Broad Regional Variations in Body-Wave Amplitudes, SDAC-TR-76-8, Teledyne Geotech, Alexandria, VA.

Douglas, A., J. A. Hudson, and V. K. Kembhavi, 1971; The Relative Excitation of Seismic Surface and Body Waves by Point Sources, Geophys. J. R. Astr. Soc., 23, p. 451-460.

Evernden, J. F., 1967; Magnitude Determination at Regional and Near-Regional Distances in the United States, Bull. Seismol. Soc. Am., 57, p. 591-639.

Evernden, J. F., 1969; Identification of Earthquakes and Explosions by Use of Teleseismic Data, J. Geophys. Res., 74, p. 3828-3856.

Evernden, J. F., 1975; Further Studies on Seismic Discrimination, Bull. Seismol. Soc. Am., 65, p. 359-391.

Evernden, J. F., and D. Clark, 1970; Investigation of P Travel-Time Curve, 2, Phys. Earth Planet. Interiors, 4, p. 1-23.

Evernden, J. F., and J. Filson, 1971; Regional Dependence of Surface-Wave Versus Body-Wave Magnitudes, J. Geophys. Res., 76, p. 3303-3308.

Ewing, W. M., W. S. Jardetzky, and F. Press, 1957; Elastic Waves in Layered Media, McGraw-Hill, New York, NY.

Farnbach, J. S., 1975; The Complex Envelope in Seismic Signal Analysis, Bull. Seismol. Soc. Am., 65, p. 951-962.

Fitch, T. J., M. W. Shields, and R. E. Needham, 1978; Comparison of Crustal Phase Magnitudes for Explosions and Earthquakes, Seismic Discrimination Semiannual Technical Summary, Lincoln Laboratory, M.I.T., Lexington, MA.

Geller, R. J., 1976; Scaling Relations for Earthquake Source Parameters and Magnitudes, Bull. Seismol. Soc. Am., 66, p. 1501-1523.

Gilbert, F., 1973; The Relative Efficiency of Earthquakes and Explosions in Exciting Surface Waves and Body Waves, Geophys. J. R. Astr. Soc., 33, p. 487-488.

Gutenberg, B., and C. F. Richter, 1956; Earthquake Magnitude, Intensity, Energy, and Acceleration, Bull. Seismol. Soc. Am., 32, p. 163-191.

Hanks, T. C., and M. Wyss, 1972; The Use of Body-Wave Spectra in the Determination of Seismic-Source Parameters, Bull. Seismol. Soc. Am., 62, p. 561-589.

Harkrider, D. G., 1970; Surface Waves in Multilayered Elastic Media: II. Higher Mode Spectra and Spectral Ratios from Point Sources in Plane Earth Models, Bull. Seismol. Soc. Am., 60, p. 1937-1988.

Haskell, N., 1964; Total Energy and Energy Spectral Density of Elastic Wave Radiation from Propagating Faults, Bull. Seismol. Soc. Am., 54, p. 1811-1841.

Haskell, N., 1966; Total Energy and Energy Spectral Density of Elastic Wave Radiation from Propagating Faults, Part II, A Statistical Source Model, Bull, Seismol. Soc. Am., 56, p. 125-140.

Haskell, N., 1969; Elastic Displacements in the Near-Field of a Propagating Fault, Bull, Seismol. Soc. Am., 59, p. 865-908.

Herrin, E., and J. Richmond, 1960; On the Propagation of the Lg Phase, Bull. Seismol. Soc. Am., 50, p. 197-210.

Hodgson, J. H., and A. E. Stevens, 1964; Seismicity and Earthquake Mechanism, in Research in Geophysics, H. Odishaw, ed., Vol. 2, M.I.T. Press, Cambridge, MA.

Hsiao, H. Y. A., 1978; Application of a Combined Source Model for Seismic Discrimination, Technical Report No. 21, Texas Instruments Report No. ALEX(01)-TR-78-09, AFTAC Contract Number F08606-77-C-0004, Texas Instruments Incorporated, Dallas, TX.

Isacks, B. L., and C. Stephens, 1975; Conversion of Sn to Lg at a Continental Margin, Bull. Seismol. Soc. Am., 65, p. 235-244.

Knopoff, L., and F. Gilbert, 1960; First Motions from Seismic Sources, Bull. Seismol. Soc. Am., 50, p. 117.

Knopoff, L., F. Schwab, and E. Kausel, 1973; Interpretation of Lg, Geophys. J. R. Astr. Soc., 33, p. 389-404.

Lambert, D. G., D. H. VonSeggern, S. S. Alexander, and G. A. Galat, 1970; The Longshot Experiment, Vol. II: Comprehensive Analysis, SDAC Report # 234, Teledyne Geotech, Alexandria, VA.

Lambert, D. G., T. C. Bache, and J. M. Savino, 1977; Simulation and Decomposition of Multiple Explosions, Systems, Science and Software, Topical Report SSS-R-77-3194, La Jolla, CA.

Landers, T. E., 1978; The Mechanism of Lg Propagation, Seismic Discrimination Semiannual Technical Summary, Lincoln Laboratory, M.I.T., Lexington, MA.

Liebermann, R. C., and P. W. Pomeroy, 1969; Relative Excitation of Surface Waves by Earthquakes and Underground Explosions, J. Geophys. Res., 74, p. 1575-1590.

Marshall, P. D., and P. W. Basham, 1972; Discrimination Between Earthquakes and Underground Explosions Employing an Improved m_b Scale, Geophys. J. R. Astr. Soc., 28, p. 431-458.

Nuttli, O. W., 1973; Seismic Wave Attenuation and Magnitude Relations for Eastern North America, J. Geophys. Res., 78, p. 876-885.

Nuttli, O. W., and S. G. Kim, 1975; Surface-Wave Magnitudes of Eurasian Earthquakes and Explosions, Bull. Seismol. Soc. Am., 65, p. 693-709.

Page, E. A., 1976; Improved Procedures for Determining Seismic Source Depths from Depth Phase Information, Final Report; AFTAC Project No. VELA T/6710, Contract Number F08606-76-C-0003, ENSCO, Inc. Springfield, VA.

Panza, G. F., and G. Caleagnile, 1975; Lg, Li, and Rg from Rayleigh Modes, Geophys. J. R. Astr. Soc., 40, p. 475-487.

Peppin, W. A., and T. V. McEvilly, 1974; Discrimination Among Small Magnitude Events on the Nevada Test Site, Geophys. J. R. Astr. Soc., 37, p. 227-243.

Press, F., G. Dewart, and R. Gilman, 1963; A Study of Diagnostic Techniques for Identifying Earthquakes, J. Geophys. Res., 68, p. 2909-2928.

Reid, H. F., 1911; The Elastic Rebound Theory of Earthquakes, Bull. Dept. Geology, University of California, 6, p. 413.

Ringdal, F., 1974; Estimation of Seismic Detection Thresholds, Technical Report No. 2, Texas Instruments Report No. ALEX(01)-TR-74-02, AFTAC Contract Number F08606-74-C-0033, Texas Instruments Incorporated, Dallas, TX.

Ringdal, F., J. S. Shaub, and D. G. Black, 1975; Documentation of the Interactive Seismic Processing System (ISPS), Technical Report No. 9, Texas Instruments Report No. ALEX(01)-TR-75-09, AFTAC Contract Number F08606-76-C-0011, Texas Instruments Incorporated, Dallas, TX.

Ringdal, R., 1975; Maximum Likelihood Estimation of Seismic Event Magnitude from Network Data, Technical Report No. 1, Texas Instruments Report No. ALEX(01)-TR-75-01, AFTAC Contract Number F08606-75-C-0029, Texas Instruments Incorporated, Dallas, TX.

Sax, R. L., 1976; Design, Simulated Operation, and Evaluation of a Short-Period Seismic Discrimination Processor in the Context of a World-Wide Seismic Surveillance System, Technical Report No. 9, Texas Instruments Report No. ALEX(01)-TR-76-09, AFTAC Contract Number F08606-76-C-0011, Texas Instruments Incorporated, Dallas, TX.

Schmidt, A. W., and K. S. Wilson, 1978; Seismic Data Preparation Procedures, Technical Report No. 22, Texas Instruments Report No. ALEX(01)-TR-78-10, AFTAC Contract Number F08606-77-C-0004, Texas Instruments Incorporated, Dallas, TX.

Sharpe, J. A., 1942; The Production of Elastic Waves by Explosive Pressures, 1. Theory and Empirical Field Observations, Geophysics, 7, p. 144-154.

Shaub, J. S., and D. G. Black, 1977; The Extended Interactive Seismic Processing System, Technical Report No. 9, Texas Instruments Report No. ALEX(01)-TR-77-09, AFTAC Contract Number F08606-77-C-0004, Texas Instruments Incorporated, Dallas, TX.

Shaub, J. S., D. A. Eastburn, D. R. Lashmit, and R. L. Sax, 1977; Documentation of the Extended Interactive Seismic Processing System (ISPSE), AFTAC Contract Number F08606-77-C-0004, Texas Instruments Incorporated, Dallas, TX.

SIPRI, 1968; Seismic Methods for Monitoring Underground Explosions, International Peace Research Institute, Stockholm.

Solomon, S. C., 1972; On Q and Seismic Discrimination, Geophys. J. R. Astr. Soc., 31, p. 163-177.

Snoke, J. A., 1975; Archambeau's Elastodynamical Source-Model Solution and Low Frequency Spectral Peaks in the Far-Field Displacement Amplitude, in Carnegie Inst. Wash. Year Book (74), Washington, D. C.

Snoke, J. A., A. T. Linde, and I. S. Sacks, 1975; Seismic Source Studies, General Introduction, Carnegie Inst. Wash. Year Book (74), Washington, D. C.

Stacey, F. D., 1969; Physics of the Earth, J. Wiley and Sons, New York, NY.

Steketee, I. A., 1958; Some Geophysical Applications of Elasticity Theory of Dislocations, Can. J. of Phys., 36, p. 1168.

Stevens, A. E., 1969; World-Wide Earthquake Mechanism, in The Earth's Crust and Upper Mantle, Geophysical Monograph 13, American Geophysical Union, Washington, D. C.

Strauss, A. C., and L. C. Weltman, 1977; Continuation of the Seismic Research Observatories Evaluation, Technical Report No. 2, Texas Instruments Report No. ALEX(01)-TR-77-02, AFTAC Contract Number F08606-77-C-0004, Texas Instruments Incorporated, Dallas, TX.

Sun, D., 1976; Source Studies in the Near- and Far-Field, Semi-Annual Technical Report No. ALEX(02)-TR-76-01-Part A, AFOSR Contract Number F44620-73-C-0055, Texas Instruments Incorporated, Dallas, TX.

Sun, D., 1977; Determination of Seismic Source Parameters from Long-Period Surface Wave Data, Technical Report No. 11, Texas Instruments Report No. ALEX(01)-TR-77-11, AFTAC Contract Number F08606-77-C-0004, Texas Instruments Incorporated, Dallas, TX.

Thirlaway, H. I. S., 1968; Diagnosing Underground Explosions and Earthquakes, Contemp. Phys., 9, p. 17.

Toksöz, M. N., A. Ben-Menahem, and D. G. Harkrider, 1964; Determination of Source Parameters of Explosions and Earthquakes by Amplitude Equalization of Seismic Surface Waves, 1, Underground Nuclear Explosions, J. Geophys. Res., 69, p. 4355-4366.

Toksöz, M. N., K. C. Thomson, and T. J. Ahrens, 1971; Generation of Seismic Waves by Explosions in Prestressed Media, Bull. Seismol. Soc. Am., 61, p. 1589-1624.

Tsai, Y. B., 1972a; Utility of Tsai's Method for Seismic Discrimination, Semi-Annual Technical Report No. 1, AFOSR Contract Number F44620-71-C-0112, Texas Instruments Incorporated, Dallas, TX.

Tsai, Y. B., 1972b; Utility of Tsai's Method for Seismic Discrimination Semi-Annual Technical Report No. 2, AFOSR Contract Number F44620-71-C-0112, Texas Instruments Incorporated, Dallas, TX.

Turnbull, L. S., 1971; The Use of Rayleigh and Love Waves to Examine the Effects of Buried Multipolar Sources, EOS (Abstract), 52, p. 863.

Turnbull, L. S., 1972; Surface Wave Radiation from a Buried Volume Relaxation Source in a Multilayered Half-Space, EOS (Abstract), 53, p. 350.

Turnbull, L. S., J. C. Battis, D. Sun, and A. C. Strauss, 1975; Source Studies in the Near- and Far-Field, Semi-Annual Technical Report No. 4-Part A, Texas Instruments Report No. ALEX(02)-TR-75-02-Part A, AFOSR Contract Number F44620-73-C-0055, Texas Instruments Incorporated, Dallas, TX.

Unger, R., 1976; Seismic Event Discrimination Using the Instantaneous Envelope, Phase and Frequency, Abstract, EOS, 57, p. 286.

Unger, R., 1978a; Automatic Detection, Timing and Preliminary Discrimination of Seismic Signals with the Instantaneous Amplitude, Phase and Frequency, Technical Report No. 4, Texas Instruments Report No. ALEX(01)-TR-77-04, AFTAC Contract Number F08606-77-C-0004, Texas Instruments Incorporated, Dallas, TX.

Unger, R., 1978b; Narrow and Broad Region Dispersion of Long-Period Surface Waves, Technical Report No. 16, Texas Instruments Report No. ALEX(01)-TR-78-04, AFTAC Contract Number F08606-77-C-0004, Texas Instruments Incorporated, Dallas, TX.

Veith, K. F., and G. E. Clawson, 1972; Magnitude from Short-Period P-wave Data, Bull. Seismol. Soc. Am., 62, p. 435-452.

Viecelli, J. A., 1973; Spallation and the Generation of Surface Waves by an Underground Explosion, J. Geophys. Res., 78, p. 2475-2487.

Von Seggern, D. H., 1972; Seismic Shear Waves as a Discriminant Between Earthquakes and Underground Nuclear Explosions, SDAC Report No. 295, AFTAC Contract Number F33657-72-C-0009, Teledyne Geotech, Alexandria, VA.

Von Seggern, D. H., 1973; Seismic Surface Waves from Amchitka Island Test Site Events and Their Relation to Source Mechanism, J. Geophys. Res., 78, p. 2467-2474.

Whalen, A. D., 1971; Detection of Signals in Noise, Academic Press, New York, NY.

APPENDIX A

VFM NARROWBAND FILTER DESCRIPTION

A cusp-shaped narrowband filter is used in many different applications throughout the routines used in obtaining discriminant measurements. This filter gives optimal time and frequency domain characteristics within the limits of the Uncertainty Principle. The goals which this filter attempts to satisfy are: (1) minimum width in the frequency domain, and (2) maximum ripple suppression in the time domain. Since the Uncertainty Principle disallows the possibility of simultaneously satisfying these two goals to an arbitrary precision, the filter was chosen to optimize these characteristics. This filter has been used to obtain accurate time separation and accurate amplitudes in separating multiple explosions. It has also been used in calculating variable frequency magnitudes (VFM) based on the maximum envelope amplitudes for the filtered signal.

Figure A-1 illustrates the filter function in the frequency domain. The cusp-shaped filter, F, is of the form:

$$F(f) = \begin{cases} 1 - \cos \pi/3 \left[\dfrac{f - (f_c - 3/2\Delta f)}{\Delta f} \right], & (f_c - 3/2\Delta f) \le f \le f_c \\ 1 - \cos \pi/3 \left[\dfrac{(f_c + 3/2\Delta f) - f}{\Delta f} \right], & f_c \le f \le (f_c + 3/2\Delta f) \\ 0, & \text{otherwise} \end{cases}$$

where

f = frequency

f_c = frequency at which the filter is centered

Δf = the desired width (in Hz) at $\frac{1}{2}$ amplitude points (-6dB points).

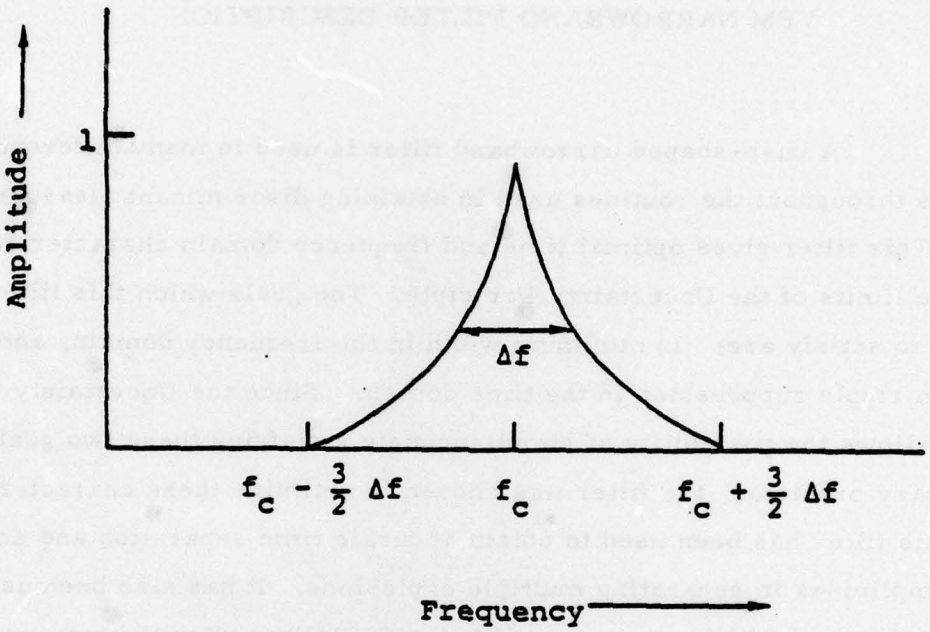

FIGURE A-1

NARROWBAND FILTER USED FOR VFM MEASUREMENT. THE WIDTH AT ONE-HALF MAXIMUM AMPLITUDE IS DESIGNATED Δf
(Lambert, Bache, and Savino, 1977)

This filter is applied to the signal in the frequency domain by multiplication of the above function with the transformed signal (Lambert, Bache, and Savino, 1977).